Digestive System

10

Abdelhamid H. Elgazzar and Saud A. Alenezi

10.1 Gastrointestinal Tract

The digestive system consists of the gastrointestinal tract, hepatobiliary system (Fig. 10.1), pancreas, and salivary glands. Nuclear medicine is concerned with the evaluation of normal and abnormal functions of the gastrointestinal tract and hepatobiliary system. To date, the role of nuclear medicine in pancreatic disorders is limited to evaluation of its tumors which is dealt with elsewhere in the book.

10.1.1 The Esophagus

10.1.1.1 Anatomic and Physiological Considerations

The esophagus is a 18–25 cm long muscular tube that passes through the mediastinum, connecting the pharynx and the stomach. The cervical esophagus is composed of striated muscles whereas the thoracic esophagus consists of smooth muscles. Physiologically, the main function of the esophagus is to transport swallowed food from the hypopharynx to the stomach. Moreover, the normal function of the esophagus prevents the regurgitation of food from the upper esophagus into the hypopharynx and gastric contents from the stomach to the esophagus. The disruption of the normal function of the esophagus results in dysphagia and/or regurgitation. Functionally, the esophagus has three components: the upper esophageal sphincter (UES), the body, and the lower esophageal sphincter (LES) [1]. The components work together to keep the esophagus empty. Esophageal motility disorders result from sphincter dysfunction or abnormal peristalsis in the body of the esophagus or both. The diagnosis and treatment of esophageal dysmotility rest on the understanding of the functional anatomy of the UES, esophageal body, and the LES.

Upper Esophageal Sphincter

The UES is a 3–4-cm-long high-pressure zone that forms a barrier between the esophagus and the pharynx. It opens and closes intermittently to allow the passage of food or liquid. The UES closure muscles comprise the cervical esophagus, cricopharyngeus, and interior pharyngeal constrictor. The UES opening muscles consist of the superior and inferior hypoid muscles and superior pharyngeal muscles [1–3]. All UES muscles are striated and are innervated by the glossopharyngeal, branches of the vagus, ansa cervicalis, and sympathetic nerves from the cervical ganglion. The vagus nerve is the major motor nerve of the UES. Nerve cell bodies of the vagus efferent fibers are located in the nucleus ambiguus (medulla oblongata). Between swallows, the UES is tonically contracted to prevent reflux of

A. H. Elgazzar (✉) · S. A. Alenezi
Department of Nuclear Medicine, Faculty of Medicine, Kuwait University, Kuwait City, Kuwait

A. H. Elgazzar (ed.), *The Pathophysiologic Basis of Nuclear Medicine*,
https://doi.org/10.1007/978-3-030-96252-4_10

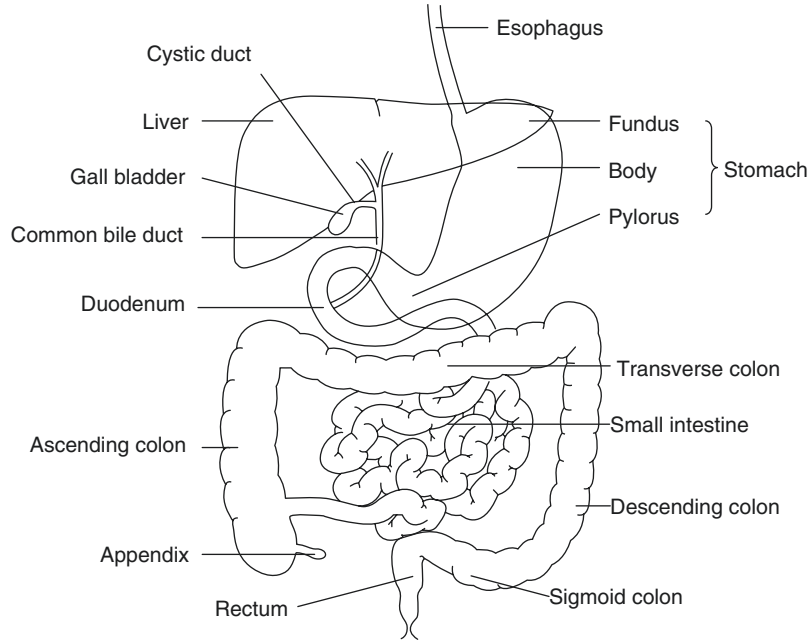

Fig. 10.1 Diagram of the relevant parts of the digestive system

esophageal contents and entry of air from the pharynx during inspiration. During swallowing, the cricopharyngeal and inferior pharyngeal constrictor muscles relax and the suprahyoid muscles contract.

Esophageal Body

The esophageal body extends from the UES to the LES and measures 18–25 cm. The esophageal wall consists of mucosa, submucosa, and the tunica muscularis and adventitia. The esophageal body is not surrounded by a tunica serosa. The esophageal mucosa is of the stratified squamous epithelium type, except for the distal 2 cm, where columnar epithelium of the gastric cardia type may be encountered. More proximal extension of gastric-type epithelium or the presence of intestinal-type columnar epithelium defines the pathological entity known as Barrett's esophagus (Fig. 10.2). Outside the epithelial lining is a thin layer of longitudinally oriented smooth muscle fibers, the muscularis mucosa. Below the muscularis mucosa is the submucosa, which consists of connective tissue. The muscularis propria is made up of an inner, circular, muscle layer and an outer, longitudinal, muscle layer. In the proximal 5% of the esophageal body, the muscularis propria is made up of striated muscle fibers. The distal 50–60% consists entirely of smooth muscle. The middle 35–40% is composed of a mixture of smooth and striated muscle fibers.

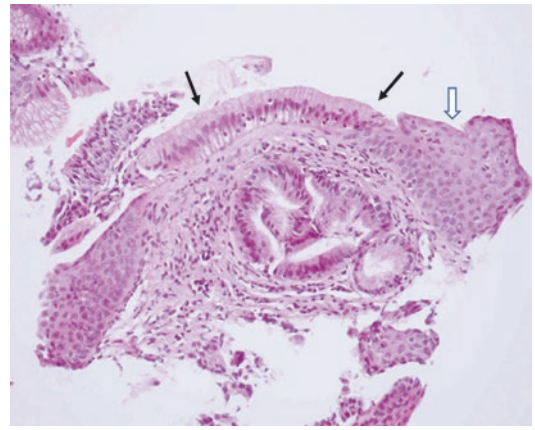

Fig. 10.2 Barrett's esophagus. *Solid arrows* point to columnar metaplasia. *Open arrow* points to the normal stratified squamous epithelium. (Courtesy of Prof. M. Elmonayeri)

Neuronal control of esophageal body motility is complex [4]. The esophageal wall receives extrinsic innervation via the vagus nerve. Striated muscle fibers are directly innervated

by postganglionic neurons originating in the nucleus ambiguus and terminating on the motor end plate. Smooth muscle fibers are controlled by preganglionic nerve fibers originating in the dorsal motor nucleus. These cholinergic nerve fibers terminate on the intrinsic neurons of the myenteric plexus located between the circular and longitudinal muscle layers. Within the myenteric plexus, two types of neurons have been identified. Excitatory neurons mediate contraction of both longitudinal and circular muscle layers via nicotinic cholinergic nerve receptors. Inhibitory neurons mediate the relaxation of mainly circular muscle fibers via noncholinergic, nonadrenergic neurotransmitters, most probably nitrous oxide and vasoactive intestinal peptide (VIP) [5]. Intrinsic sensory (afferent) neurons are within Meissner's plexus located in the submucosa. Sensory impulses are conveyed to the central nervous system via both vagal and thoracic sympathetic nerve fibers.

Swallowing initiates a progressive series of coordinated propulsive contractions throughout both the striated and the smooth muscle portions of the esophageal body. This form of esophageal motor activity is referred to as primary peristalsis. Intraluminal distention of the esophageal body results in a peristaltic wave at or proximal to the site of distention. This wave is termed secondary peristalsis and serves to clear the esophagus from contents that have not been cleared by primary peristalsis, or refluxed gastric contents. Primary and secondary peristaltic waves have similar amplitudes and travel at a velocity of 3–5 cm/s.

Deglutitory inhibition is a unique physiological phenomenon whereby repetitive swallowing inhibits all esophageal body activity while the LES is relaxed. A normal peristaltic contraction will follow the last swallow of such a series and clear the esophagus completely [6].

Lower Esophageal Sphincter

The LES is a high-pressure zone measuring 2–5 cm in length located between the esophageal body and the stomach. Ultrastructural studies show that this high-pressure zone consists of a specialized thickened region of the circular muscles layer of the distal esophagus, albeit the muscle fibers are not circular, rather they are organized as clasp and sling fibers [7]. At rest the sphincter is tonically contracted with a normal pressure ranging from 10 to 45 mmHg. The basal LES tones are determined by three factors: myogenic tone that is independent of neural influences, cholinergic excitatory tone, and nitrergic inhibitory tone. The LES relaxes after swallowing. Relaxation is mediated by the nitrergic inhibitory neurons. The LES may also relax without swallowing, a phenomenon referred to as transient lower esophageal sphincter relaxation (TLESR). These relaxations are believed to play a major role in the pathogenesis of gastroesophageal reflux disease.

A number of endogenous compounds affect the LES tone when administered in pharmacological doses. For instance, large doses of gastrin increase the tone of LES. Exogenous substances such as beta-adrenergic receptor agonists and calcium channel blockers may induce relaxation of the LES.

10.1.1.2 Esophageal Motor Disorders

Disorders of the UES and Cervical Esophagus

Motor disorders affecting the skeletal (proximal) part of the esophagus result from either neurological abnormalities affecting the extrinsic innervation of the proximal esophagus, or skeletal muscle or neuromuscular disorders. More specifically these include:

- Neurological diseases
  - Cerebrovascular accident
  - Parkinsonism
  - Amyotrophic lateral sclerosis
  - Cranial nerve palsy
- Skeletal muscular disorders
  - Dermatomyositis
  - Polymyositis
  - Muscular dystrophy
- Cricopharyngeus dysfunction
- Others
  - Myasthenia gravis
  - Amyloidosis

Table 10.1 Classification of primary esophageal body and LES disorders

Achalasia
Nonspecific esophageal dysmotility
Hypercontractile esophagus
Nutcracker esophagus
Hypertensive lower esophageal sphincter
Hypocontractile esophagus
Ineffective esophageal motility
Hypotensive lower esophageal sphincter
Discoordinated motility
Diffuse esophageal spasm

Because of the difficulty of transferring food bolus from the hypopharynx into the esophageal body across the UES, most patients experience choking or regurgitation of liquids and/or solids. Videofluoroscopy is the best diagnostic modality for diagnosing oropharyngeal dysphagia. Scintigraphy is of limited value.

Disorders of Esophageal Body and LES

Disorders of the distal esophageal body (smooth muscle) and LES can be broadly classified into achalasia and nonspecific esophageal dysmotility according to conventional stationary esophageal manometry (Table 10.1).

Achalasia

Achalasia is a primary motor disorder of the esophagus with absence of peristalsis and insufficient lower esophageal sphincter relaxation [8].

It is the best-studied motor disorder of the esophagus. It occurs at a rate of 1:100,000 and affects both sexes equally. Age of onset is usually 25–65 years. It results from the degeneration of the inhibitory myenteric neurons in the body and the LES region. This leads to a hypertensive LES which relaxes poorly and also causes aperistalsis in the body of the esophagus. Patients usually present with dysphagia to liquids and solids. Barium esophagogram may show dilatation of the esophagus and "bird beaking" of the distal esophagus. Esophageal manometry confirms the diagnosis of achalasia. Typically, there is incomplete relaxation of the LES and aperistalsis. LES hypertension is detected in 20–40% of patients [7]. Although these changes are highly suggestive of achalasia, they are by no means pathognomonic. Other conditions that might mimic achalasia include adenocarcinoma of the cardia, esophageal squamous cell carcinoma, Chagas' disease, and lung cancer.

Several other spastic disorders have been characterized in patients with noncardiac chest pain (Table 10.1). They all share a similar clinical presentation. Diffuse esophageal spasm (DES) is the most severe form. It is less common than achalasia. The mean age at presentation is 40 years. Patients frequently complain of intermittent nonprogressive dysphagia for solids and liquids. Hot or cold liquids and stress may precipitate chest pain. Some patients with DES progress to achalasia.

Nonspecific Esophageal Dysmotility

Nonspecific esophageal motility disorders are further classified into hypercontractile, hypocontractile, and discoordinated motility. Patients with hypercontractile esophagus usually present with chest pain and dysphagia. Nutcracker esophagus is a hypercontractile disorder characterized by increased lower esophageal peristalsis amplitude and duration. Hypertensive LES is associated with an LES resting pressure of >45 mmHg [9].

Patients with hypocontractile esophageal disorders complain of heartburn, regurgitation, and occasional dysphagia. Ineffective esophageal motility is characterized by low-amplitude peristalsis. Hypotensive LES is defined as an LES pressure below 10 mmHg. A number of systemic conditions are associated with esophageal hypocontractility including scleroderma, diabetes mellitus, and amyloidosis.

Diffuse esophageal spasm is a rare condition that presents with atypical chest pain that can radiate to the throat and back. Dysfunction in nitrous oxide synthesis or degradation is believed to be the cause of the spastic component. The manometric hallmark of diffuse esophageal spasm is simultaneous discoordinated contractions in more than 20% of swallow. The resultant tertiary contractions give the corkscrew appearance on barium swallow.

Gastroesophageal Reflux Disease

Gastroesophageal reflux disease (GERD) involves the reflux of chyme from the stomach to the esophagus. The LES may relax spontaneously and transiently 1–2 h after the patient has eaten, allowing gastric contents to regurgitate into the esophagus. The acid is normally neutralized and cleared by peristalsis from the esophagus within 3 min and the tone of the sphincter is stored. When the reflux does not cause symptoms, it is known as physiological but in some individuals it may cause a spectrum of inflammatory responses in the esophagus. GERD is the most prevalent condition originating from the gastrointestinal tract. It is estimated than 20% of the Western adult population suffers from heartburn more than three times a month [9]. It is particularly important in the pediatric age group. Also, GERD is common among pregnant women, especially during the third trimester.

The typical symptom of GERD is heartburn. However, a number of atypical symptoms are also linked to GERD, such as noncardiac chest pain, hoarseness, asthma, water brash, teeth erosion, and halitosis.

Most children affected with gastroesophageal reflux (GER) are between 6 months and 2 years old; they suffer from poor weight gain, vomiting, aspiration, choking, asthmatic episodes, stridor, apnea, and failure to thrive. A small amount of physiological reflux occurs in infants and resolves spontaneously by 8 months of age. The Tuttle acid reflux test is generally considered the reference standard but is technically demanding. The radionuclide method has a number of potential advantages. It is physiological, easily performed, well tolerated by the patient, and quantitative and involves a low radiation dose to the child.

Pathophysiology

GERD is a multifactorial process. Causes of GERD can be categorized as follows: (a) decreased pressure of LES, (b) transient increase in intra-abdominal pressure, and (c) short intra-abdominal esophageal segment. Mechanisms involved are summarized in Table 10.2. As mentioned earlier, transient LES relaxation appears to be the most common mechanism of GERD, especially in patients without endoscopic evidence of esophagitis [10]. In patients with moderate to severe esophagitis, LES incompetence plays a more important role in promoting reflux. The relation between a sliding hiatus hernia and GERD is controversial. Although most patients with severe GERD have hiatus hernia, most patients with hiatus hernia are asymptomatic. Recent data suggest that a large hiatus hernia may impair acid clearance [11, 12].

Table 10.2 Mechanisms of gastroesophageal reflux disease

Mechanism	Causes
Anti-reflux barrier	Transient LES relaxation
	Incompetent LES
	Sliding hiatus hernia
Esophageal clearance	Impaired peristalsis
	Decreased salivary output
Refluxate composition nature	Acid
	Pepsin
	Bile salts
	Pancreatic enzymes
Gastric factors	Delayed gastric emptying
	Acid hypersecretion
	Helicobacter pylori
Defective esophageal mucosal protection	Lack of HCO_3 secretion
	Lack of mucus secretion

Esophageal body peristalsis plays an important role in clearing refluxed acid in both the upright and the supine position. Defective primary or secondary peristalsis leads to incomplete clearance of acid. Furthermore, salivary HCO_3 usually neutralizes acid that remains in contact with the esophageal mucosa. Thus, impaired salivation may contribute to mucosal injury [13].

There is consensus about the fact that the potency of the contents of the refluxate, particularly acid/pepsin, is important in the pathogenesis of reflux esophagitis. Bile and pancreatic enzymes may be additional contributing factors.

Delayed gastric emptying is documented in 6–30% of patients with GERD. Theoretically,

gastric stasis can contribute to GERD. However, the relative importance of delayed gastric emptying is not well established [13]. *Helicobacter pylori* has recently been implicated as having a potential role in the pathogenesis of GERD [5]. *H. pylori* may secrete proinflammatory substances that can damage esophageal mucosa and sensitize vagal afferent nerves or lead to the reduction of LES tone. In contrast, there are data suggesting a protective role for *H. pylori* against GERD [6].

Finally, a significant proportion of patients with proven esophagitis do not have increased exposure to acid/pepsin. These patients probably have disruption of mucosal defense mechanisms such as the mucus layer, intercellular junctional complexes, intracellular mechanisms of handling acid, and blood flow to the esophagus [14].

10.1.2 The Stomach

10.1.2.1 Anatomic and Physiological Considerations

Anatomic Features

The stomach is a storage sac located between the esophagus and duodenum (Fig. 10.1). The proximal stomach consists of the cardia, fundus, and body. The antrum forms the distal stomach and is separated from the duodenum by the pyloric ring. The wall structure of the stomach is similar to that of the rest of the gastrointestinal tract, i.e., it consists of the mucosa, submucosa, muscularis propria, and serosa. However, unlike other parts of the gastrointestinal tract, the muscularis consists of three layers—circular, longitudinal, and oblique. This facilitates distension of the stomach and storage of food. The muscle layer in the antrum is modified to aid the mixing of food. The pyloric ring regulates the emptying of the stomach.

Overall Functions

Besides storage, the stomach has a number of exocrine, paracrine, and endocrine functions. The exocrine secretions consist of HCI and pepsin produced by the mucosal parietal cells and chief cells, respectively. These cells are located in the fundus and body of the stomach. Most cells within the lamina propria and submucosa are responsible for the main paracrine function, namely, the release of histamine, which in turn stimulates the parietal cells to secrete acid. The antrum secretes the hormone gastrin which enhances gastric emptying and acid secretion.

The intrinsic factor (IF) is a glycoprotein secreted by parietal cells. It binds to Vitamin B-12. The IF-B12 complex in turn binds to specific receptors on the terminal ileal epithelium. Without IF, B12 cannot be absorbed and pernicious anemia develops. Usually failure to secrete IF results from gastric atrophy which causes the destruction of parietal cells.

Gastric Motor Physiology

The motor activity of the stomach serves two main functions: (a) to act as a reservoir for ingested meal and ensure timed delivery of food particles to the duodenum at a rate compatible with optimal digestion and (b) to disperse solids into small particles and to mix them with gastric juice. The functions are accomplished by the coordinated activity of three functionally distinct parts of the stomach: (a) the proximal stomach, including the fundus and proximal body; (b) the distal stomach, including distal body and antrum; and (c) the pylorus, as part of the pyloroduodenal unit.

The proximal stomach has three muscle layers, longitudinal, circular, and oblique. No myoelectrical activity is recorded from the fundus during fasting except for the interdigestive migratory motor complexes (see below). In the fed state, the fundus exhibits two forms of motor activity: receptive relaxation and accommodation. Receptive relaxation refers to the reduction in proximal stomach tone initiated by swallowing or pharyngeal stimulation. Accommodation is reflex relaxation of the proximal stomach in response to gastric distention. It is not induced by swallowing or pharyngeal stimulation. Truncal vagotomy abolishes both receptive relaxation and accommodation, suggesting that they are mediated by the vagus nerve. Some gastrointestinal peptides such as cholecystokinin, secretin, VIP, and gas-

trin induce proximal stomach relaxation, whereas motilin increases fundic pressure [15, 16].

The distal stomach is comprised of two muscle layers: the longitudinal and circular. Slow waves or slow pacer potentials originate in the pacemaker region, located on the greater curvature of the stomach near the junction of the proximal and distal stomach. Slow waves pace the normal 3 min^{-1} corpus-antral peristalsis, which mixes solid and liquid food with gastric juice and triturates larger particles. The distal gastric motor activity is regulated by cholinergic and noncholinergic, vagal efferent nerve fibers. Cholinergic pathways stimulate antral contraction whereas noncholinergic vagal nerve stimulation inhibits antral activity through VIP and possibly nitrous oxide release from inhibitory neurons within the myenteric plexus.

The pyloric sphincter functions, in coordination with the duodenum, as a sieve allowing particles l mm or smaller to pass into the duodenum in 2–4-mL aliquots with each gastric peristalsis [17]. Emptying of inert liquids such as 0.9% saline follows first-order kinetics; i.e., the volume of liquid emptied into the duodenum in a given time is a constant fraction of the volume that remains in the stomach (Fig. 10.3) [18]. Emptying of digestible solid particles is characterized by a lag phase and a linear phase (Fig. 10.4) [19]. However, the caloric density, viscosity, osmolarity, and volume of any specific meal will influence gastric emptying rates. Fibrous material in the stomach is emptied in the interdigestive state by migrating myoelectrical-contractile complexes comprising 3–10 min of strong lumen-obliterating antral contractions [8].

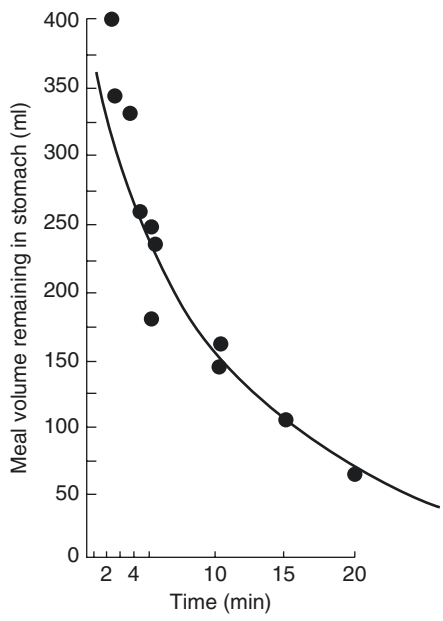

Fig. 10.3 Gastric emptying of 0.9% normal saline follows first-order kinetics. (From [18])

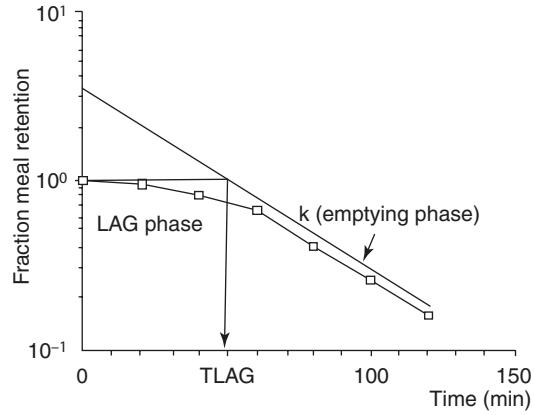

Fig. 10.4 Emptying of digestible solid particles lag phase and a linear phase. The *curve* represents modified power exponential function. (From Siegel et al. [19])

10.1.2.2 Disorders of Gastric Emptying

Conditions that cause abnormal gastric emptying can be divided into two groups: disorders associated with delayed emptying and disorders associated with dumping (Table 10.3). Diabetes is one of the most common causes of delayed gastric emptying in clinical practice. Most afflicted patients have had type I diabetes for more than 10 years, complicated by autonomic and peripheral neuropathy. Delayed emptying of both solids and liquids is attributed to the dysfunction of the proximal and distal stomach, as well as to increase pyloric resistance [20, 21].

Idiopathic gastroparesis is also encountered frequently in patients with bloating, early satiety, and nausea. The exact cause is unclear but it may be related to post-viral gastroenteritis [5]. Delayed gastric emptying is a known and frequent complication of gastric surgery. For instance, vagotomy delays emptying of solids but

Table 10.3 Causes of gastric dysmotility

Condition	Causes
	Mechanical obstruction
	Gastric outlet obstruction (e.g., tumor, peptic ulcer)
	Small intestinal obstruction
	Decreased gastric motility
	Postsurgical gastroparesis (vagotomy Roux-en-Y, fundoplication, etc.)
	Endocrine disorders (DM, hypothyroidism, Addison's disease, hyper- or hypoparathyroidism)
	Drugs (narcotics, anticholinergics, calcium channel blockers)
	Connective tissue diseases (e.g., scleroderma, SLE)
	Muscular disorders (myotonic dystrophy, dermatomyositis)
	Paraneoplastic
	Post-viral
	Neurological disorders (migraine, CVA, Parkinson, dysautonomia)
	Intestinal pseudo-obstruction
	Idiopathic gastroparesis
	Others (anorexia nervosa, uremia, ischemic gastroparesis, pregnancy)
Rapid gastric emptying (dumping)	Duodenal ulcer disease (including ZE syndrome)
	Vagotomy
	Antrectomy
	Idiopathic

promotes liquid emptying. Similarly, antrectomy can cause rapid emptying of undigested solids and liquids due to the loss of mixing function and loss of pyloric resistance. Symptoms of delayed gastric emptying include early satiety, nausea, vomiting, postprandial abdominal bloating, distention, and pain. The symptoms of gastroparesis are nonspecific and cannot be easily differentiated from those of mechanical obstruction. Other diseases such as gastritis, irritable bowel syndrome, and nonnuclear dyspepsia may cause similar complaints.

10.1.2.3 Duodenogastric Reflux

Duodenogastric reflux (DGR) has been suggested to occur in normal individuals in both fasting and postprandial periods [22, 23], although others have suggested that it does not occur physiologically [24]. The amount of refluxed bile in normal subjects is reported to be small and clears rapidly from the stomach [25]. This feature helps separate normal from abnormal subjects in the fasting state.

Table 10.4 Causes of duodenogastric reflux

Causes	
Duodenal ulcer	Gastritis
Acute cholecystitis	Chronic cholecystitis
Enteritis	Pancreatitis
Gastric carcinoma	Surgery
Post-traumatic stress ulceration	Gastric surgery/ vagotomy
Duodenal hematoma	Cholecystectomy
Erosive esophagitis	Gallstone dyspepsia
Physiological/unknown cause	

Pathologically, DGR has been associated with many conditions (Table 10.4), including postgastrectomy/vagotomy, gastric and duodenal ulcers, cholecystitis, and gastritis [26]. In some of these conditions, such as duodenal ulcer, duodenal hematoma, and cholecystitis, duodenal irritation is probably the underlying mechanism. Other causes may irritate the duodenal mucosa by the adjacent pancreatic inflammation. Slavin also proposed that the deficiency of pancreatic secretions can explain DGR since volume, the alkaline pH, and the physiological components of the pancreatic secretions may be important for maintaining the outward flow of gastric contents [27].

10.1.3 The Intestines

10.1.3.1 The Small Intestine

Anatomic and Histologic Considerations

The small intestine is a hollow muscular cylinder that measures 5–6 m in length. It consists of three regions: duodenum, jejunum, and ileum. The intestinal wall is made up of four layers: the mucosa, the submucosa, the muscularis, and the serosa. The small intestinal mucosa is fashioned into villi and crypts to increase the surface area and enhance the absorptive function of the small bowel. The mucosa of the villi consists of absorp-

tive columnar epithelial cells (enterocytes) and mucus-secreting goblet cells. Within the crypts the most common cell type is the undifferentiated crypt cell which secretes chloride and water into the lumen. The crypt also contains pluripotent stem cells. Furthermore, the small bowel harbors the enteroendocrine cells which secrete a number of hormones including secretin, cholecystokinin, gastrin, gastric inhibitory peptide, motilin, glucagon, vasoactive intestinal peptide, somatostatin, and others. These hormones play an important role in gastrointestinal motility. Finally, the intestinal mucosa and lamina propria contain the largest lymphoid organ in man: the gut-associated lymphoid tissue (GALT) [28]. The latter consists of:

- M-cells
- Intraepithelial lymphocytes (IELs)
- Peyer's patches (lymphoid follicles)
- Lamina propria T and B lymphocytes
- Dendritic cells
- Macrophages

The M-cells are specialized epithelial cells overlying lymphoid follicles. Because they are not covered by mucus, antigens can bind to M-cells which take in the antigens, process them, and present them to lymphocytes and macrophages. However, the binding to antigens is highly selective. For instance, only pathogenic bacteria can attach to M-cells, whereas commensals cannot. IELs are specialized T lymphocytes situated between the basolateral membranes of mucosal epithelial cells and the lamina propria. They appear to have an important immunologic function as they express CD45RO a marker of memory cells. Dendritic cells are derived from the bone marrow and reside beneath M-cells. They capture antigens, carry them across the mucosal barrier, and present them to T lymphocytes.

The submucosa consists of connective tissue, lymphocytes, plasma cells, macrophages, mast cells, fibroblasts, eosinophils, nerve fibers, ganglion cells (Meissner's plexus), blood vessels, and lymphatics.

The muscularis is made of inner circular and an outer longitudinal muscle fibers. Between these two layers of smooth muscle lies the myenteric plexus, the network of intramural neurons that is essential for all coordinated and organized motor activity. The extrinsic (autonomic) nerves affect the gastrointestinal motility by means of these enteric nerves.

Functional Considerations

Most of the digestion and absorption of nutrients takes place in the small bowel. Moreover, the motor function of the small bowel ensures the mixing of chyme with digestive enzymes and the propulsion of chyme toward the colon. Also, the small bowel plays an important role as a first line of defense against pathogenic microorganisms and harmful food antigens.

In most instances, nutrients cannot be absorbed by the cells that line the gastrointestinal tract in the forms in which they are ingested. *Digestion* is the breakdown of ingested molecules into small ones via reactions catalyzed by enzymes produced by the gastrointestinal organs.

The small intestinal epithelium participates in digestion by secreting oligosaccharidases such as lactase, enterokinase, and peptidases.

Absorption refers to the process of transporting molecules through the epithelial lining of the gastrointestinal tract into the blood or lymph.

Water, electrolytes, monosaccharides, amino acids, small peptides, glycerol, fatty acid, vitamins, and minerals are all absorbed via a number of mechanisms including passive diffusion, facilitated diffusion, active transport, and endocytosis. Although absorption takes place along the entire length of the small intestine, the mucosa in certain regions selectively absorbs specific molecules. For instance, iron is primarily absorbed in the duodenum and proximal jejunum, whereas the terminal ileal mucosa has specific receptors for binding and absorbing vitamin B-12 and bile salts [29].

Under physiological conditions the small bowel exhibits two main motor patterns. During the fed state, and as a result of contact with nutrients, a number of neuronal and hormonal signals are elicited including afferent vagal stimulation and the release of cholecystokinin which mediate *segmentation* and *peristalsis. Segmentation* is the

most frequent movement in the small bowel and is characterized by closely spaced contractions of the circular muscle layer. These contractions divide the small intestine into short neighboring segments. Segmentation helps mix chyme with digestive enzymes. *Peristalsis*, on the other hand, is the progressive contraction of successive sections of circular smooth muscle resulting in the propulsion of chyme toward the colon. Furthermore, during the fed state, the small intestine especially the duodenum exerts negative feedback control on gastric emptying via neural and hormonal mechanisms (secretin, cholecystokinin, and gastric inhibitory peptide).

During the fasting phase, the small intestine exhibits a different pattern of motility characterized by bursts of intense electrical and contractile activity separated by periods of lack of activity. This pattern is called *migrating myoelectric complex* (MMC). In humans MMC occurs every 90–120 min, originates from the stomach, and sweeps through the small bowel till the terminal ileum. The function of MMC is to clear undigested particles and propagate them to the colon [30].

Small Intestinal Dysmotility

Motor disorders of the small bowel can lead to symptoms and signs of "functional" as opposed to mechanical small bowel obstruction. Patients frequently complain of abdominal distension, bloating, and abdominal pain, and when small intestinal dysmotility is associated with gastroparesis, nausea, and vomiting may be prominent. On physical examination, the abdomen is usually distended and bowel sounds are diminished. Features of bacterial overgrowth may be observed.

Small intestinal dysmotility may be acute or chronic. Acute dysmotility is termed adynamic ileus and is commonly seen following abdominal surgery, severe septicemia, or electrolyte disturbances such as hypokalemia. Chronic dysmotility is termed pseudo-obstruction (Table 10.5).

Most cases of pseudo-obstruction are secondary to endocrine and metabolic causes, such as diabetes mellitus and hypothyroidism; neurological disorders, such as Chagas' disease and Parkinsonism; or drug induced (e.g., phenothiazines, narcotics). Primary pseudo-obstruction is rare. Few cases are due to familial visceral neuropathies and myopathies. However, the majority of cases of primary pseudo-obstruction are sporadic.

Table 10.5 Motor disorders of the small intestine

Cause	Mechanism	Outcome
Acute illness	Impaired smooth muscle contraction	Adynamic ileus
	Altered neurotransmission	
Pregnancy	Decreased smooth muscle contraction (progesterone)	Slow transit
Diabetes mellitus	Autonomic dysfunction	Slow or rapid transit
Scleroderma	Smooth muscle fibrosis	Weak contractions
	Neuronal loss in gut wall	Slow transit
Primary pseudo-obstruction	Neuronal loss, plexus degeneration	Weak contractions
		Abnormal MMC
		Slow transit
Myopathies	Myocyte and mitochondrial abnormalities	Weak segmentation and peristalsis

Malabsorption

Malabsorption syndrome is an alteration in the ability of the GI tract, usually the small intestine to absorb one or more nutrients adequately from diet into the bloodstream. These may include fats, proteins, carbohydrates, vitamins, or others. This may result from acquired or congenital defects. The syndrome may present with anemia (most commonly vitamin B-12, folate, and iron deficiency); diarrhea; steatorrhea (excessive amount of fat in the stool); abdominal distention edema; malnutrition and weight loss; muscle cramping due to decreased vitamin D, calcium, and potassium levels; muscle wasting and atrophy due to decreased protein absorption and metabolism; and perianal skin burning, itching, or soreness due to frequent loose stools. Protein depletion can lead to impaired bone formation and osteoporosis, and calcium deficiency leads to weak-

ening and demineralization of the bone, causing osteomalacia.

Common causes of malabsorption syndrome include inflammatory bowel disease, tropical sprue, Whipple's disease, lactase deficiency, and parasitic diseases; other causes are past intestinal surgeries, bacterial overgrowth, gluten enteropathy (nontropical sprue), AIDS, radiation to the abdomen, diabetes, lymphoma, or motility disorders. In addition to small bowel disease, malabsorption can occur in those who have had portions of their stomachs removed surgically. The pancreas produces enzymes that help digest food, so if a condition exists where enzymes are not being produced, it can result in maldigestion or malabsorption. This could include chronic alcoholic pancreatitis, trauma, cystic fibrosis, tumors, or postsurgical states. The diagnosis of malabsorption syndrome and identification of the underlying cause can require extensive diagnostic testing. Generally, an endoscopy is performed under mild sedation, at which time a biopsy can be obtained to be analyzed under the microscope. In addition, various blood tests are helpful to determine if a malnourished condition exists. These tests may include serum cholesterol; serum sodium, potassium, and chloride; serum calcium; serum protein and albumin; serum vitamin A and carotene; D-xylose test; Schilling test; and others. Stool collections and cultures are useful as well as certain breath and hormone tests. Scintigraphic imaging and quantitation is also used in some forms.

Protein-Losing Enteropathy (PLE)

PLE is a condition in which excess protein loss into the gastrointestinal lumen is severe enough to produce hypoproteinemia. It occurs with many of the previously listed conditions causing malabsorption. Furthermore, diseases such as constrictive pericarditis, congestive heart failure, intestinal lymphangiectasia, nephrotic syndrome, and systemic lupus erythematosus may also cause protein loss from the gastrointestinal tract without any observable mucosal lesions in the bowel. The mechanism of the loss of plasma protein into the gastrointestinal tract in these diseases is not yet fully understood [5].

The previously reported materials used for the detection of protein loss have many limitations, such as rapid reabsorption of the radiolabel, unstable protein binding both in vivo and in vitro, and limited availability. The need for measurement of fecal radioactivity over 3–4 days has also been a drawback with some of the methods in which these materials are used. Imaging with other radioisotope-labeled materials such as ^{111}In chloride and ^{111}In transferrin has been reported [6].

^{99m}Tc–labeled HSA has been used to image protein-losing enteropathy since its introduction in 1986 [31]. Serial imaging for up to 24 h is useful in detecting protein loss from the gut, possibly because of the intermittent nature of this protein loss. Tc-99m HSA is also useful in viewing the entire gastrointestinal tract at one time to permit detection of multiple potential sites of protein loss. A new scintigraphic method using ^{99m}Tc-labeled dextran was first described in 1995 by Bhatnagar et al. [32]. This method demonstrates significant intestinal radiotracer accumulation at 3–4 h postinjection in 22 patients, giving information about localization and extension of the disease. In 4 of 12 healthy subjects, there was minimal abdominal accumulation occurring late in the study [33]. These polysaccharides of molecular weight between 60,000 and 90,000 are being used as a plasma expander and, in radioactive tagged form, for lymphoscintigraphy and blood pool agents. Add brief details on the procedure.

Vitamin B-12 Malabsorption

Vitamin B-12 deficiency due to pure dietary inadequacy of this vitamin is very rare and occurs mainly in strict vegetarians. More often gastrointestinal disorders, atrophic gastritis, pernicious anemia, congenital lack or abnormality of gastric IF, or total or partial gastrectomy cause malabsorption and consequent deficiency of this vitamin. Diseases involving the distal ileum such as Crohn's disease, intestinal stagnant loop syndrome, and rarely congenital selective ileal malabsorption with proteinuria (Imerslund-Grasbeck syndrome) may also result in malabsorption of vitamin B-12.

10.1.3.2 The Colon

Anatomic and Functional Considerations

The colon is a tubular structure that extends from the ileocecal valve to the anal verge (Fig. 10.1). It measures approximately 1–5 m and consists of the cecum; ascending, transverse, descending, and sigmoid colon; and rectum. Like the small intestine, the colonic wall consists of the mucosal submucosa, muscularis, and serosa. However, the colonic mucosa lacks villi. Also, unlike the small intestine, the external longitudinal muscular layer is gathered into three flat longitudinal ribbons of smooth muscle called teniae coli. The continuous contractions of the teniae coli cause sacculations of the wall termed haustrations.

The primary function of the colon is to absorb water and electrolytes from its contents and to pack feces until defecation. The motility of the colon is geared toward this function. As stated above, throughout the colon, localized segmental contractions take place and result in mixing chyme. In the cecum and ascending colon, retrograde (antipropulsive) contractions also occur. The net effect of these motility patterns is to slow transit and facilitate the absorption of water and electrolytes. Periodically, massive contractions start in the proximal colon to propel fecal material toward the sigmoid colon where it is stored. One to three times a day, mass contractions sweep the stool toward the rectum. Distension of the rectum by feces initiates the defecation reflex which is mediated by the pelvic nerves and integrated at the level of the sacral spinal cord.

Pathophysiology of Relevant Colon Diseases

Inflammatory Bowel Disease

Inflammatory bowel disease (IBD) refers to two disorders: Crohn's disease (CD) and ulcerative colitis (UC). Both conditions are characterized by chronic relapsing intestinal inflammation. UC affects the colon only, and the inflammation is limited to the mucosa + submucosa in most cases. CD can affect the entire gastrointestinal tract from mouth to anus. The inflammation in CD is granulomatous and transmural. Besides inflammation of the gut, IBD is associated with a number of systemic manifestations including anterior uveitis, axial and peripheral arthropathy, primary sclerosing cholangitis, erythema nodosum, and pyoderma gangrenosum.

The etiology of IBD is not totally settled. Proposed factors include environmental, infectious, genetic, autoimmune, and host factors. After first described by Burrill B. Crohn, Crohn's disease was considered an infectious disease. Crohn's disease and ulcerative colitis were thought to be autoimmune diseases, and currently, microbial factors, as well as other direct environmental influences, have been proposed [34].

A lot of research has been performed to discover potential genes linked to IBD. One of the early linkages discovered was on chromosome 16 (IBD1 gene), which led to the identification of the NOD2 gene (now called CARD15) as the first gene clearly associated with IBD (as a susceptibility gene for Crohn's disease). Studies have also provided strong support for IBD susceptibility genes on chromosomes 5 (5q31) and 6 (6p21 and 19p). None of these mechanisms has been implicated as the primary cause, but they are postulated as potential causes.

The pathophysiology of IBD is still incompletely understood and is under active investigation, but the common end pathway is inflammation of the mucosal lining of the intestinal tract, causing ulceration, edema, bleeding, and fluid and electrolyte loss. The inflammation of the intestinal mucosa includes both acute inflammation with neutrophilic infiltration and chronic with mononuclear cell infiltration, predominantly lymphocytes [35].

Many of the immunologic and molecular mechanisms that mediate inflammation have been elucidated in recent years. Three groups of factors seem to play a role: genetic predisposition, mucosal immune dysregulation, and environmental agents (Table 10.6). The importance of genetic factors in the pathogenesis of IBD is evidenced by familial aggregation of CD and UC cases. Approximately 10–20% of patients with IBD have an affected relative. Concordance among monozygotic twins especially in CD also

Table 10.6 Pathogenesis of inflammatory bowel disease

Genetic predisposition	Environmental factors	Immunologic dysregulation
Family clustering	Infectious agents	Proinflammatory mediators
NOD_2 gene variants	Dietary antigens	Anti-inflammatory mediators
Gene loci on Chr. 2,3,12	Intestinal commensals	

supports the notion of genetic predisposition. . One of the early linkages discovered was on chromosome 16 (IBD1 gene), which led to the identification of the NOD2 gene (now called CARD15) as the first gene clearly associated with IBD (as a susceptibility gene for Crohn's disease). Studies have also provided strong support for IBD susceptibility genes on chromosomes 5 (5q31) and 6 (6p21 and 19p). None of these mechanisms has been implicated as the primary cause, but they are postulated as potential causes [35].

This gene mediates the innate immune response to microbial pathogens. Similarly a number of other susceptibility genes have been identified in relation to CD and UC.

In genetically predisposed individuals, environmental factors can precipitate the disease by inducing an abroad immunologic response characterized by an imbalance between anti-inflammatory mediators.

The mucosal immune system plays a central role in the pathogenesis of IBD. A defective mucosal barrier may allow the uptake of microbial and ingested antigens. Under physiological conditions, GALT selectively removes harmful antigens. This process is mediated by the dendritic cells which are the main antigen presenting cells in GALT. The interaction of dendritic cells with T lymphocytes results in immunosuppression (tolerance) toward commensals and beneficial antigens. In IBD patients, tolerance is lost due to a number of immunoregulatory abnormalities including an imbalance between proinflammatory and anti-inflammatory mediators in favor of the former. For instance, the levels of IL-1, IL-6, IL-18, tumor necrosis factor alpha (TNF alpha), and interferon gamma are raised in patients with CD (TH1 response), whereas the levels of IL-1ra, TGF beta, 4-Y, IL-10 (TH2 response), and prostaglandin E_2 are reduced. The role of TNF alpha is of particular therapeutic significance. Monoclonal antibodies to TNE alpha have been shown to be effective in treating CD.

The rising incidence of IBD especially CD in recent years is highly suggestive of the role of environmental factors in modulating the immune response. Furthermore, a number of studies have shown a positive correlation between smoking and CD and a negative association with UC. Other factors that have been implicated as environmental precipitants of IBD include the use of NSAIDS, antibiotics, infective diarrheal illnesses, and increased intake of refined sugar. In the genetically susceptible rodent model of IBD, colitis does not develop when the gut is sterile, and IBD is precipitated by the introduction of bacteria into the diet [36, 37].

The primary pathophysiologic change of UC is inflammation of the mucosa and the submucosa and formation of crypt abscesses and mucosal ulceration with skip areas. The small intestine is essentially not involved. UC primarily involves the mucosa and the submucosa, with formation of crypt abscesses and mucosal ulceration.

CD consists of segmental involvement by a nonspecific granulomatous inflammatory process involving all layers of bowel with skip areas. The disease involves the small bowel in addition to the colon, and rectal sparing is typical. Less commonly it involves the mouth, tongue, esophagus, stomach, and duodenum.

Acute Appendicitis

The appendix is a diverticulum of an average of 10 cm in adults arising from the posteromedial wall of the cecum with its fixed to the cecum, while the remainder of the appendix is free. This fact accounts for its variable positions (retrocecal, subcecal, retroileal, pre-ileal, or pelvic) and behind much of the diversity in clinical presentations among patients with acute appendicitis [38].

The pathophysiology of appendicitis begins with obstruction of the narrow appendiceal lumen by causes, including fecaliths, lymphoid hyperplasia (related to viral illnesses such as upper respiratory infections, mononucleosis, or gastroenteritis), gastrointestinal parasites, foreign bodies, and Crohn's disease. Continued secretion of mucus results in elevated intraluminal pressure, leading to tissue ischemia, overgrowth of bacteria, transmural inflammation, appendiceal infarction, and possible perforation. Inflammation may subsequently extend into the parietal peritoneum and adjacent structures causing abdominal abscesses.

Acute appendicitis is the most common reason for emergency abdominal surgery and must be differentiated from other causes of abdominal pain. The overall diagnostic accuracy achieved by medical history, physical examination, and laboratory tests has been approximately 80% as the presentation may be atypical. In atypical cases, ultrasonography and computed tomography (CT) may help lower the rate of unnecessary surgeries. The accuracy rates for ultrasonography range from 71 to 97% and the modality is highly operator dependent and difficult in patients with a large body habitus. The accuracy rate of CT scanning is between 93 and 98%. However, there is controversy regarding the use of contrast media and which CT technique is best. Additionally, radiation exposure, cost, and possible complications from contrast media are disadvantages [4].

Colorectal Cancer

The incidence of colorectal cancer is highest in developed countries, such as the USA and Japan, and lowest in developing countries in Africa and Asia. It is the third most common type of cancer in both men and women in the USA. Pathologically most (over 95%) of colorectal cancers are adenocarcinomas. Surgery, chemotherapy, radiation therapy, and immunotherapy are the lines of treatment. Nuclear medicine has an important role in the follow-up to detect recurrence (see Chap. 12). FDG-PET has an important role as it is more sensitive than computed tomography for the detection of metastatic or recurrent colorectal cancer (Fig. 10.5) and may improve clinical management in more than 25% of cases [39]. It is of particular importance to differentiate post-therapy fibrosis and inflammation from viable tumor in the presacral region.

Gastrointestinal Bleeding

The localization of the specific bleeding site in patients presenting with acute GI bleeding remains a serious clinical problem. Scintigraphy has emerged as the imaging modality of first choice for localizing bleeding sites in the lower gastrointestinal tract.

Acute gastrointestinal bleeding (GIB) can be divided into bleeding in the upper (proximal to the ligament of Treitz) or lower tract. If acute upper GIB is a possibility, lavage with a nasogastric tube should identify acute or subacute bleeding. Endoscopy will localize 80–97% cases of acute upper bleeding; of these, 75% will resolve spontaneously or with conservative medical therapy and 10% will require surgery. Because of the length and tortuosity of the colon and contamination of fecal matter and blood, endoscopy is not that successful in lower GIB cases. Peptic ulcers are the most common cause of upper GIB; other causes include gastritis, esophageal varices, Mallory Weiss tear, esophagitis with or without hiatal hernia, and carcinoma [40]. The three leading causes of lower GIB are diverticular disease, angiodysplasia, and colorectal cancer. Other causes include inflammatory bowel disease, ischemic colitis, infectious colitis (inflammation of the colon due to an **infective** cause, including bacterial, viral, fungal, or parasitic), and anorectal disease (Table 10.7). This bleeding usually resolves spontaneously in 80% of cases and rebleeds in 25%. Angiodysplasias account for 20% of significant lower GIB and tend to rebleed.

Meckel's diverticulum is a vestige of the omphalomesenteric duct that is present in about 2% of the population with two thirds younger than 2 years. It is an outpouch usually found on the antimesenteric border of the ileum, 50–80 cm proximal to the ileocecal valve. Ectopic gastric mucosa is present in about 30% of cases. Nearly all diverticula responsible for

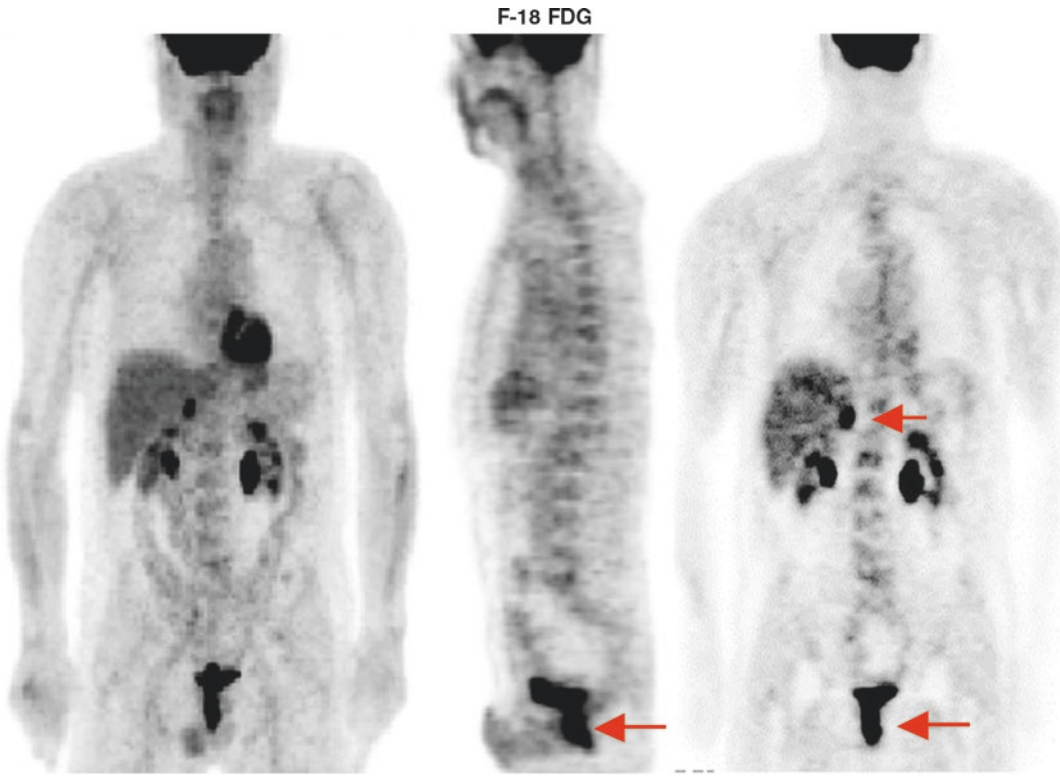

Fig. 10.5 F-18 FDG study of a patient who had rising CEA 5 years after resection of rectal adenocarcinoma. MRI and CT were inconclusive. Five biopsies were obtained from the rectum and were negative. The FDG study shows clearly viable local tumor recurrence and metastases in the right adrenal gland (*arrows*)

Table 10.7 Causes of GI bleeding[a]

Upper gastrointestinal bleeding
Esophageal, gastric, and duodenal ulcers
Mallory Weiss tears
Esophagitis, gastritis, duodenitis, pancreatitis
Neoplasms
Vascular malformations
Varices
Lower gastrointestinal bleeding
Post-polypectomy bleeding
Ischemic colitis
Colorectal polyps/neoplasms
Inflammatory bowel disease
Infectious colitis
Meckel's diverticulum
Neoplasia
NSAID ulcers
Dieulafoy's lesion
Anorectal conditions **as** rectal varices **and radiation** proctitis

[a] [41–44]

rectal bleeding contain ectopic gastric mucosa. Bleeding, which is usually massive and painless, may result from ileal mucosal ulceration due to acid secretion.

Scintigraphy and computed tomography angiography (CTA) are the most important noninvasive imaging tests that can identify presence of and help locate the site of bleeding [41]. Patients with lower GIB should be stabilized and supported while diagnostic studies are performed. More commonly, a nuclear medicine study is performed first to localize the bleeding because it is more sensitive for slow or intermittent bleeding, which is a common occurrence. If the scan is positive, arteriography can be employed to deliver vasopressin or embolic agents selectively into the bleeding artery. The most recent ACR appropriateness criteria guidelines for stable patients with lower GI bleeds give equal weight to Tc-99m RBC scan and CTA [45].

10.1.4 Salivary Gland

10.1.4.1 Anatomic and Physiologic Considerations

The major salivary glands include the parotid and the submandibular gland. The parotid gland is located behind the mandible and consists of a superficial and a deep part. The main parotid duct (Stensen's duct) runs anteriorly to pierce the buccinator muscle, opening on a papilla on the buccal mucosa opposite the second upper molar tooth. The submandibular gland is smaller than the parotid and lies in the submaxillary triangle just below the mandible. The main duct (Wharton's duct) passes forward and medially to open on a papilla lateral to the frenulum at the base of the tongue. The sublingual glands are situated anteriorly in the floor of the mouth above the mylohyoid muscle, and each gland opens into the oral cavity through several small ducts.

Salivary glands secrete saliva which is a clear, viscous, and watery fluid that contains two major types of protein secretions, a serous secretion containing the digestive enzyme ptyalin and a mucus secretion containing the lubricating aid mucin. Saliva also contains large amounts of potassium and bicarbonate ions and to a lesser extent sodium and chloride ions as well as several antimicrobial constituents, including thiocyanate, lysozyme, immunoglobulins, lactoferrin, and transferrin. Accordingly saliva provides many several functions including antimicrobial activity, mechanical cleansing action, control of pH, removal of food debris from the oral cavity, lubrication of the oral cavity, remineralization, and maintaining the integrity of the oral mucosa.

10.1.4.2 Pathophysiology of Relevant Disorders

Nuclear medicine-relevant conditions affecting salivary glands are numerous. These include inflammatory, neoplastic, and mechanical disorders affecting the parenchyma and duct system. Xerostomia is defined as dry mouth resulting from reduced or absent saliva flow. It is not a disease but is a symptom of various medical conditions. Xerostomia may result from such conditions as mumps, Sjögren's syndrome, sarcoidosis, radiation-induced atrophy, and drug sensitivity.

Inflammation of salivary glands usually presents as diffuse enlargement of the glands, unilateral or bilateral. Bilateral enlargement is caused by inflammation (mumps, Sjögren's syndrome), granulomatous disease (sarcoidosis), or diffuse neoplastic involvement (leukemia and lymphoma). The vast majority of salivary neoplasms occur in the parotid gland. Over two thirds represent benign mixed or pleomorphic adenomas. Warthin's tumor is another benign tumor that can be bilateral. The more common malignant tumors include mucoepidermoid carcinoma, adenocarcinoma, and squamous cell carcinoma. Plain films are of limited use for evaluating these tumors. Sialography in conjunction with CT is the preferred technique [46, 47]. The CT sialogram demonstrates the location of the tumor within the gland and also defines any involvement of the deep structures of the neck.

The duct system of the parotid and the submandibular glands can be demonstrated by sialography, and the technique is particularly valuable in the diagnosis of diseases which affect the duct system such as calculus, stricture, and sialectasia.

10.1.5 Ascites

Ascites is the accumulation of excess fluid within the peritoneal cavity. It is most frequently encountered in patients with cirrhosis and other forms of severe liver disease, but a number of other disorders may lead to either transudative or exudative ascites. Serous effusion into the peritoneum occurs in cases of general edema of both the cardiac and renal type and is sometimes abundant; some fluid may accumulate also in severe anemias and wasting disease. The most severe ascites, however, results from portal obstruction, the most common cause being cirrhosis of the liver. Hepatic vein occlusion (Budd–Chiari syndrome) is also accompanied by gross ascites.

The pathogenesis of ascites is complex, and multiple factors have been postulated to

be involved. In cirrhosis the major vascular obstruction is post-sinusoidal, and the flow of lymph is considerably augmented. The lymphatic vessels, including the thoracic duct, are dilated but nevertheless appear inadequate to deal with the increased volume of lymph. Fluid oozes from the liver surface; this is called the weeping liver.

Another factor in the pathogenesis of ascites is hypoalbuminemia, since if this is combined experimentally with portal vein obstruction, ascites develops. It has been postulated that the major factor in the formation of ascites is retention of salt and water by the kidney, followed by an outflow of fluid into the peritoneal cavity. Another factor to consider in the pathogenesis of ascites is the increased capillary pressure in the splanchnic area secondary to portal hypertension. This leads to the formation of transudate.

Surgical management of ascites includes various shunt operations. Most are performed as therapy for esophageal bleeding. Which shunt operation is most effective in relieving ascites has not been established; in fact, ascites is reduced after any type of portosystemic shunt as a consequence of decreased portal flow and decreased intrahepatic congestion. Among the most commonly performed shunts, splenorenal and splenocaval shunts and their variants have proven effective in relieving ascites. Transjugular intrahepatic portosystemic shunt (TIPS) has been used to reduce portal hypertension in patients with bleeding esophageal varices. TIPS has been shown to relieve intractable ascites as well.

The peritoneovenous shunt is a pressure-activated shunt devised by LeVeen. One line of this shunt lies free in the peritoneal cavity, and the venous opening of the efferent inserts into the SVC near its entrance into the right atrium. Flow into the shunt is maintained if there is 3–5 cmH_2O pressure gradient between the valve and its venous end. Radionuclide studies using Tc99m-macroaggregated albumin (MAA) injected intraperitoneally are used to evaluate the patency of the shunts [48–50].

10.1.6 Gastrointestinal Scintigraphy

10.1.6.1 Radionuclide Esophageal Transit Time Study

This study has proven useful and sensitive in detecting esophageal disorders and its involvement in certain systemic disorders.

The patient should fast for 4–6 h. A dose of 250–500 μCi Tc-99m-SC in 10 mL of water is taken through a straw. The multiple-swallow technique is preferred over the single-swallow test because of the considerable intraindividual variations in esophageal emptying among normal subjects and patients. It is preferable to do the imaging with the subject in the supine position to eliminate the effect of gravity; images of 1 s each are acquired to characterize the esophageal transit. Delayed images at 10 min may be helpful in patients with significant stasis of radioactivity in the esophagus. A time-activity curve can be generated; the esophageal transit time is the time interval between the peak activity of the proximal esophageal curve and the peak activity of the distal esophageal curve.

The normal transit time is 15 s, with a distinct peak in each third of the esophagus. A slowing of bolus progression can be noted at the mid-esophagus because of compression by the tracheal bifurcation and aortic arch. Prolonged transit time might be found in several esophageal and systemic disorders such as achalasia, progressive systemic sclerosis, diffuse esophageal spasm, nonspecific motor disorders, nutcracker esophagus, Zenker's diverticulum (an outpouch above the UES that is acquired), esophageal tumors, and esophageal stricture.

10.1.6.2 Gastroesophageal Reflux Study

The patient should fast for 4 h. The dose is 0.5–1 mCi Tc-99m-SC in 300 mL of acidic orange juice. Imaging is performed with the subject in a supine position at a rate of 1 frame/10 s for 60 min. All frames should be reviewed with contrast enhancement. GER is seen as distinct spikes of activity into the esophagus (Fig. 10.6).

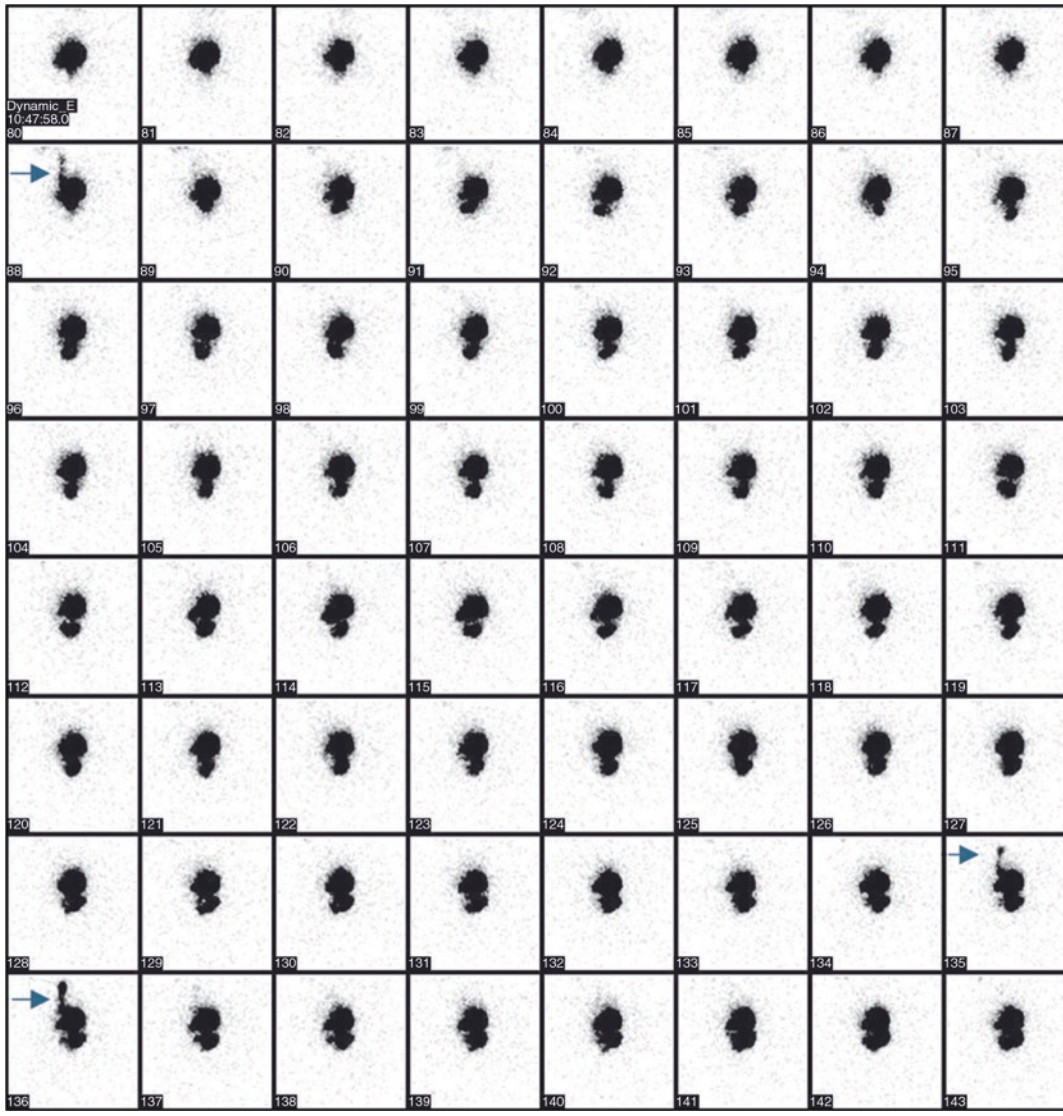

Fig. 10.6 A gastroesophageal reflux study obtained using ^{99m}Tc-sulfur colloid for a 2-year-old boy demonstrates reflux in three frames (*arrows*)

The episodes of reflux are graded as high or low level, by duration (less or more than 10 s), and by their temporal relationship to meal ingestion. The salivagram can often reveal aspiration when a GER study is negative.

This scintigraphic study has 89% correlation with the acid reflux test. The evidence of pulmonary aspiration is valuable in the pediatric age group, though it is seen in up to 25% of cases of aspiration with reflux.

10.1.6.3 Gastric Emptying Study

The patient should avoid smoking, since it affects emptying, and should fast overnight. The dose is 0.5–1.0 mCi Tc-99m-SC mixed with egg white or liver pâté as a solid meal. Dynamic images can be taken for 60 min or longer (Figs. 10.7 and 10.8), and if necessary, static delayed images are taken every 15 min until at least 50% of the stomach activity (content) has gone into the bowel. Normally, the stomach should empty 50% of the

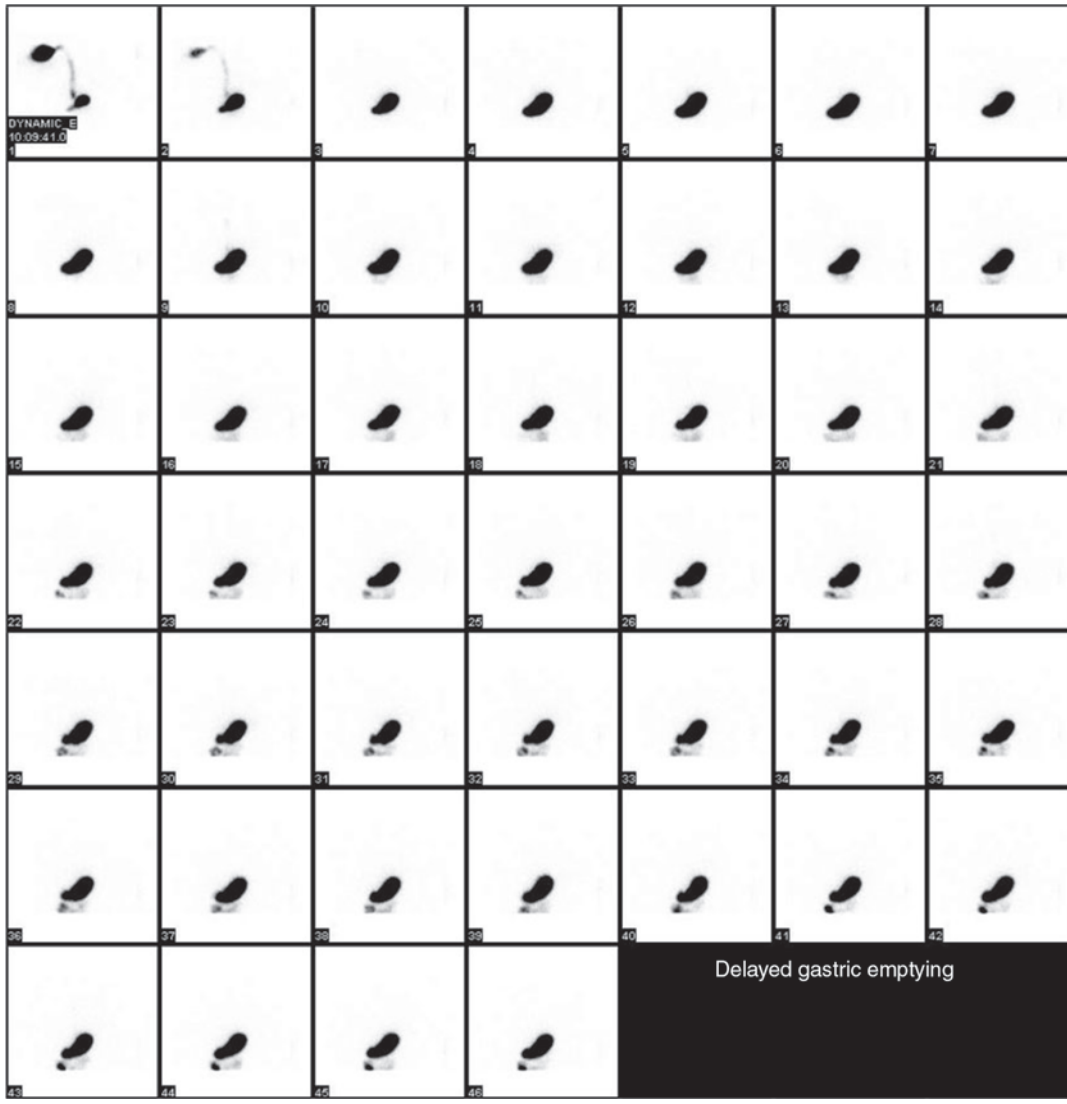

Fig. 10.7 Abnormal gastric emptying study. ^{99m}Tc-sulfur colloid gastric emptying study is shown. Gastric emptying half-clearance time was more than 160 min. Note activity in the stomach is not decreasing with time indicating delayed clearance. Compare with the normal pattern in Fig. 10.8

activity measured at time zero, by 90 min. The lag phase corresponds to maximal filling of the distal stomach when trituration has been completed and the suspended solid particles begin to empty. Lag phase abnormality may be the earliest finding in diabetic gastroparesis and can be corrected by the drugs used to treat this condition [15, 21]. Solids leave the stomach in a linear fashion. Acutely delayed emptying is seen in stress (as in cold or pain), due to drugs (morphine, anticholinergics, levodopa, nicotine, beta blockers) and due to hyperglycemia and hypokalemia.

Chronically delayed gastric emptying is encountered most frequently in gastric outlet obstruction, postvagotomy, gastric ulcer, scleroderma, dermatomyositis, hypothyroidism, diabetes mellitus,

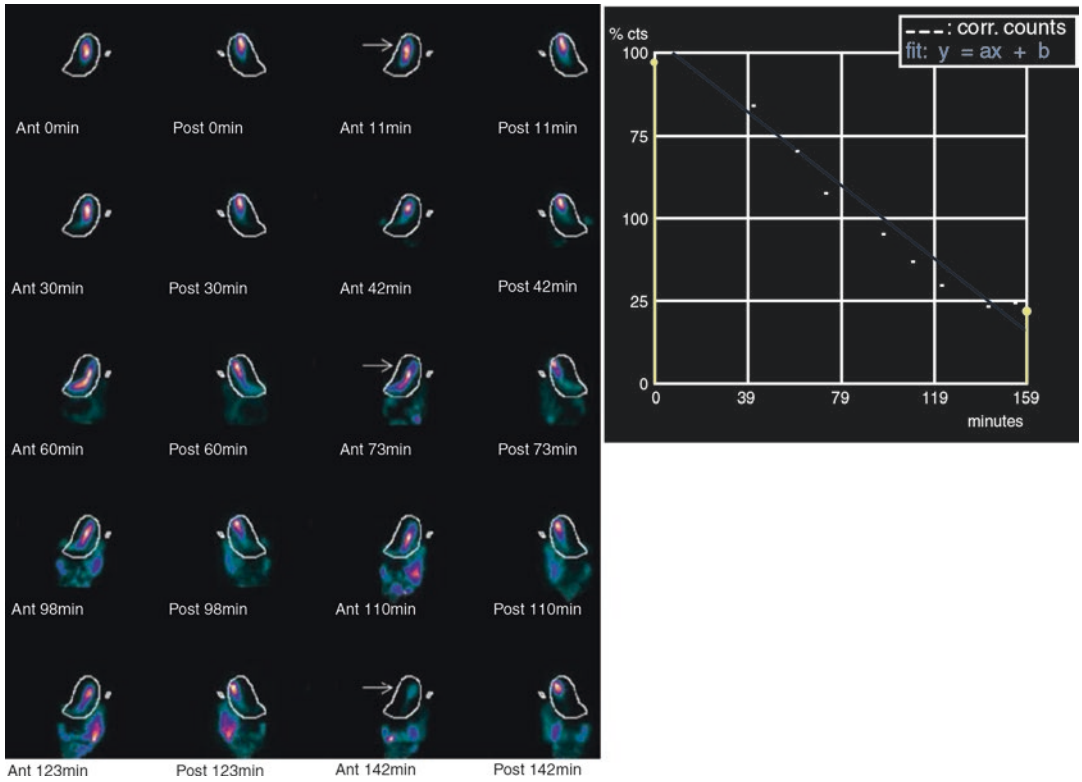

Fig. 10.8 Normal gastric emptying study. The study revealed normal gastric emptying quantitatively. Note the decreasing activity of gastric activity with time during the study, indicating prompt clearance

amyloidosis, and uremia. Abnormally rapid gastric emptying is found in gastric surgery, Zollinger-Ellison syndrome, duodenal ulcer, hyperthyroidism, and diabetes.

It should be noted that the reproducibility of gastric emptying studies is only moderately as in 30% of studies repeat studies can be different [51]. Accordingly, the diagnosis of gastroparesis based on a single study may occasionally be inaccurate.

An ingestible, telemetric device (the wireless motility capsule: WMC) is now commercially available, enabling the measurement of both regional and total GI transit times in a minimally invasive manner without radiations is an alternative to scintigraphy. The wireless motility capsule measures pH, pressure, and temperature throughout the GI tract, and is used also to calculate gastric emptying [52].

10.1.6.4 Duodenogastric Reflux Study

The way of detecting duodenogastric reflux is to administer a radiopharmaceutical that can go to the duodenum without passing through the stomach. This can be achieved by using hepatobiliary radiopharmaceuticals in conjunction with stimulation of the gall bladder to empty by a fatty meal. This helps to increase the activity in the duodenum and thus to detect the reflux. The usual protocol is to acquire dynamically for 60 min following i.v. administration of Tc99m-IDA derivative (Fig. 10.9). The fatty meal is then ingested by the patient and another dynamic study is obtained for 30 min.

10.1.6.5 Gastrointestinal Bleeding Localization Study

This radionuclide study can detect a bleeding rate as low as 0.1 mL/min. The two common

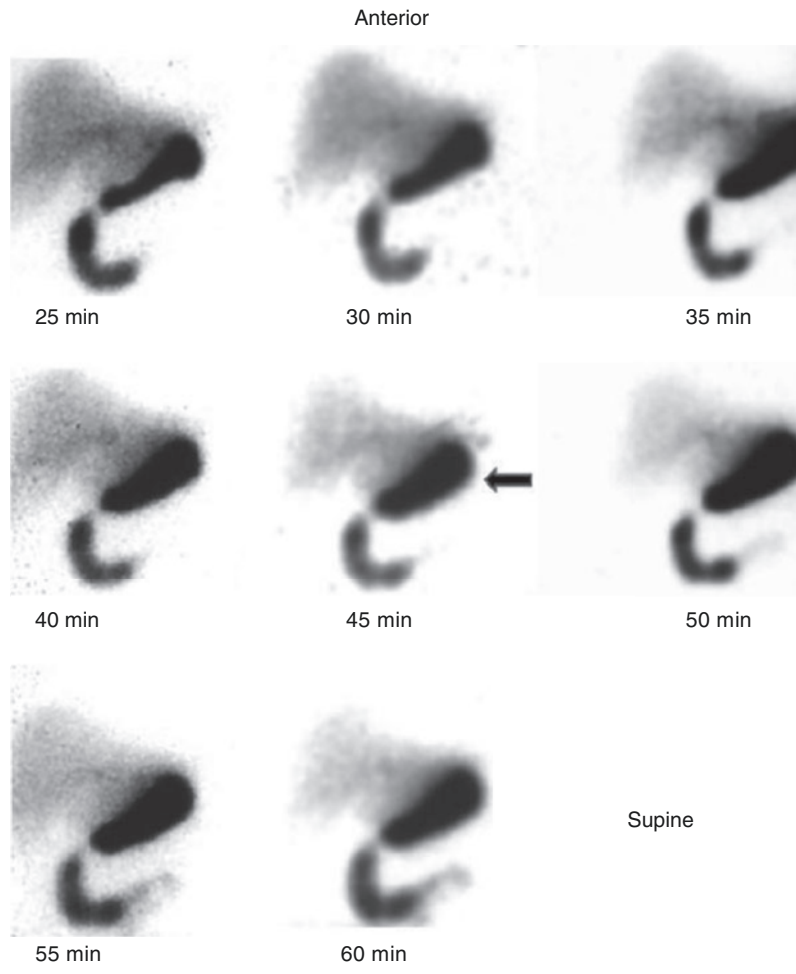

Fig. 10.9 Representative images of a hepatobiliary study of a 32-year-old male patient suspected of having acute cholecystitis. In addition to the nonvisualized gallbladder by 60 min shown in the images presented, significant duodenogastric reflux is seen (*arrow*)

indications for a radionuclide bleeding scan are as follows:

1. Suspected acute ongoing or intermittent lower GIB of unknown localization with nondiagnostic endoscopy.
2. Follow-up of known bleeding to assess treatment effectiveness.

A radionuclide bleeding scan plays only a very small role in the evaluation of upper GIB because of the high accuracy of endoscopy and because of potential interference from radiotracer activity normally excreted by the gastric mucosa. All patients with prior aortic graft surgery and GIB should be considered to have an aortoenteric fistula until proven otherwise.

Two radiopharmaceuticals are available for the study of lower GIB: Tc-99m-labeled RBCs and Tc-99m-sulfur colloid.

1. Using Tc-99m-labeled RBCs is the most commonly used method. The patient's RBCs should be labeled in vitro to get the highest labeling efficiency. Imaging is begun with injection of the radiolabeled RBCs, where dynamic images are taken at a rate of 1 frame/10–60 s. Rapid bleeding can be detected with first-minute flow images taken at a rate of 1 s/frame. The extravasation manifests as focal activity that appears during the blood pool phase, initially intensifies, and moves anterograde and retrograde in a bowel-like trajectory on subsequent images

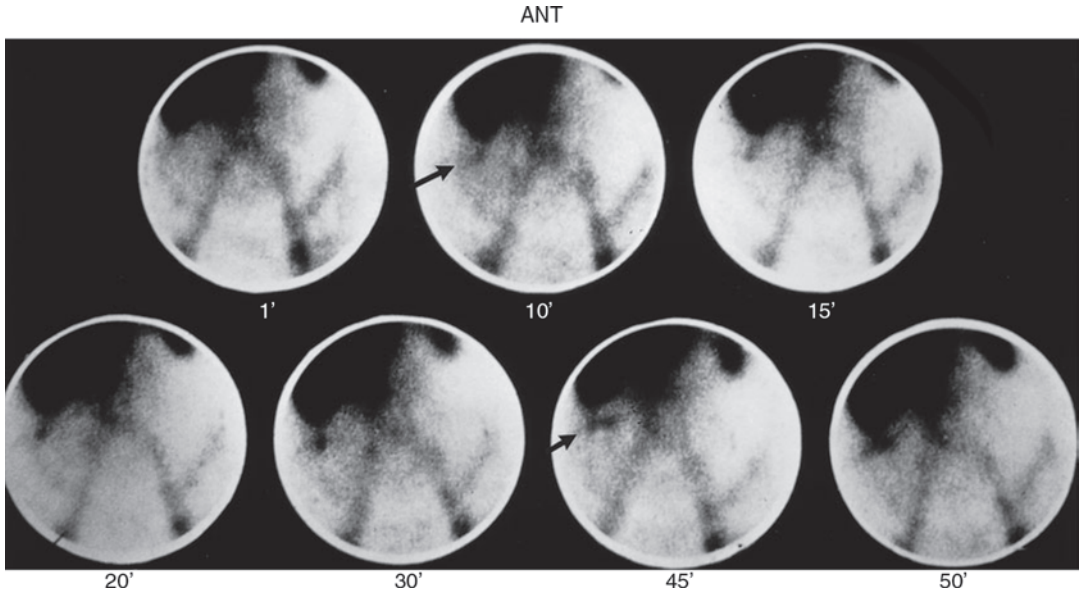

Fig. 10.10 ^{99m}Tc-labeled RBC study for localization of gastrointestinal bleeding showing a focus of extravasated activity in the right hepatic flexure, which progressed later during the study (*arrows*)

(Fig. 10.10). It is extremely important to view the study in a cine mode, which can clarify difficult cases. If transit time is rapid, 1 mg glucagon can be given i.v. to reduce bowel motility. The sensitivity of this cinematic method is more than 90% [53].

To localize the bleeding site, 5 cc or more of extravasation may be needed. The patients can be monitored for up to 24 h; however, the site of extravasation may be easily misinterpreted [54]. A negative radionuclide study is good evidence that angiography will not detect the site of hemorrhage.

2. In the Tc-99m-sulfur colloid method, the study can be performed in approximately 30 min, in cases of active lower GIB (if no time is available for labeling the RBCs) where time is vital for the management of the patient. This tracer is cleared from the circulation with a half-time of 2.5–3.5 min. By 12–15 min, most of the activity is cleared from the vascular system (background), resulting in a high target-to-background ratio. The clearance is delayed in patients with diffuse liver disease. The study is fast and sensitive with quick results, but intermittent bleeding sites may be missed. Small bowel bleeding can be differentiated from colonic bleeding by the appearance of blood filling multiple loops of small bowel.

The technique of Tc-99m-labeled RBCs is preferred. However, for acute or continuous bleeding, a Tc-99m-SC study may be used, and in this case, images are taken for 30 min, which can detect a blood loss of 0.1 mL/min. If this is negative or blood loss is known to be intermittent, a labeled RBC study is used.

10.1.6.6 Meckel's Diverticulum Study

Scintigraphy is performed using Tc-99m-pertechnetate, since it is taken up by the gastric mucosa contained in Meckel's diverticulum (Figs. 10.11 and 10.12). The radiotracer accumulates in and is excreted from the mucus-secreting cells in the ectopic gastric mucosa regardless of the presence of parietal cells.

The patient should be fasting for 4–6 h to reduce gastric secretion passing through the bowel. With Tc-99m-pertechnetate, Meckel's diverticulum appears at the same time as the stomach and the activity increases in intensity with the stomach; it may change in position during the study and may empty its contents

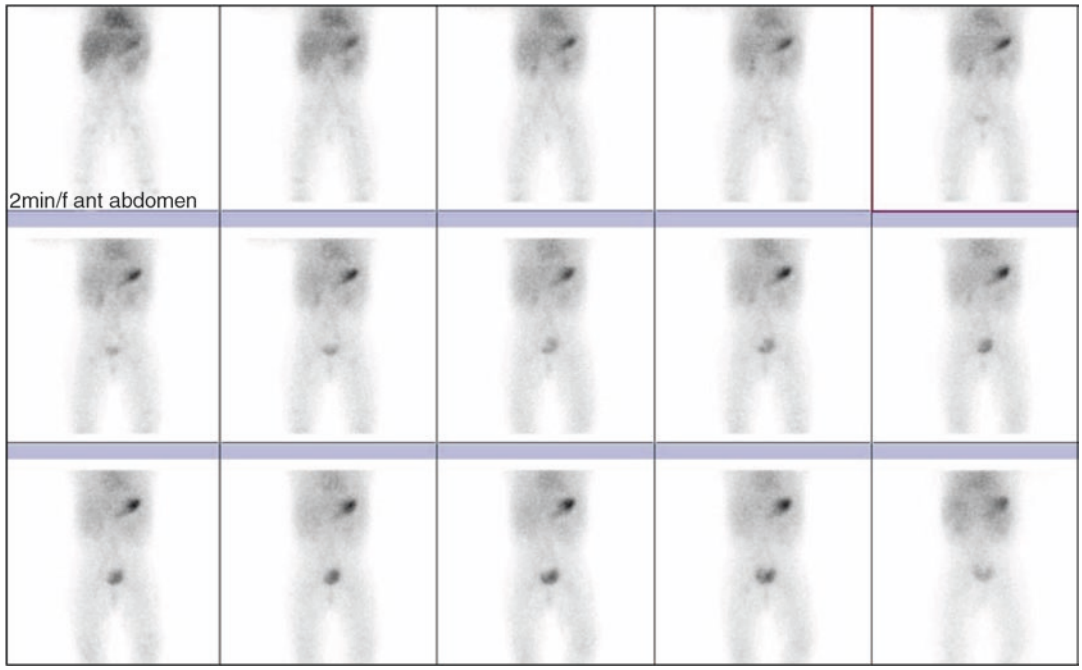

Fig. 10.11 Negative Meckel's diverticulum study

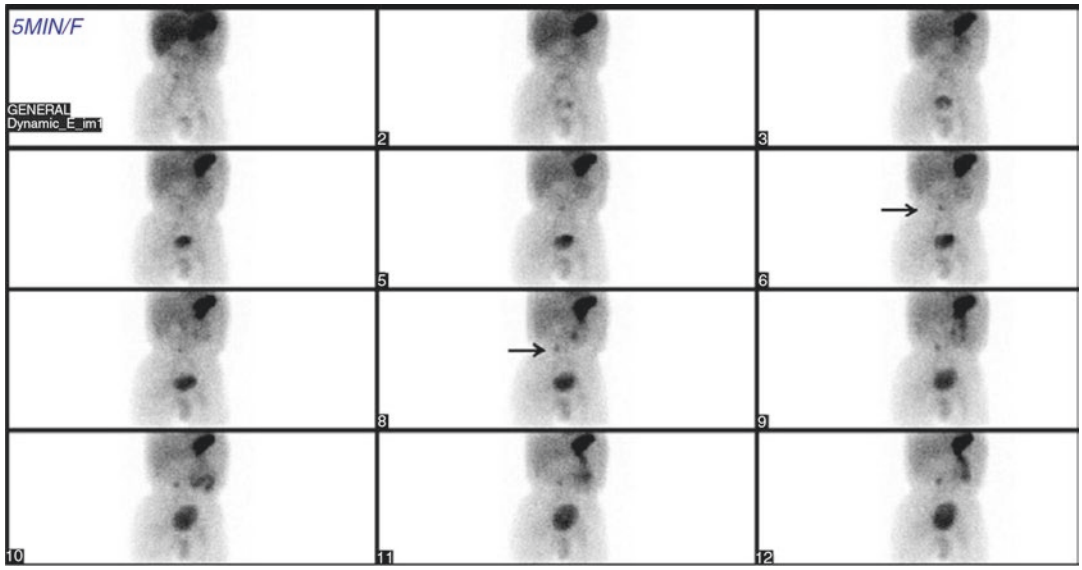

Fig. 10.12 Positive study for Meckel's diverticulum (*arrows*)

into the bowel. Pharmacological intervention improves the sensitivity of the study. Cimetidine enhances gastric uptake and blocks pertechnetate release from the mucosa. Glucagon is given i.v. 10 min after pertechnetate to inhibit peristalsis and delay emptying of gastric contents into the small bowel.

Any blood leaking into the bowel would be apparent, although it would not show the rounded appearance of Meckel's diverticulum. Among the

false-positive cases are renal transplant, renal pelvis, ureter, bladder diverticulum, iliac vessels and uterus, ectopic gastric mucosa in small bowel other than Meckel's diverticulum, infection (as in acute appendicitis), and intussusception. Among the false-negative cases are absence of ectopic gastric mucosa in the diverticulum and diverticulum hidden by bladder or stomach. The sensitivity of Tc-99m-pertechnetate is overall more than 85%, but it drops after adolescence because patients asymptomatic throughout childhood are less likely to have ectopic gastric mucosa. In a recent study on children under 18 years of age, the sensitivity, specificity, PPV, NPV, and accuracy values were 84%, 97%, 90%, 95%, and 94%, respectively [55].

10.1.6.7 Imaging of Inflammatory Bowel Disease

The diagnosis of inflammatory bowel disease (IBD) needs a complex workup. Besides verifying the disease itself, it is fundamental to assess disease extent and activity and to detect associated complications, to help select the most effective treatment and for follow-up. Scintigraphy with radiolabeled leukocytes (Fig. 10.13) is able to provide a complete survey of the whole intestinal tract, both the small and large bowel, and detects septic complications successfully with negligible risk. Radionuclide procedures are useful in establishing or ruling out IBD in patients with intestinal complaints, in assessing disease severity, and in the evaluation of extraintestinal septic complications [56]. Radiolabeled leukocytes studies offer an accepted radionuclide method for imaging inflammation. Because of many advantages of tecnetium-99m (^{99m}Tc) over indium-111 (111In), ^{99m}Tc-HMPAO-leukocyte scintigraphy is preferred for the investigation of IBD. The ^{99m}Tc-HMPAO-leukocyte scintigraphy technique is highly accurate within the first few hours postinjection. It can reliably assess disease activity, but a normal scintigraphy does not exclude mild inflammation [57]. Recently the immunoscintigraphy with ^{99m}Tc-antigranulocyte antibodies has been carried out; however, ^{99m}Tc-HMPAO is the first-choice agent with SPECT/CT preferred (Figs. 10.13 and 10.14). FDG-PET/CT is very helpful in localization of activity . It is an excellent method for the noninvasive quantification of bowel inflammation and in assessing advancement of the disease [58]. For more details, please refer to Chap. 4.

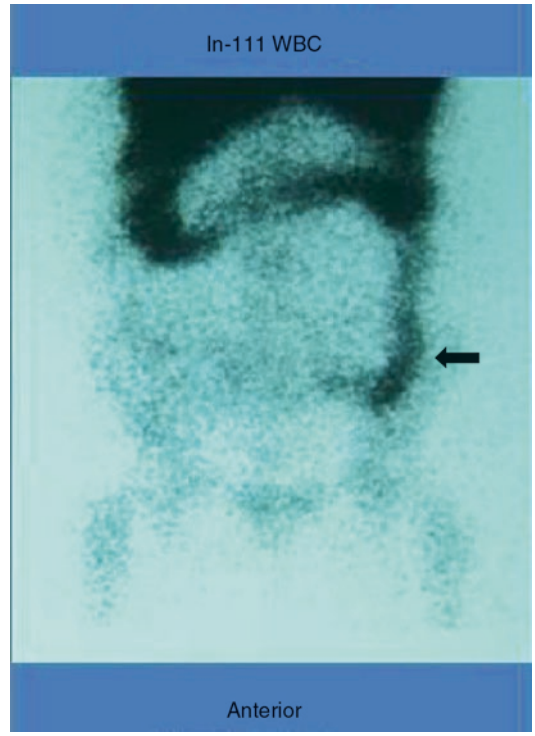

Fig. 10.13 In 111 WBC study in a patient with known inflammatory bowel disease showing significant uptake by the colon (*arrow*) indicating active disease

10.1.6.8 Salivary Gland Imaging

Several modalities can be used for the diagnosis of salivary gland disorders. Standard radiographs are of limited value. Sialography is particularly useful for duct system conditions. Parenchymal diseases like tumors are better shown by CT and US. CT can be combined with sialography, and this combination is currently the most sensitive technique for localizing small tumors [46]. Scintigraphy is needed in some conditions that cannot be evaluated by morphologic modalities particularly functional conditions such as xerostomia.

Salivary gland scintigraphy is carried out after 5–15 mCi (185–550 MBq) of Tc99m-pertechnetate injected in the patient intravenously.

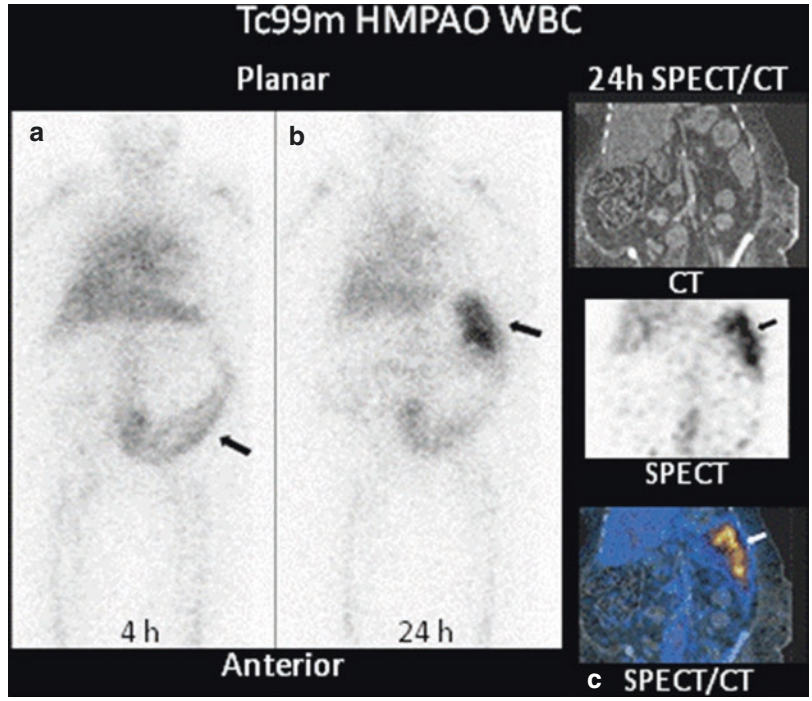

Fig. 10.14 In 111 WBC study of a patient with inflammatory bowel disease. On 4-h In-111 WBC images (**a**), there is mild diffuse labeled WBC accumulation in the descending and sigmoid colon (arrow). On 24-h images (**b**), the accumulation in the upper part of the descending colon and splenic flexure are more intense (arrow). SPECT/CT (**c**) more clearly shows the uptake in the colon's splenic flexure (arrow) since there is a superimposition of the spleen and splenic flexure on planar images

Dynamic images are obtained as 1-min frames for 15–20 min. The patient is asked to drink two glasses of water before the study, and a sialagogue (20-mL lemon juice) is given at 10 min to stimulate salivation. The images are obtained for the anterior face and neck in the sitting position, using a low-energy, high-resolution collimator. Extra images for right and left laterals are obtained for 2 min each to localize the activity. Regions of interest (ROI) are drawn and a graph is plotted to assess the function of the salivary glands.

Findings on a normal scan are a stepwise rising curve of activity with an abrupt drop after the sialagogue and a subsequent rise again (Fig. 10.15). In Sjögren's syndrome there will be decreased accumulation of radiotracer compared with the thyroid gland and delayed clearance (Fig. 10.16). In Warthin's tumor (adenolymphoma), there is an intense increase in the focal area of activity because it mimics thyroid tissue in pertechnetate uptake [59–61].

10.1.6.9 Imaging of Appendicitis

Radioisotope imaging using labeled white blood cells and more recently antigranulocyte antibody technetium (99mTc) fanolesomab (NeutroSpec) has been used for appendicitis imaging patients with equivocal signs and symptoms of appendicitis. Localized uptake of tracer in the RLQ suggests appendiceal inflammation. Tc99m HMPAO labeled leukocyte showed a sensitivity of 90–98% and specificity of 92–96% [62, 63]. Recent reports suggest a possible role of FDG-PET/CT to diagnose appendicitis [64].

10.1.6.10 Scintigraphic Non-imaging Procedures

Carbon-14 Breath Tests

This simple carbon-14 breath test has been utilized increasingly in recent years in gastrointestinal practice. The test is based on detection and quantitation of radioactive carbon dioxide originating in the stomach or small intestines and exhaled through the respiratory system after being absorbed into the blood stream. This is based on the ability of the *H. pylori* urease enzyme to break down an isotope-labeled urea solution ingested by the patient into carbon dioxide and ammonia [65]. The test is useful in

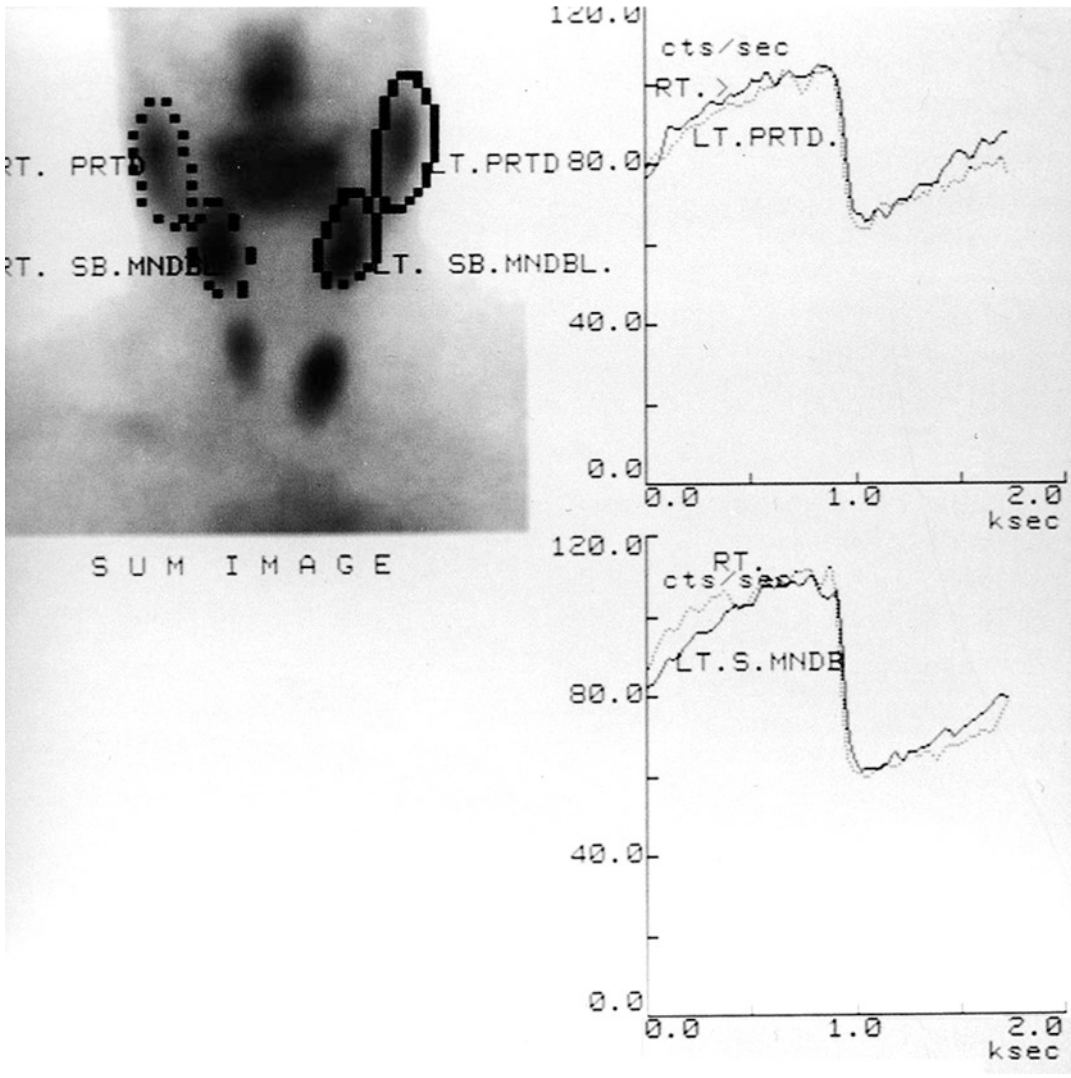

Fig. 10.15 Normal pattern on a salivary radionuclide study. Note the adequate accumulation of the radiotracer with good clearance

the diagnosis of several disease processes, particularly *Helicobacter pylori* infections, lactose intolerance, and malabsorption due to bacterial deconjugation of bile acids.

Helicobacter pylori Infections

Helicobacter pylori has been known for many years and was previously called *Campylobacter pylori* or *Campylobacter pyloridis*. It is a small, curved, gram-negative rod found in the stomach (Fig. 10.17) and duodenum of many individuals. The prevalence correlates best with socioeconomic status. In the USA, the overall probability of infection is 20–30%. Among African-Americans the probability is about 50%, and approximately 60% of immigrants such as Latinos are affected. The infection approaches 90% in third-world countries, where it occurs in 10% of children between the age of 2 and 8 years per year and most teens become infected [65–72].

H. pylori infection is known to be associated with several pathological disorders. The organism causes the most common type of nonerosive gastritis, which characteristically involves the antrum

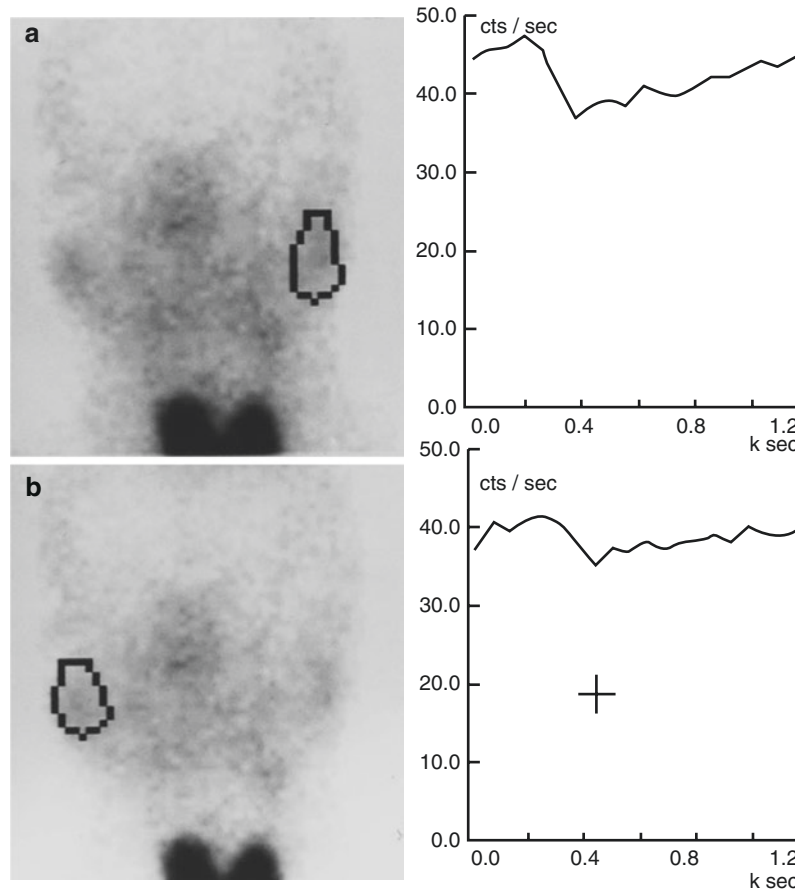

Fig. 10.16 ^{99m}Tc-pertechnetate salivary gland study showing poor uptake and clearance of the radiotracer in a patient with Sjögren's syndrome. Visually (**a**) and on time-activity curves (**b**)

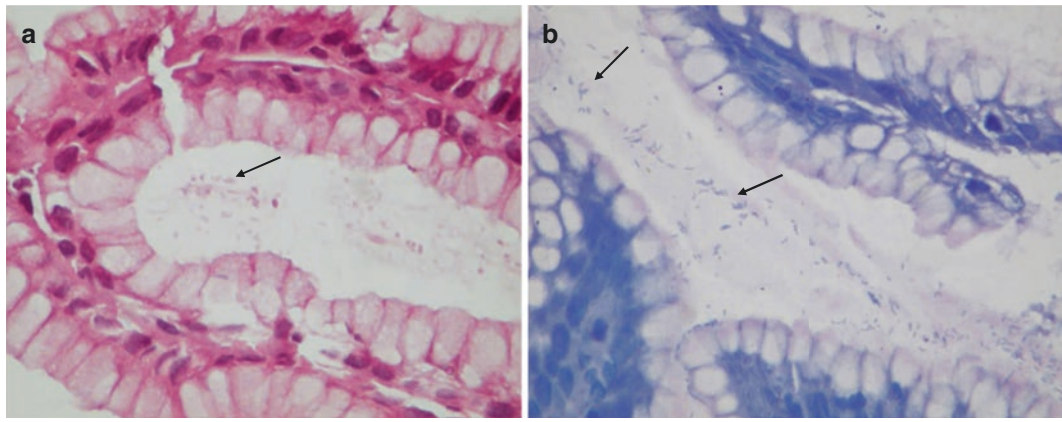

Fig. 10.17 *Helicobacter pylori* as seen on H & E stain (**a**) and Giemsa stain (**b**). (Courtesy of Prof. M. Elmonayeri with thanks)

and body of the stomach. It is found in almost all patients with duodenal ulcers and approximately 80% of those with gastric ulcer. Other conditions such as gastric adenocarcinoma and lymphoma, chronic fatigue syndrome, and acne rosacea are also linked to the organism [63, 64]. Recently it has also been suggested to be involved in the pathogenesis of coronary artery disease.

The diagnosis of *H. pylori* may be obtained by endoscopy specimen, by a blood test identifying anti-*Helicobacter* infection antibody or by a carbon-13 or carbon-14 urea breath test. Endoscopy is needed in many cases to detect ulcers and other gross pathological changes. During endoscopy, biopsy material is obtained and examined microscopically, in addition to culturing for *H. pylori*. However, endoscopy cannot be used just to find whether *Helicobacter* infection is present and is not justified as a follow-up technique to evaluate the response to therapy. Antibody testing, on the other hand, has the shortcoming of not being suitable for patient follow-up since antibodies decline slowly after treatment and may remain elevated long after *Helicobacter* has been killed.

H. pylori is able to fight stomach acid containing a large amount of the enzyme urease. Urease converts urea, present in the saliva and gastric juices, into bicarbonate and ammonia, which are strong bases and act as acid-neutralizing agents around the *H. pylori*, protecting it from the stomach acidity. This action of urea hydrolysis is the basis of carbon-14 and carbon-13 urea breath tests (Fig. 10.18).

The test can be performed using a capsule or a liquid containing a minimal amount (2 μCi) of carbon-14 urea. The patient swallows a drink or capsule and 10–20 min later, samples of breath are taken with the patient blowing into a small bottle of liquid. The amount of radioactive carbon dioxide in blood and expired in breath is detected and quantitated by scintillation counter. In the presence of *H. pylori* infections, the count will be higher than normal. Carbon-14 urea contains a tiny amount of radioactive material, which passes out of the body in a day or so in the urine or breath [73]. The amount of radioactive exposure to the patient from the test is less than the individual normally receives in a half day from nature [67]. It is also equivalent to the radiation dose that an individual absorbs when flying in an airplane for 1 h. Since urea is present in saliva, patients must brush and rinse their teeth before taking the test.

Lactase Deficiency

Acquired lactase deficiency is a common disorder of carbohydrate absorption. The deficiency of intestinal lactase leads to decreased hydrolysis of ingested lactase in the small intestinal cells as occurs normally. Lactase is one of the most common disaccharides in diet and is a main constituent of milk and other dairy products. The intact lactose is not absorbed and increases the osmotic effect of the small intestinal contents, with subsequent outpouring of liquid into the intestinal lumen. This will result in increased intestinal motility with abdominal cramps, distention, and diarrhea when a patient ingests milk [74, 75].

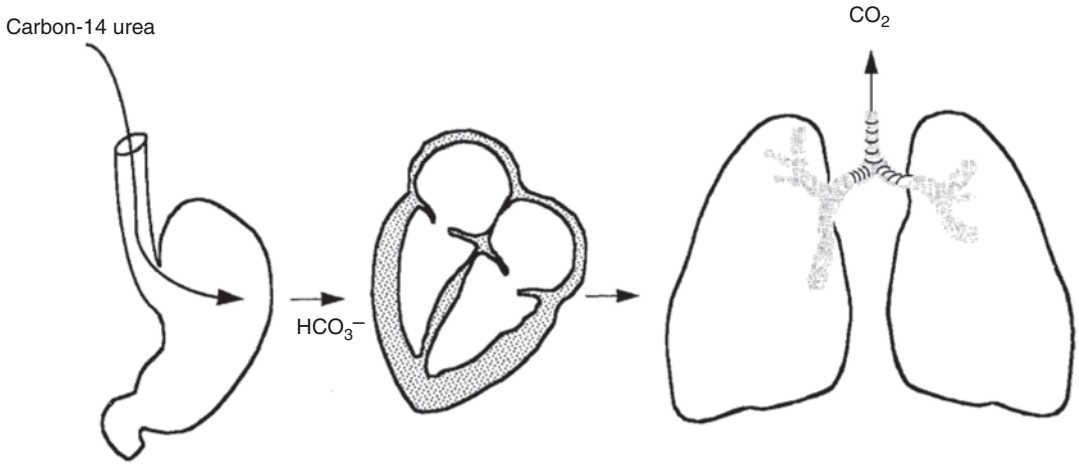

Fig. 10.18 The principle of carbon-14 breath tests

For lactose intolerance, lactose-1-C-14 together with carrier lactose (50 g) dissolved in 400 mL of water is used. In patients with lactose intolerance, lactase deficiency leads to the inability to split lactose into glucose and galactose and subsequently to CO_2. When carbon-14-labeled lactose-1 is administered to patients with lactase deficiency, there will be decreased exhalation of labeled carbon dioxide.

Malabsorption Secondary to Bacterial Overgrowth

Bacterial overgrowth is one of the major reasons for luminal phase malabsorption. Bacterial overgrowth causes deconjugation of bile salts which are absorbed and cycled normally through the enterohepatic circulation but are ineffective in micelle formation. Since micelle formation is essential for the normal absorption of free fatty acids and monoglycerides, malabsorption results. Carbon-14-glycine cholate and more recently the carbon-14-xylose breath test are useful in the diagnosis of malabsorption secondary to bacterial overgrowth [75, 76]. Since carbon-14-glycine cholate is a conjugated bile salt, it is absorbed by the ileum and metabolized in the liver. Only a small portion is attached normally by bacteria and causes deconjugation leading to the formation of carbon dioxide that is exhaled. The deconjugation increases with increased bacterial colonization in the intestines, and consequently the amount of labeled carbon dioxide present in the exhaled breath increases [77]. This test is useful in the diagnosis of blind or stagnant loop syndrome and of ileal absorptive function.

Schilling Test

This procedure uses an oral test dose of radiolabeled cyanocobalamin (usually ^{57}Co-B-12) with or without added Intrinsic factor (IF). The absorption is most frequently measured indirectly by measuring the urinary excretion of the radiolabeled vitamin B-12. The vitamin is flushed out into a 24-h collection of urine sample by a large parenteral dose (1 mg) of nonradioactive vitamin B-12 injected intramuscularly usually 1 h after administration of the oral test dose. The test is done once without IF and then repeated with IF. A convenient method is to use two radioisotopes of cobalt, ^{58}Co-labeled cyanocobalamin with IF and ^{57}Co-cyanocobalamin without IF (often referred to as the Dual-Isotope method). Normal subjects with no abnormality of Vitamin B-12 absorption show urinary excretion of free radioactive vitamin B-12 of 9% or more, with IF-bound to free cobalamin ratio of between 0.8 and 1.2.

10.2 Hepatobilitary system

10.2.1 Anatomical and Physiological Considerations

The liver is the largest organ in the body, weighing between 1200 and 1800 g. The liver lies in the abdominal cavity, where it is split into a large right and a small left lobe by the falciform ligament extending from the anterior abdominal wall. The Couinaud classification divides the liver into eight independent segments numbered 1–8, each of which has its own vascular inflow, outflow, and biliary drainage. The Couinaud segments and their corresponding traditional nomenclature are shown in Fig. 10.19.

Within the lobes and segments are multiple, smaller anatomical units called liver lobules. These lobules are formed of plates of hepatocytes, which are the functional cells of the liver. In addition, the parenchyma of the liver is composed of another type of cells: the reticuloendothelial cells or Kupffer's cells. Almost 90% of the reticuloendothelial cells in the body are found in the liver. The sinusoids are capillaries located between the plates of hepatocytes; they receive a mixture of venous and arterial blood from branches of the portal vein and the hepatic artery, respectively. Blood from the sinusoids drains to central veins that continue to empty into the hepatic vein, which enters the inferior vena cava. Kupffer's cells line the sinusoids and destroy microorganisms.

The liver has digestive, metabolic, hematological, and immunological functions. The hepatocytes synthesize approximately 1 L of bile per day and secrete it into the bile canaliculi, which are small channels between the hepatocytes. The bile canaliculi empty into bile ducts that unite and finally

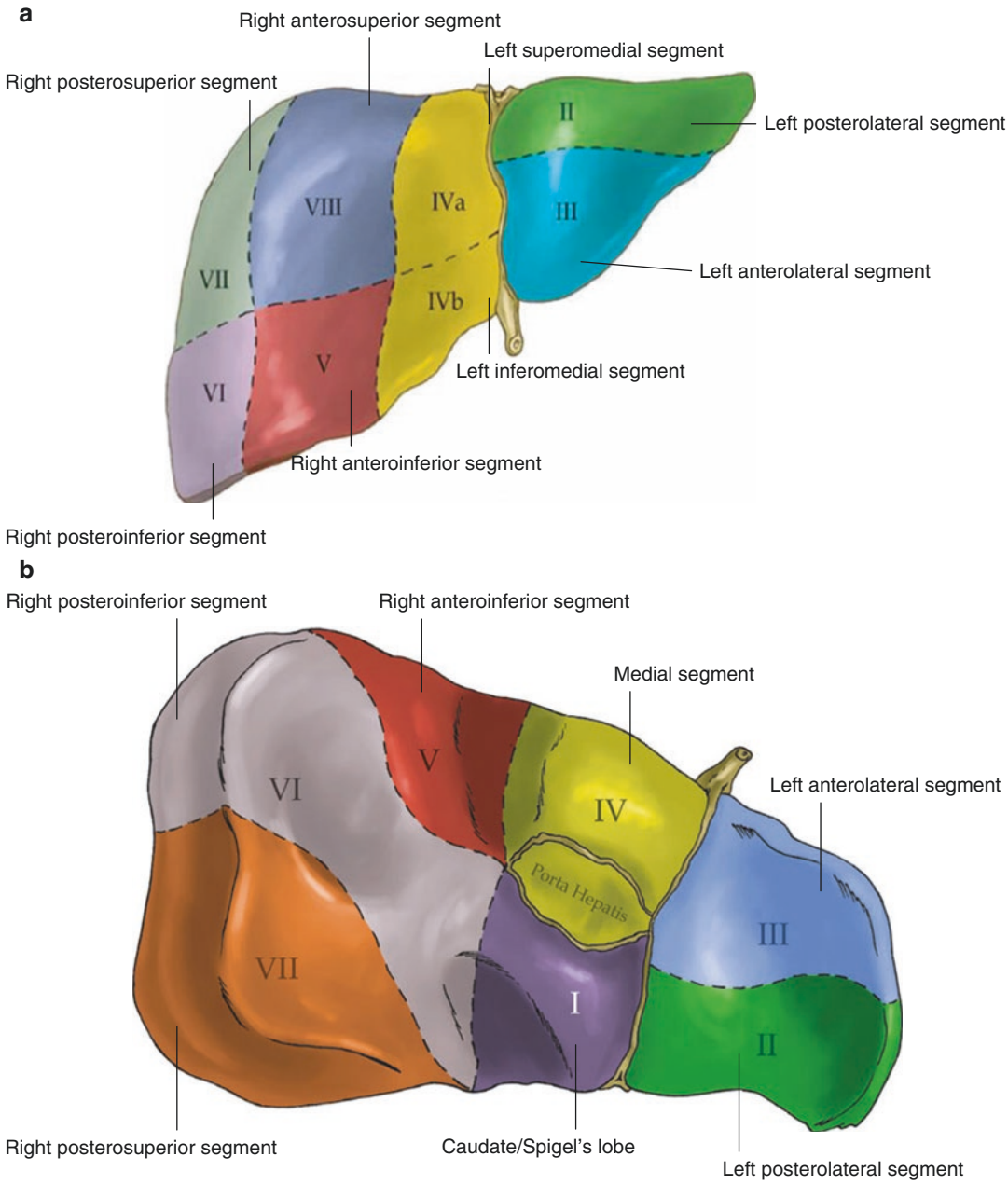

Fig. 10.19 (**a**, **b**) The Couinaud segments of the liver. (**a**) Anterior surface view; (**b**) visceral surface view. *I*, caudate/Spigel's lobe; *II*, left, posterolateral segment; *III*, left anterolateral segment; *IVa*, left superomedial segment; *IVb*, left inferomedial segment; *V*, right anteroinferior segment; *VI*, right posteroinferior segment; *VII*, right posterosuperior segment; *VIII*, right anterosuperior segment

form the right and left hepatic ducts, which join to form the common hepatic duct. Past the point where the cystic duct begins, the hepatic duct is called the common bile duct, which drains into the duodenum through the major duodenal papilla. Bile is necessary for fat digestion and absorption. Unconjugated bilirubin is converted to water-soluble, conjugated bilirubin by hepatocytes and is secreted with bile. The gallbladder stores bile and ejects it when chyme enters the duodenum and stimulates the

secretion of cholecystokinin. The hepatocytes are capable of regeneration. Most regeneration takes place in the left lobe in disease states such as alcoholic damage or chronic hepatitis.

10.2.2 Hepatobiliary Radiopharmaceuticals

Several radiopharmaceuticals are used for scintigraphic assessment of liver and hepatobiliary disorders (Table 10.8). Technetium-99m (Tc-99m)-sulfur colloid (SC) is a radiopharmaceutical for liver/spleen imaging. This compound is cleared by cells of the reticuloendothelial system: approximately 85% by Kupffer's cells in the liver, 10% by the spleen, and 5% by the bone marrow. Tc-99m-phytate is also used for liver/spleen imaging in some countries. However, due to smaller particle size, its splenic uptake is significantly less than that of SC.

Iminodiacetic acid derivatives are used for cholescintigraphy. Tc-99m-disofenin (2,6-diisopropyl iminodiacetic acid (DISIDA)) and Tc-99m-mebrofenin (2,4,6-trim-ethyl, 5-bromoiminodiacetic acid (BrIDA)) are exclusively used for cholescintigraphy by most laboratories in the USA. Various other iminodiacetic acid (IDA) compounds are available in other countries. These compounds, after being injected intravenously, are bound to plasma albumin, transported to the liver, and actively taken up by the hepatocytes via carrier-mediated, non-sodium-dependent, organic anionic pathways similar to those responsible for bilirubin uptake [84]. The IDA compounds are not conjugated. They are excreted into the bile canaliculi by both active and passive transport mechanisms [85]. Compared with Tc99m-disofenin, mebrofenin demonstrates higher hepatic excretion and lower urinary excretion, especially in patients with a high bilirubin level [85]. Depending on the agents used, 2–15% of the injected dose is excreted in urine. The more severe the hepatic dysfunction, the greater the renal excretion [86, 87].

Tc-99m-aglactosyl-neoglycoalbumin (Tc-99m-NGA) and Tc-99m-galactosyl human serum albumin (Tc-99m-GSA) are liver imaging agents that bind to the hepatocyte-specific asialoglycoprotein membrane receptors (ASGCP receptor) [78, 79]. These agents have been used primarily to evaluate the functional liver mass/reserve in various clinical settings.

10.2.3 Evaluation of Liver Diseases

10.2.3.1 Functional Hepatic Mass/Reserve

Assessment of hepatic functional reserve is important prior to major hepatic resection for predict-

Table 10.8 Radiopharmaceuticals for hepatobiliary scintigraphy (cholescintigraphy)[a]

Radiopharmaceutical	Uptake mechanism	Use
Tc-99m sulfur colloid	Kupffer cell	Focal nodular hyperplasia, splenosis, liver function
Tc-99m red blood cells	Blood pool distribution	Hemangioma, splenosis
Tc-99m disofenin	Extracted and excreted by the liver similar to bilirubin	Gall bladder and hepatobiliary disorders
Tc-99m MAA	Blood flow, capillary occlusion	Hepatic arterial perfusion
Tc-99m mebrofenin	Extracted and excreted by the liver similar to bilirubin	Gall bladder and hepatobiliary disorders
F-18 FDG	Glucose metabolism	Tumor/infection imaging
Gallium-67 citrate	Iron binding	Tumor/infection imaging
Tc-99m-aglactosyl-neoglycoalbumin (Tc-99m-NGA) and Tc-99m-galactosyl human serum albumin (Tc-99m-GSA)	Binding to the hepatocyte-specific asialoglycoprotein membrane receptors	Assessment of functional liver mass/reserve

[a] [78–83]

ing the outcome of surgery because postoperative liver failure can significantly affect the clinical course. This may require imaging of both the anatomical structure of the liver and the regional functional reserve. Hepatobiliary scintigraphy with technetium-99m (^{99m}Tc) iminodiacetic acid or ^{99m}Tc galactosyl human serum albumin (GSA) has been used to assess regional hepatic function. Galactosyl human serum albumin (GSA) is a ligand specific to the asialoglycoprotein receptor present exclusively on the plasma membrane of hepatocytes. GSA is bound only by this receptor and then providing valuable information about receptor population density as well as functioning hepatocyte mas [79, 83]. Tc-99m GSA does not compete with bilirubin, which is an additional advantage in the evaluation of hepatic reserve in patients with hyperbilirubinemia [88].

10.2.3.2 Primary Hepatic Neoplasms and Tumor-Like Conditions

Hepatocellular Carcinoma

While hepatocellular carcinoma (HCC) usually displays marked arterial vascularity on dynamic perfusion imaging, its appearance on static colloid imaging (focally decreased activity) is nonspecific. Sulfur colloid imaging can be used to differentiate regenerating nodules from HCC in a cirrhotic liver. The presence of colloid uptake typically represents regenerating nodules, while decreased uptake is nonspecific but may include HCC [89].

Depending on the degree of differentiation, approximately 40–50% of HCCs concentrate hepatobiliary tracers (Fig. 10.20), i.e., Tc-99m-IDA or Tc-99m-PMT. The degree of uptake seems to correlate with tumor differentiation, as well as with survival [90, 91]. Tc-99m-IDA uptake was seen in 70% of well-differentiated tumors, in 30% of moderately differentiated tumors, and in no poorly differentiated tumors [90]. In another series of 162 patients, the median survival of 82 patients with increased tumor uptake on delayed Tc-99m-PMT imaging was 1013 days, compared with 398.5 days in 80 patients with no tumor uptake [91].

Uptake of hepatobiliary tracers on delayed imaging can be present in other liver lesions that contain hepatocytes, such as focal nodular hyperplasia (FNH) [92]. Kotzerke et al. claimed that the distinction between FNH and HCC is possible with 3-phase imaging (perfusion, 5–10 min, and 2–3 h) [93]. In their series, most FNH exhibited normal or increased uptake at 5–10 min, whereas most HCC displayed decreased or no uptake during this phase.

Gallium-67 and thallium-201 were used in the past for evaluation of HCC in various clinical settings. However, the utility of these tracers in HCC appears to have been replaced largely by positron-emitting tracers recently.

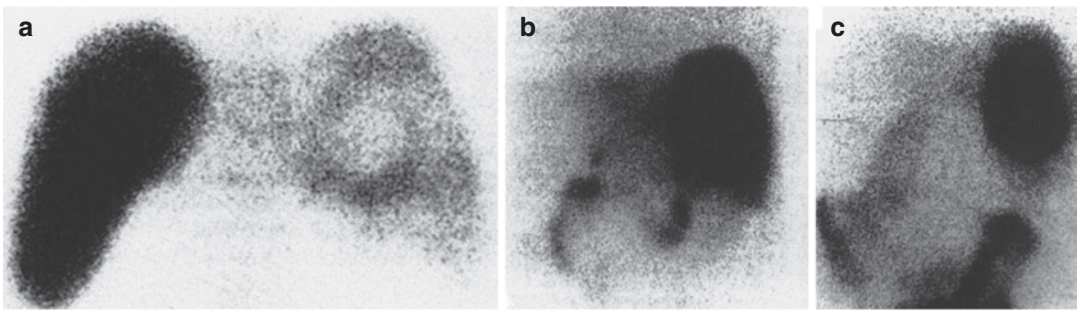

Fig. 10.20 (**a**) Hepatic scintigraphy with Tc-99m-SC in a patient with hepatoma complicating liver cirrhosis. A defect is observed in the posterior view. (**b**) Hepatic scintigraphy with Tc-99m-DISIDA 15 min after tracer administration (posterior view). Marked tracer uptake fills the cold area previously observed, as well as the rest of the liver parenchyma. (**c**) Hepatic scintigraphy with Tc-99m-DISIDA 3 h after tracer administration (posterior view). Tracer is clearly retained in the HCC area while it has been excreted from the nontumoral liver. (Reprinted from Calvet et al. [90] with permission)

10.2.3.3 Hepatic Hemangioma

Hemangioma is the most common benign tumor of the liver. Cavernous hemangioma occurs at all ages but most commonly in adults. Most hemangiomas are of the cavernous type, constituted by dilated nonanastomotic vascular spaces lined by flat endothelial cells and supported by fibrous tissue. Thrombi in different stages of organization are often encountered. Long-standing lesions can show extensive hyalinization or calcification [94–96].

The classic finding of hepatic cavernous hemangiomas (HH) on Tc-99m-RBC imaging was described as lack of increased activity on early flow images and a gradual increase in activity on blood pool images over time [97] while HCCs show increased flow as well as increased activity on delayed images; however, other studies found no cases in which HCC demonstrated increased activity on either planar or SPECT-delayed images [98]. In addition, perfusion in small and/or deeply situated lesions is difficult due to the limited resolution of dynamic imaging. Moreover, it quickly became obvious that the sensitivity of planar Tc-99m-RBC imaging is unacceptably low, ranging from 30 to 53% [98–104]. The sensitivity of SPECT RBC imaging is but still heavily dependent on the lesion size. Reports published in the 1990s showed overall sensitivity of 70–80% using single-head SPECT [101–103, 105]. Using triple-head cameras [99, 104], the sensitivity was 17–20% for the detection of lesions smaller than 1 cm, 65–80% for lesions between 1 and 2 cm, and virtually 100% for lesions equal to or larger than 1.4 cm (Fig. 10.21). It is remarkable that the specificity and positive-predictive value of both planar and SPECT RBC (Fig. 10.22) imaging is essentially 100% [98–104]. For all of these reasons, neither flow nor delayed planar imaging needs to be a

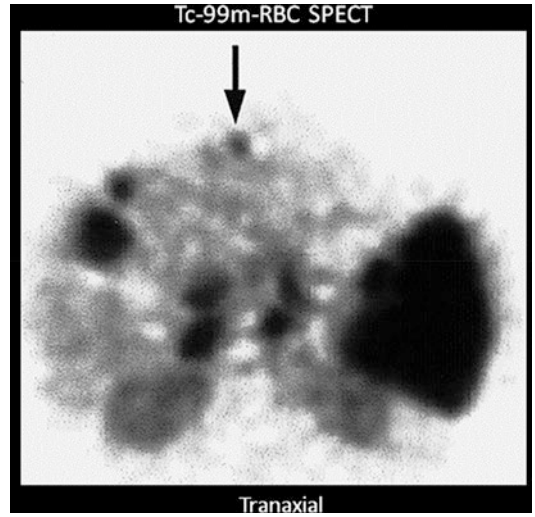

Fig. 10.21 Selected image of Tc-99m-RBC SPECT images of the liver reveal multiple hemangiomas. The smallest one (*arrow*) was 0.7 cm

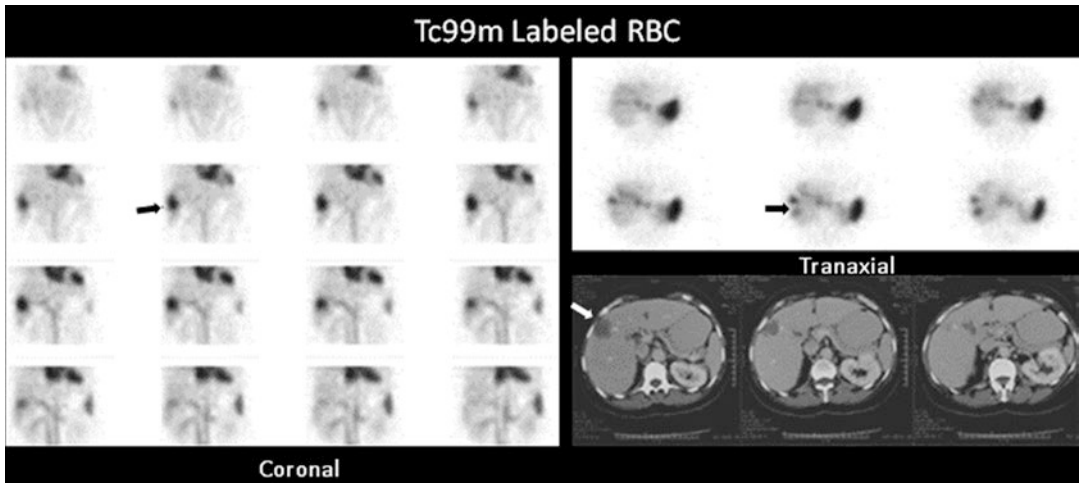

Fig. 10.22 Representative images of a tomographic radionuclide hemangioma study showing a solitary hemangioma (*arrow*) corresponding to the finding on CT but clarifying its nature with high specificity

routine part of the Tc-99m RBC study for evaluation of HH.

False-negative results were reported in cases of HH with extensive thrombosis and/or fibrosis [97]. Several false-positive cases related to various malignancies, including HCC as mentioned above, angiosarcomas, metastases, and hepatic lymphoma, have been reported in the literature [105–107]. However, the occurrence of such false-positive results seems extremely rare in view of the 100% specificity in virtually all studies other than case reports.

When dedicated SPECT imaging is performed, a lesion situated adjacent to large intrahepatic vessels, inferior vena cava, or right kidney needs to be cautiously evaluated to avoid either false-negative or false-positive results [108]. A SPECT/CT hybrid system is becoming more widely available, and fusion imaging lowers the false results [109, 110].

Tc-99m RBC SPECT imaging was reported to be more useful than MRI for evaluation of HH in 1990 because of the lower cost and higher specificity [111]. Despite its near-perfect specificity and positive-predictive value, Tc-99m RBC imaging does not appear to be fully utilized, which may be in part due to improved specificity of other anatomical imaging modalities [112, 113]. Given that, a new prospective head-to-head comparison of SPECT/CT with MRI or ultrasound for evaluation of HH may be needed.

10.2.3.4 Focal Nodular Hyperplasia

Focal nodular hyperplasia contains variable quantities of normal hepatic cellular elements, including Kupffer's cells, hepatocytes, and bile ducts arranged in a characteristic pattern. The characteristic triad suggesting FNH has been described as arterial blood flow (Fig. 10.23), normal colloid uptake, and accumulation of Tc-99m-IDA tracer [115].

Thirty to seventy percent of FNHs have either normal or increased Tc-99m-colloid uptake (Fig. 10.23a) [97, 116], reflecting the variable quantity of Kupffer's cells. Decreased Tc-99m-colloid uptake may be seen in approximately one-third of cases (Fig. 10.23b) [116]. Because of the presence of hepatocytes in FNH, Tc-99m-IDA scintigraphy has also been evaluated for the diagnosis of FNH. Of 25 FNHs in a study, 19 (76%) showed hyperperfusion during the flow phase and 23 (92%) appeared as focal regions of increased uptake during the clearance phase of hepatobiliary imaging. Normal sulfur colloid uptake was seen in 16 (64%) [92]. The detectability of FNH by Tc-99m-IDA scintigraphy was 92%, greater than that of CT (84%) or MRI (84%).

10.2.3.5 Hepatocellular Adenoma

Hepatocellular adenomas typically appear as photopenic defects on Tc-99m-colloid scintigraphy. In the past, this was attributed to the absence of Kupffer's cells [117]. However, a pathological study demonstrated that all hepatic adenomas studied contained Kupffer's cells [118]. Yet most of these lesions (77%) did not demonstrate Tc-99m-colloid uptake for unknown reasons. The authors found no significant histological difference between those lesions that accumulate colloids and those that do not. They also suggested that adenoma should be added to the differential diagnosis of a hepatic lesion with Tc-99m-colloid uptake because of the presence of uptake in 23% of their cases.

10.2.4 Biliary Tract Diseases

Bile flowing through the common hepatic duct may flow either into the gallbladder or through the common bile duct (CBD) into the duodenum. The quantity of bile flowing in either direction is determined to a major degree by the pressure developed by the sphincter of Oddi. In normal individuals, bile flows into the gallbladder when the sphincter of Oddi is contracted. Foods containing lipids and amino acids enter the duodenum and cause release of endogenous cholecystokinin (CCK) from the duodenum to the upper jejunum, which in turn contracts the gallbladder, dilates the sphincter of Oddi, and increases bile secretion from the hepatocytes. All of these enhance the flow of bile into the duodenum.

On a typical normal cholescintigram performed with Tc-99m-IDA agents, the CBD and gallbladder are visualized 10–20 min following

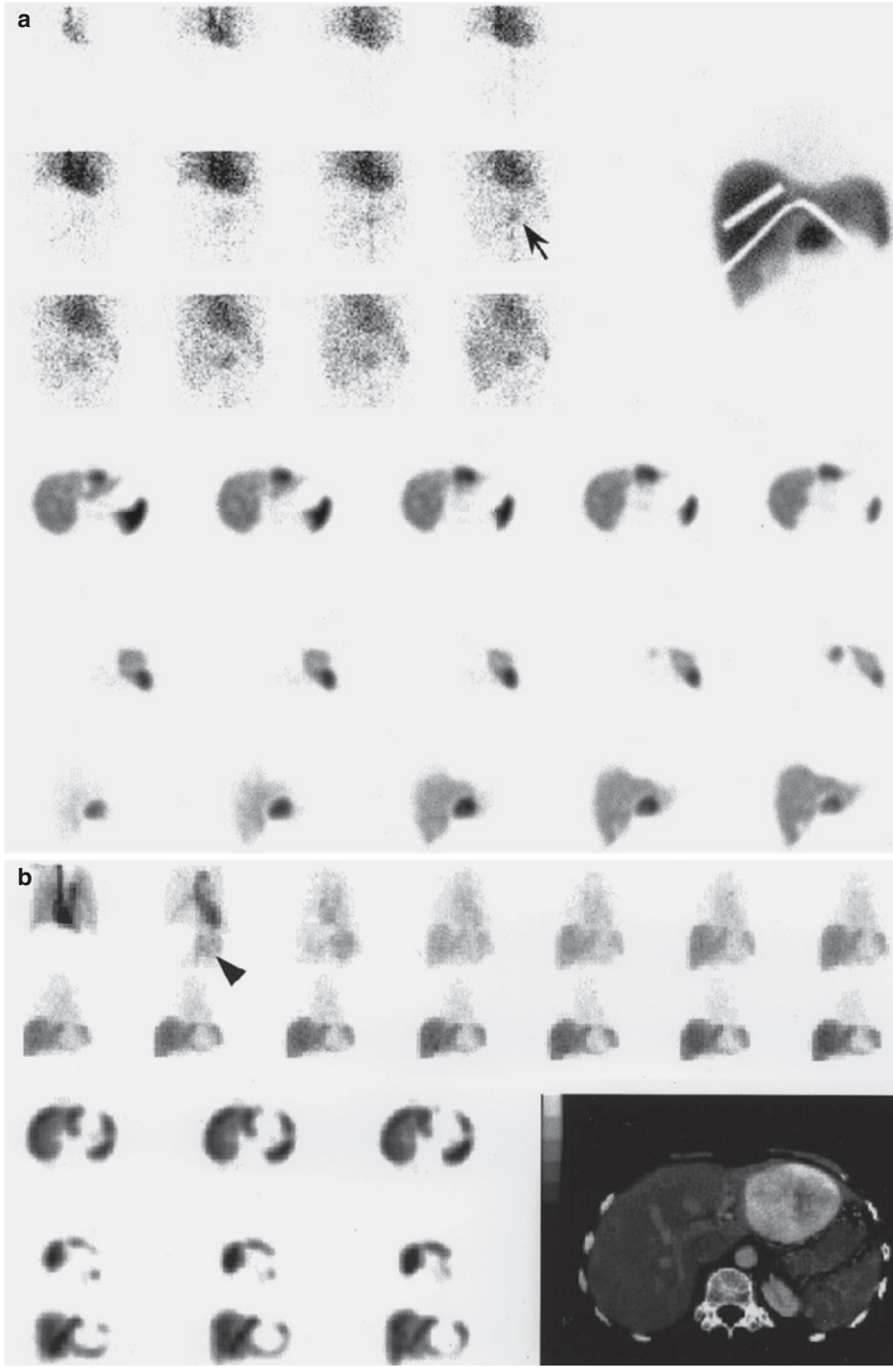

Fig. 10.23 (**a**, **b**) Tc-99m sulfur colloid studies in two cases of focal nodular hyperplasia. While both case **a** and case **b** show increased early arterial flow (*arrow, arrowhead*), colloid uptake is increased in case **a** and decreased in case **b** on delayed views. (Reprinted from Kim et al. [114] with permission)

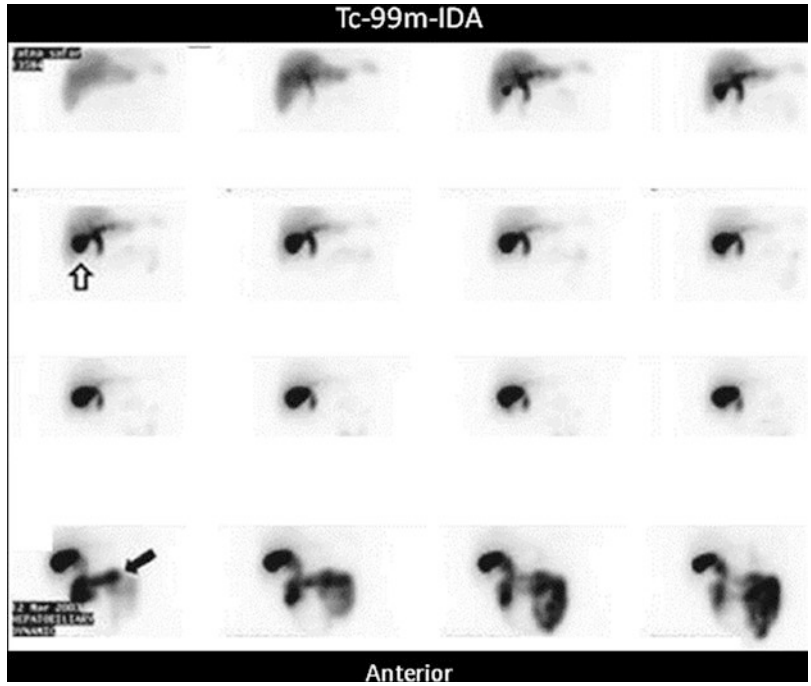

Fig. 10.24 Normal radionuclide hepatobiliary study with prompt visualization of gall bladder (*open arrow*) and intestinal activity (*solid arrow*)

the intravenous administration of Tc-99m-IDA (Fig. 10.24). Visualization of the small bowel varies depending on the sphincter tone and the degree of gallbladder filling.

10.2.4.1 Acute Cholecystitis

Although it is generally known that acute cholecystitis in 90–95% of cases begins with obstruction of the neck of the gallbladder or the cystic duct by a gallstone, some authors feel that obstruction does not necessarily lead to acute cholecystitis [119]. Nevertheless, obstruction is present in almost all cases of acute cholecystitis. There are other important factors in the pathogenesis of acute cholecystitis, including chemical factors such as prostaglandins and bacterial growth . Injury to the gallbladder mucosa by a mechanical or chemical factor stimulates the epithelial cells to secrete fluid. Active fluid secretion in the obstructed gallbladder lumen increases the intraluminal pressure, which may cause impairment of circulation and ischemia of the gallbladder mucosa (Fig. 10.25) and wall. Distention of the gallbladder further enhances formation of

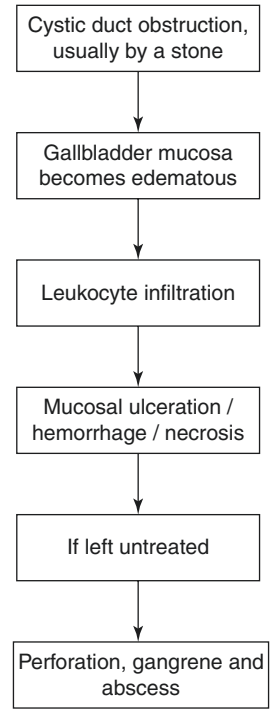

Fig. 10.25 Pathophysiologic features of acute cholecystitis

prostaglandin, establishing a vicious cycle [120]. Active fluid secretion in the gallbladder wall is markedly reduced by morphine. The acceleration of the process can be reduced by morphine [121].

Approximately 60–70% of patients report prior attacks that resolved spontaneously. The factors regulating the intraluminal pressure may determine the course of an attack of acute cholecystitis. Of the 75% of patients with acute cholecystitis who experience remission of symptoms, approximately one quarter will experience a recurrence of cholecystitis within 1 year, and 60% will have at least one recurrent attack within 6 years [122]. Therefore, the histological pattern of acute cholecystitis is superimposed upon chronic inflammatory changes in at least 90% of cholecystectomy specimens [123].

Acalculous form of acute cholecystitis is less common (less than 10%) of patients with acute cholecystitis [124]. Despite the absence of gallstones, the cystic duct is frequently obstructed by viscous bile, sludge, cellular debris or edema associated with dehydration [125]. Precipitating factors include severe trauma or burns, the postpartum period following prolonged labor, a major operation, prolonged parenteral hyperalimentation, vasculitis, obstructing tumor of the gallbladder, and parasitic infestation of the gallbladder. It also may be seen with a variety of other systemic diseases (sarcoidosis, cardiovascular disease, tuberculosis, syphilis, actinomycosis, etc.) [122]. Apart from the absence of stones, the pathology of acalculous and calculous cholecystitis is essentially identical [126].

10.2.4.2 Imaging for Acute Chelecyctitis

Acute cholecystitis is the most common indication for cholescintigraphy, which is considered the procedure of choice for its diagnosis [127]. Generally, nonvisualization of the gallbladder up to 4 h after radiotracer administration or within 30 min after the administration of morphine sulfate is interpreted as consistent with cystic duct obstruction, provided that there is normal hepatic uptake and excretion. Gallbladder visualization anytime during imaging virtually excludes the presence of acute cholecystitis. The study can be obtained as planar, SPECT, or SPECT/CT.

Meta-analysis of 2466 patients showed a sensitivity of 97% and specificity of 90% [127]. Conventional imaging protocols frequently require delayed imaging for up to 4-h postinjection or even up to 24 h in patients with severe intercurrent disease to achieve a sufficiently high level of accuracy. Delayed imaging is logistically inconvenient. It can be potentially disadvantageous to the patient, and it may not be feasible in some clinical settings. Efforts to increase the specificity of the test and/or to shorten the total imaging time were made using pharmacological interventions, which include morphine augmentation and CCK pretreatment [128].

Despite the superiority of cholescintigraphy over ultrasonography (US) for evaluation of acute cholecystitis that has been known for decades and confirmed repeatedly as the best single noninvasive test for the diagnosis of acute checystitis [128]. US is still often the first diagnostic test being ordered in many institutions. A most recent (and seemingly largest) meta-analysis report, including 57 studies and 5859 patients, published in 2012 confirmed that cholescintigraphy has the highest diagnostic accuracy of all imaging modalities in the detection of acute cholecystitis [129].

10.2.4.3 Causes of False-Positive Results of Cholescitigraphy for Acute Cholesystitis

Several conditions are known to be potential causes for false-positive results on cholescitigraphy resulting in false non visualization of gall bladder (Table 10.9). Insufficient fasting will result in gallbladder contraction induced by circulating endogenous CCK, thereby inhibiting

Table 10.9 False-positive cholescintigraphy for acute cholecytitis

1. Non-fasting (less than 3–4 h)
2. Prolonged fasting (more than 24 h)
3. Total parentenral nutrition
4. Severe concurrent disease
(a) Severe postoperative complications
(b) Massive trauma
(c) Sepsis
(d) Acute respiratory syndrome
5. Hepatocellular disease
6. Chronic cholecystitis

bile flow into the gallbladder. Delayed imaging and certain interventions are used to minimize false-positive results.

Secondary Scintigraphic Signs of Acute Cholecystitis

Rim Sign

This pattern represents increased IDA activity in the liver parenchyma around the gallbladder fossa "rim sign" (Fig. 10.26). The presence of this sign is frequently associated with acute cholecystitis, which is often complicated, i.e., gangrenous gallbladder [128]. This pericholecystic activity appears to be caused by increased blood flow to [130] and/or delayed bile excretion from inflamed liver parenchyma adjacent to an inflamed gallbladder [131].

At times, a rim sign with marked tracer retention may mimic the gallbladder appearance

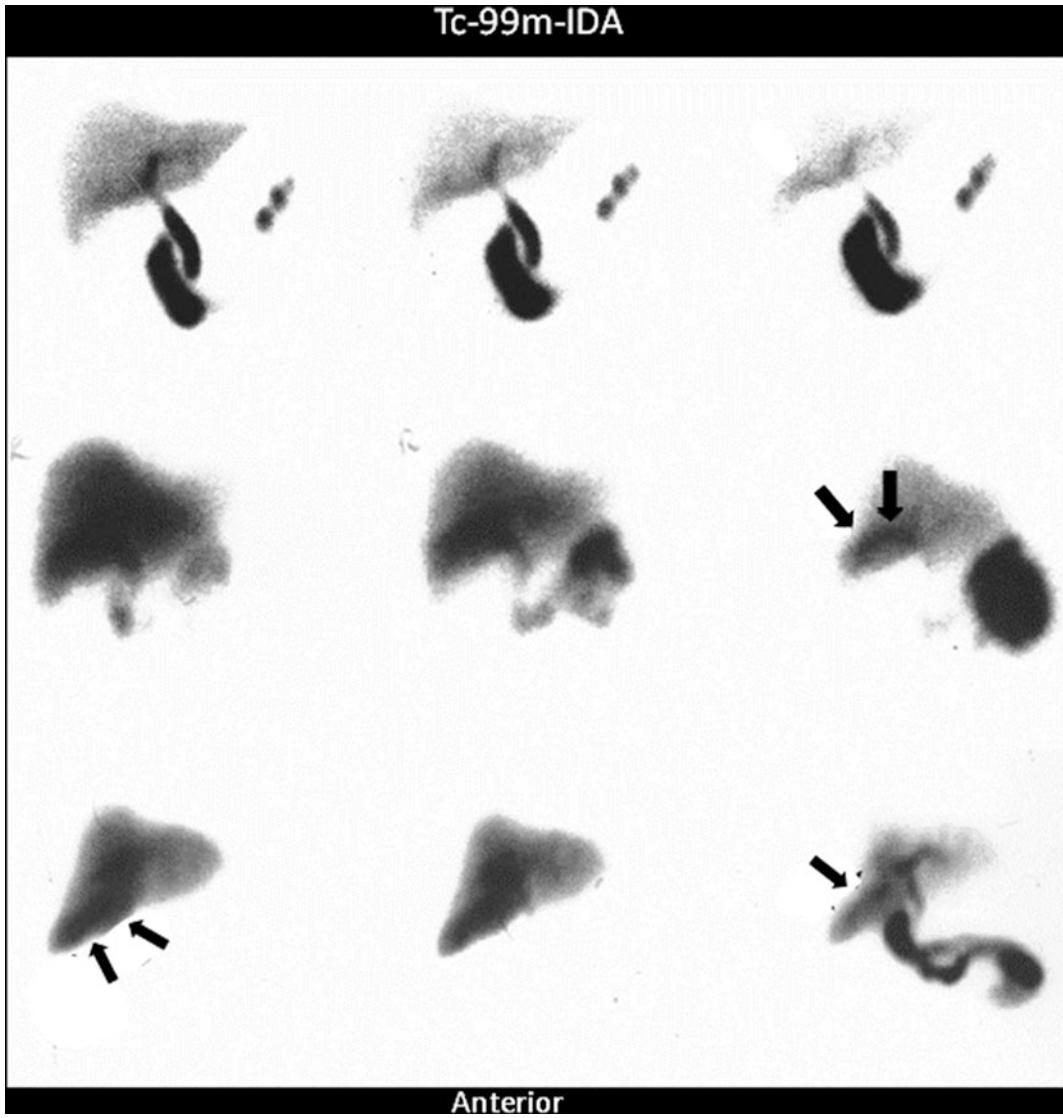

Fig. 10.26 A spectrum of rim signs. A mild rim sign is seen in the Tc-99m-IDA study of patient 1 (*arrow*). The rim sign in patient 2 is quite prominent and clearly seen as a rim. The rim sign in patient 3 is more diffuse and may be confused with the gallbladder. However, this activity is present on the early image (*large arrows*) even before the tracer activity appears in the bile ducts. (From Kim [108] with permission)

(patient 3 in Fig. 10.26), in which case the presence of such activity on the early images before the appearance of bile duct activity can help to exclude the possibility of gallbladder filling. The rim sign, though suggestive of acute cholecystitis, is not sufficiently specific to obviate interventions such as delayed imaging or morphine augmentation.

10.2.4.4 Chronic Acalculous Biliary Syndromes

This group includes chronic acalculous cholecystitis, cystic duct syndrome, and gall bladder dyskinesis. Approximately 98% of patients with symptomatic gallbladder disease have gallstones. Occasionally, patients have signs and symptoms of gallbladder disease, but no stone can be demonstrated by repeated ultrasound or oral cholecystography [132]. Chronic biliary-type pain in patients with no stones may be due to chronic acalculous biliary disorders, including chronic acalculous cholecystitis, cystic duct syndrome, a functional disorder such as gallbladder dyskinesia, and sphincter of Oddi dysfunction. Nonbiliary disease such as the irritable bowel syndrome may cause the same symptoms. Sincalide has been used for the evaluation of gallbladder ejection fraction (GBEF) or sphincter of Oddi response in this patient group to determine who might benefit from cholecystectomy, sphincterotomy, or smooth muscle relaxants.

The pathological findings of chronic acalculous cholecystitis are nearly identical to those of chronic calculous cholecystitis, except for the absence of stones [133]. Intermittent acalculous cystic duct obstruction and chronic ischemia with active inflammatory changes have both been postulated as possible pathogenic mechanisms.

The cystic duct syndrome results from a partial acalculous obstruction or narrowing of the cystic duct [124], which may be due to fibrosis, kinking, or adhesion.

Gallbladder dyskinesia histologically show no abnormal findings. Abnormal and/or inhomogeneous CCK receptors within the gallbladder, which cause a paradoxical or inhomogeneous response to cholecystokinetic agents, were suggested as a possible mechanism [134]. In this condition, right upper quadrant pain occurs following meals as a result of increased intraluminal gallbladder pressure. Other possible mechanisms of impaired gallbladder motility include a primary smooth muscle disorder and altered release of endogenous CCK [135].

In cholesterosis, the mucosa of the gallbladder is studded with minute yellow lipid flecks, producing the strawberry appearance [125]. In some patients suspected of having chronic acalculous biliary disease, cholesterosis has occasionally been the only histological finding, without evidence of other diseases [136]. Although cholesterosis is not often of clinical significance [125], cholecystectomy is indicated when the condition is symptomatic.

Biliary Sphincter (Sphincter of Oddi) Stenosis/Obstruction

Biliary Sphincter disorder occurs mostly in patients after cholecystectomy. It is much more common in female patients can be classified into two broad categories: stenosis (by stone or a fixed structural narrowing) and dyskinesia (functional disorder: a primary disorder of tonic/phasic motor activity) [137].

Measurement of the sphincter of Oddi pressure using sphincter manometry is considered the gold standard for the diagnosis. An elevated basal pressure (>40 mmHg) is considered the only consistent manometric criterion which is correlated with patients' symptoms and also with relief of symptoms with therapy [138].

The treatment of choice for patients with sphincter of Oddi stenosis is endoscopic sphincterotomy.

Hepatobiliary imaging with or without pharmacological intervention has also been shown to be useful in patients with SOD, and investigations have focused primarily on patients after cholecystectomy. A number of parameters have been derived from the time-activity curves of the liver parenchyma, hilum, CBD, entire hepatobiliary tract (liver and bile ducts), and bowel. These include the time of peak activity (T_{max}), excretion half-time ($T1/2$), percentage of excretion at a certain time (i.e., 45, 60 min), excretion rate, and mean transit time. Visual parameters such as

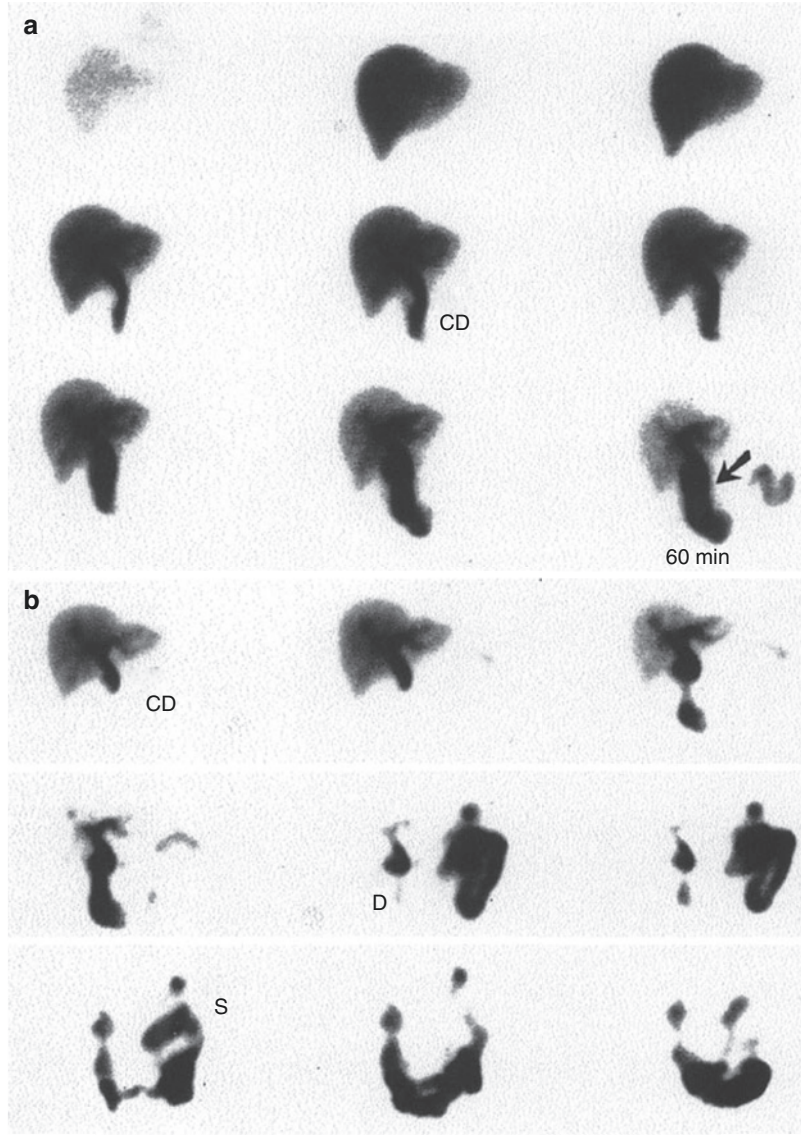

Fig. 10.27 (**a**, **b**) SOD: stenosis. This 50-year-old woman was seen at 3 years' postcholecystectomy with chronic recurrent pain. ERCP showed no mechanical obstruction, but the basal sphincter of Oddi pressure was elevated (45 mmHg). (**a**) Preoperative cholescintigraphy shows delayed hepatobiliary clearance with retention of activity in the common bile duct (*CD*) at 60 min (*arrow*). Increasing activity within the duodenum (*D*) is noted. A second preoperative study (not shown here) with constant CCK infusion (40 ng/kg/60 min) was not significantly different (i.e., there was a fixed papillary stenosis). (**b**) Postsphincterotomy study in the same patient shows significant improvement with rapid hepatobiliary and common duct clearance compared with the preoperative study. *S*, stomach. (Reprinted from Ziessman [139] with permission)

the time of first appearance of the intrahepatic biliary tree, and the bowel, CBD emptying, and CBD-to-liver ratio (comparison of CBD activity at 60 min with liver activity at 15 and 60 min) have been added to the above semiquantitative parameters [139].

These parameters have also been found useful in assessing the benefit of endoscopic sphincterotomy (Figs. 10.27 and 10.28) [140].

Although scintigraphic studies on this subject have focused primarily on the differentiation between the presence and absence of SOD, it can be also useful in discriminating between stenosis and functional dyskinesia [140] (Fig. 10.29).

10.2.5 Interventions in Cholescintigraphy

Several drugs, including cholecystokinin (CCK), morphine, and phenobarbital, have been used to alter biliary kinetics at different levels (i.e., hepatocytes, gallbladder, and/or sphincter of Oddi) in an effort to increase the efficacy of hepatobiliary

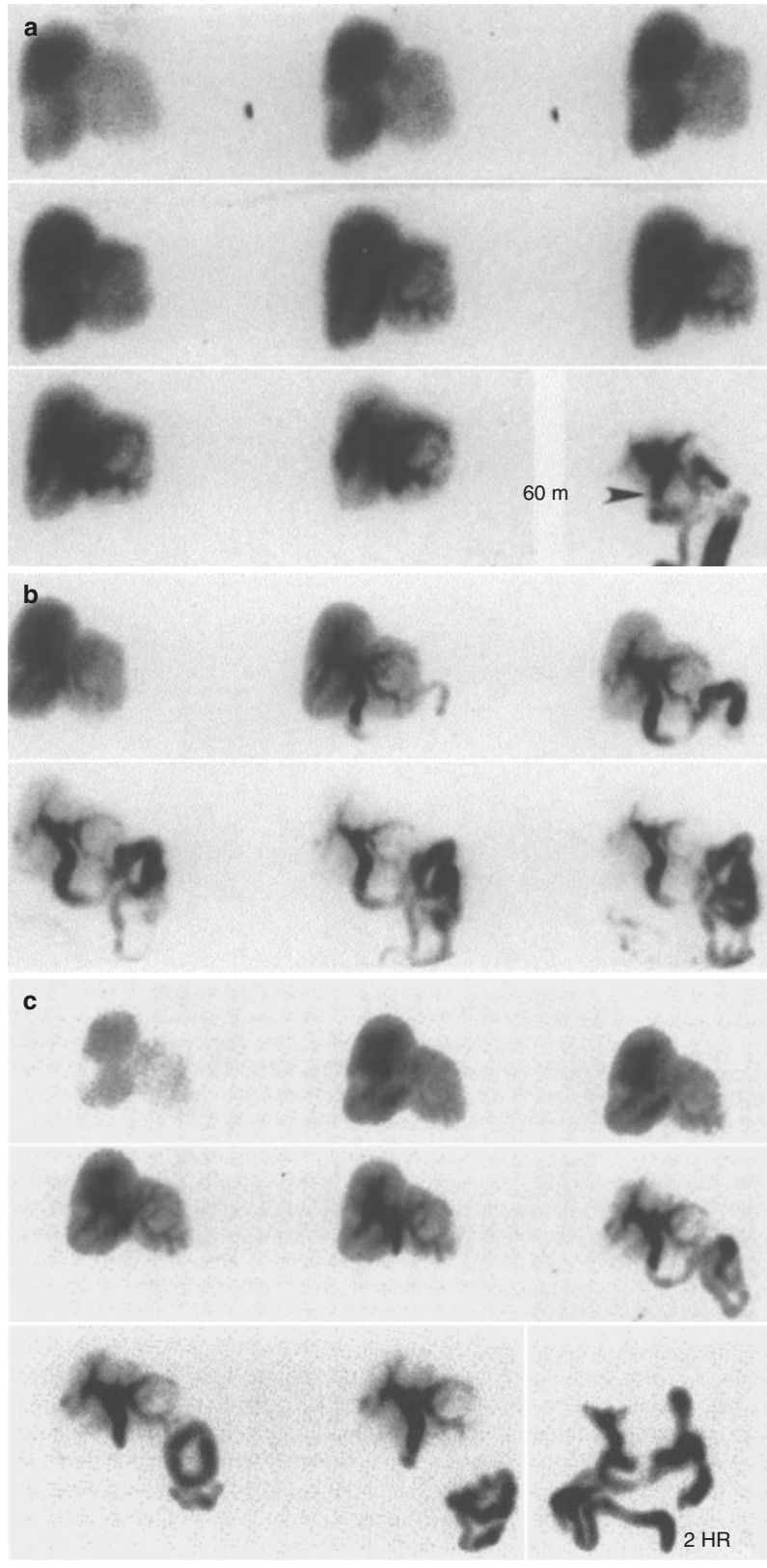

Fig. 10.28 (**a**–**c**) SOD: dyskinesia. Postcholecystectomy pain syndrome. An ERCP showed no mechanical obstruction. The sphincter of Oddi pressure was 48 mmHg. A sphincterotomy was performed. (**a**) Preoperative study. Sequential analog images over 60 min show a prominent intrahepatic collection system with dilatation in the region of the common hepatic duct at 60 min. A delayed image at 2 h shows that the obstruction is really at the level of the sphincter of Oddi (*arrowhead*). (**b**) Preoperative study with a continuous infusion of sincalide, 40 ng/kg/60 min. Hepatobiliary clearance is more rapid than the study without CCK. However, at the end of 60 min, there is retained activity in a prominent common duct. This is an obstructed dyskinetic sphincter of Oddi. (**c**) Postsphincterotomy study. There is still prominent retention in the common duct, but hepatobiliary clearance has significantly improved since the baseline study (**a**) and, interestingly, looks similar to the preoperative CCK study (**b**). (From Ziessman [139] with permission)

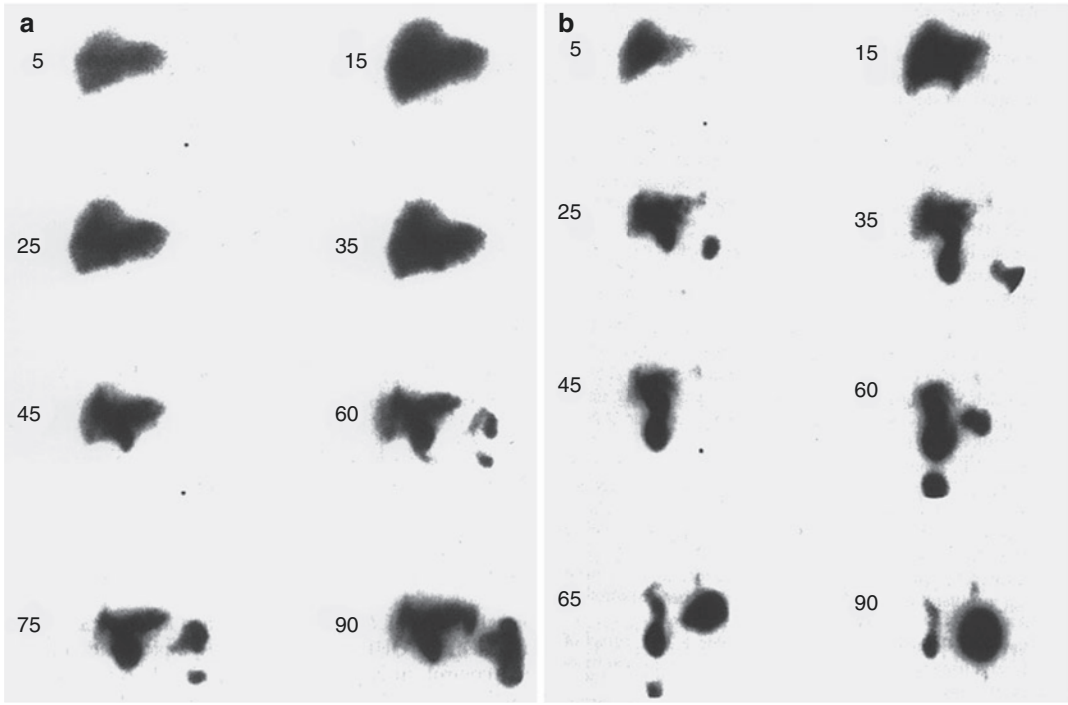

Fig. 10.29 (**a**) Stenosis of the sphincter of Oddi (structural SOD). Biliary tree activity is initially visualized at 25 min after injection of Tc-99m-IDA. The CBD and intrahepatic biliary tree appear prominently at 45 min and do not change significantly during amyl nitrate inhalation from 60 to 90 min. (**b**) Sphincter of Oddi dyskinesia (functional SOD). Biliary tree activity is first visualized at 15 min. The CBD and intrahepatic biliary tree appear prominently from 25 up to 60 min. The small bowel is first visualized at 25 min. Note a marked decline in CBD activity during amyl nitrate inhalation from 60 to 90 min. (From Madacsy et al. [141] with permission)

imaging. Sincalide, a synthetic C-terminal octapeptide of CCK, has been used in the diagnosis of acute cholecystitis in order to empty the gallbladder before cholescintigraphy, so that gallbladder filling can be enhanced during the study if the cystic duct is patent. These agents are also used to evaluate gallbladder ejection fraction (GBEF) and/or sphincter of Oddi response in patients with suspected chronic, acalculous biliary tract diseases to determine who might benefit from cholecystectomy or sphincterotomy.

10.2.5.1 Cholecysystokinin (CCK) Administration

CCK is a polypeptide hormone normally released from mucosal cells of the proximal small bowel in response to fat and protein ingested. CCK is bound to receptors in the gall bladder and sphincter of Oddi resulting in gall bladder wall contraction and sphincter of Oddi relaxation. CCK can be used in several situation as one of the interventions with cholescintigraphy. It may be administered before cholescintigraphy or after the 60 min study ends (Table 10.10).

Table 10.10 Uses of CCK associated with cholescitigraphy

1. Administration prior to cholescitigraphy
(a) Prolonged fasting and total parenetral nutrition
(b) Suspected biliary sphincter (Sphincter of Oddi) dysfunction
2. Administration after 60 min study
(a) Chronic acalculous cholecystitis
(b) Differentiate common bile duct obstruction from functional etiology
(c) Exclude acalculous form of acute cholecystitis when gall bladder is visualized

CCK Pre-cholescingraphy Administration for the Diagnosis of Acute Cholecystitis

Administration of CCK prior to injection of Tc-99mIDA will induce gallbladder empty-

ing with a reduction of intraluminal pressure. It was introduced as a means of reducing potential false-positive results for acute cholecystitis and of shortening the total imaging time [140]. The rationale of this approach is that gallbladder emptying before initiating the study is generally followed by more reliable gallbladder filling during the cholescintigraphy. Although sincalide pretreatment of all patients may not be necessary, it is often used in conditions such as alcoholism and total parenteral nutrition and during a prolonged fasting state, because functional resistance to tracer inflow may result from distention of the gallbladder with viscous contents. Fasting for 24 h or longer is a routine indication for the preadministration of sincalide in many laboratories.

It should be noted that a meticulous sincalide infusion technique is important to ensure good gallbladder emptying. At a dose of 0.02 μg/kg the drug is infused slowly over 30 and up to 60 min [85]. If this long infusion is logistically inconvenient, a 3-min infusion at the physiological rate of 3.3 ng/kg/min [86], or an infusion for up to 10 min at the same or slightly lower rate approximately 15–30 min before injection of Tc-99m-IDA, is probably adequate for this application.

CCK Pre-cholescingraphy Administration for Suspected Biliary Sphincter (Sphincter of Oddi) Dysfunction

CCK is infused at a dose of 0.02 μg/kg over 3–10 min 15 min prior to injection of IDA derivative and then study is carried out for the initial standard of 60 min [85]. If the condition is not post-cholecystectomy, longer infusion for 45–60 min is carried out after the initial cholescintigraphy study and GBEF is determined since if it is useful in predicting the outcome of sphincterotomy.

CCK Post-cholescingraphy Administration for Acalculous Biliary Syndromes

Determination of GBEF after CCK administration is important for confirmation of this group of disorders and also in predicting the outcome of surgery. The technique for administration of CCK is of the utmost importance. The degree of gallbladder emptying is dependent on the CCK dose and rate of administration, as well as on the total number of receptors in the gallbladder wall smooth muscle. Spasm of the neck of the gallbladder and decreased GBEF may occur due to unphysiologically high serum levels of sincalide following a bolus injection. This paradoxical response is attributable to the different threshold level of the CCK receptors in the body and fundus of the GB and cystic duct. The cystic duct does not contract when the dose of CCK is physiological. Therefore, this agent should not be given as a bolus. Although infusion of 20 ng/kg sincalide over 2–4 min (an average dose rate of 6.6 ng/kg/min) was once a popular technique [140–145], this dosage protocol has also been demonstrated to be unphysiological [86, 145]. Aside from frequent incomplete gallbladder emptying, infusion of 20 ng/kg over 3 min or less is often associated with such side effects as abdominal discomfort, pain, and nausea.

Comparison of various sincalide doses for a 3-min infusion technique demonstrated that 10 ng/kg (the rate of 3.3 ng/kg/min) produces maximal gallbladder emptying [86]. With further increase of the dose rate, i.e., 20 ng/kg/3 min, the GBEF actually decreases. The normal GBEF value using 10 ng/kg/3 min was established as greater than 35%. Falsely reduced GB emptying associated with a 3-min infusion of 20 ng/kg of sincalide is illustrated well in Fig. 10.30 [146]. However, Ziessman et al. showed that even the infusion at a so-called physiological rate (10 ng/kg infused over 3 min) produces an excessively variable GBEF response to establish a clinically useful and reproducible normal range compared with the same dose infused over a longer period, i.e., 10 ng/kg infused for 60 min [147]. Although the optimal dose and duration of infusion is the subject of some controversy, a long infusion seems to produce more complete gallbladder emptying and less severe side effects than a short infusion, probably due to the 2.5-min plasma half-life of sincalide. When performing and interpreting sincalide-augmented hepatobiliary imaging, it is important to adhere to a specific sincalide infusion technique and to use normal GBEF values that have been validated for that particular method. Recently, an interdisciplinary

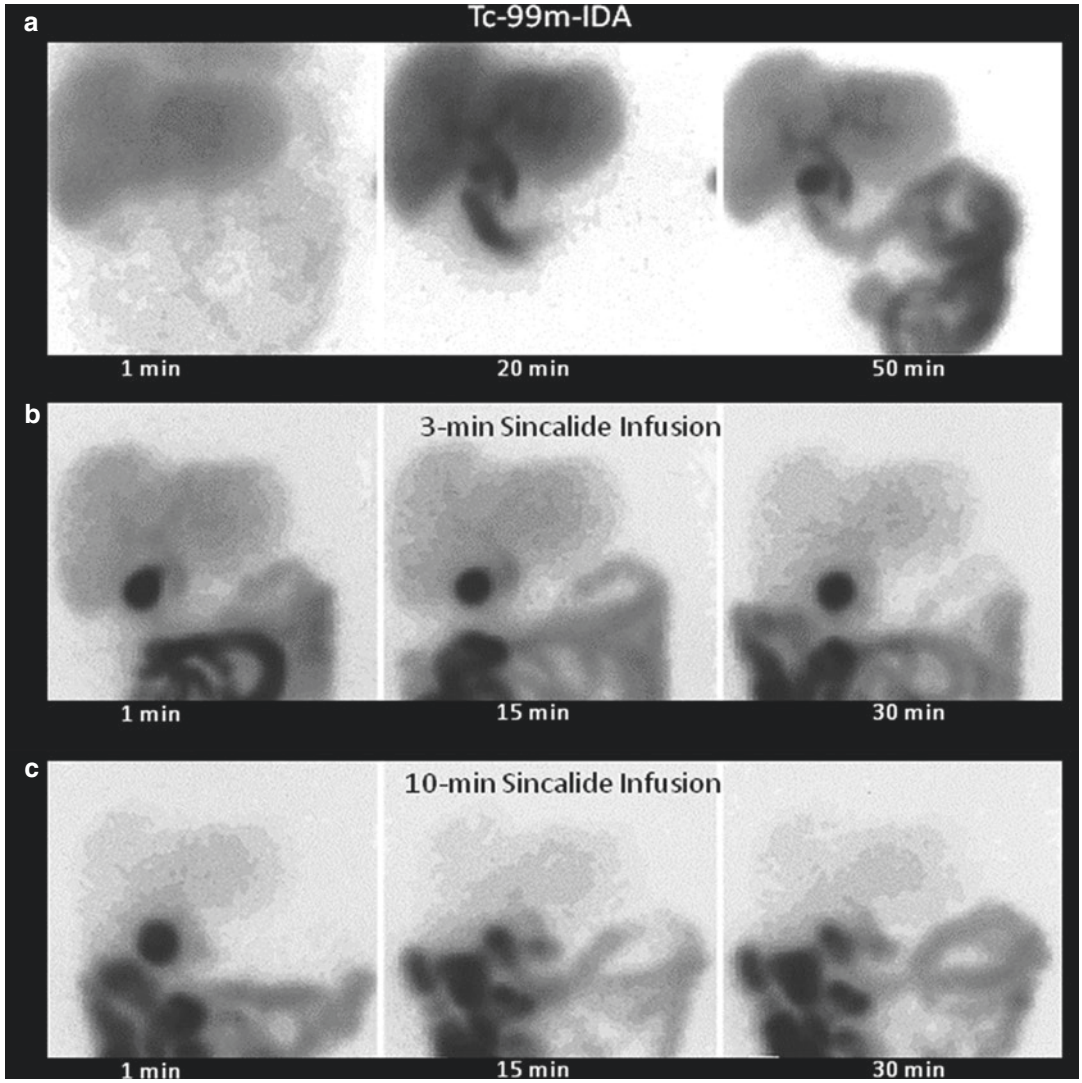

Fig. 10.30 A hepatobiliary scan using Tc-99m-IDA performed in a patient with suspected chronic acalculous biliary disease. The scan shows prompt visualization of the GB and small bowel (**a**). Following a 3-min infusion of 20 ng/kg sincalide, the GB is poorly contracted, with an EF of approximately 10% (**b**). Immediately after this, a 10-min infusion of the same dose produced a GBEF of 80% (**c**)

panel suggested that the optimal sincalide infusion method is 20 ng/kg/60 min with 38% as the lower limit of normal GBEF [148].

Various fatty meals have been evaluated as an alternative to sincalide. However, controversy exists over the use of fatty meals versus sincalide. The major disadvantage of meal stimulation is that an abnormal GB response may result from factors other than the GB, such as poor gastric emptying, pancreatic insufficiency, celiac disease, or abnormal bowel transit [149–153]. The onset of meal-induced GB emptying can also vary during different phases of the migrating motor complex at the time of ingestion [154]. The choice between fatty meal and sincalide can probably be made on the basis of the population being studied. Meal stimulation would be preferable when GB function in relation to the rest of the GI tract needs to be evaluated. However, evaluation of GB function independent of the

digestive process may be better achieved with sincalide when different patient populations are studied [155]. Nonetheless, a fatty meal can serve as an alternative in the case that sincalide is not available for clinical use. However, when used, careful attention should be paid to the fat content, texture, taste, manner of administration, and measurement time sequence, all of which need to be standardized [156]. Normal values for each center must be established when choosing a meal.

In summary, the overall data favor the use of this test for the diagnosis of chronic acalculous gallbladder and cystic duct disease. A low GBEF can probably be interpreted as indicating a high probability for symptomatic relief after surgery, and vice versa. Bayes' theorem should then be applied, especially for the group with a normal EF, to make a clinical decision according to the posttest probability from a clinical suspicion (pretest probability) and the GBEF (test probability).

10.2.5.2 Morphine Augmentation

Bile is secreted continuously from the liver into the biliary system. The proportion of bile flowing into the gallbladder or the duodenum depends on the relative resistance to flow determined mainly by the contractile state of the gallbladder and the sphincter of Oddi. The resistance of the sphincter of Oddi is considered the principal factor in the regulation of the intracholedochal pressure and of the common bile duct-gallbladder pressure gradient [157]. The administration of morphine sulfate (morphine) results in contraction of the sphincter of Oddi. This, in turn, causes an increase in the intraductal pressure and forces the bile to flow into the gallbladder if the cystic duct is patent [158–160]. A widely used protocol an alternative to delayed imaging involves the administration of 0.04 mg/kg morphine intravenously over 3 min at 1 h after the injection of radiotracer, provided that activity is seen in the bowel. Generally, morphine is not administered during the first hour because (1) the gallbladder is visualized within 1 h in the majority of patients undergoing cholescintigraphy and (2) delayed filling of the gallbladder or delayed excretion into the bowel, suggesting the presence of chronic cholecystitis or other biliary tract disease, could be missed by the early administering morphine. After morphine administration, imaging is continued for an additional 30 min. Typically, the gallbladder is visualized within 30 min if the cystic duct is patent If visualization does not occur within 30 min, the findings are interpreted as consistent with acute cholecystitis (Fig. 10.31). Therefore, the entire study can be terminated at 90 min in contrast to 4 h or more with conventional delayed imaging without morphine augmentation. Reports by Chen et al. and Kim et al. [161, 162] show that morphine administration helps to visualize the gallbladder in 32–42% of patients with gallbladder nonvisualization at up to 60–90 min despite sincalide pretreatment. These results suggest that sincalide pretreatment alone is not sufficient to detect all patent cystic ducts.

Variants Associated with CCK and Morphine Intervention

Significantly delayed tracer excretion into the bowel associated with prompt and progressive gallbladder filling can be a normal variant seen in the fasting state [163]. Morphine administered to the patient prior to the study can have the same result. This finding is well known and is now actually used in a positive way to enhance gallbladder visualization during cholescintigraphy.

In a series by Kim et al., approximately 40–50% of subjects with prompt gallbladder filling showed a markedly delayed biliary-to-bowel transit after sincalide pretreatment (Fig. 10.32) compared with only 4% of patients who did not receive sincalide [164]. Delayed biliary-to-bowel transit, when present, should not necessarily be read as abnormal, i.e., as hyperacute or partial CBD obstruction. However, a hyperacute or partial CBD obstruction may not be totally excluded in certain clinical settings, although this pattern, with intact gallbladder visualization, is not typical of CBD obstruction. In such a situation, CCK administration can help to exclude CBD obstruction by inducing gallbladder contraction and demonstrating bowel activity [164].

Oates et al. [165] and Shih et al. [166] reported that morphine administration increases the frequency and the degree of duodenogastric reflux.

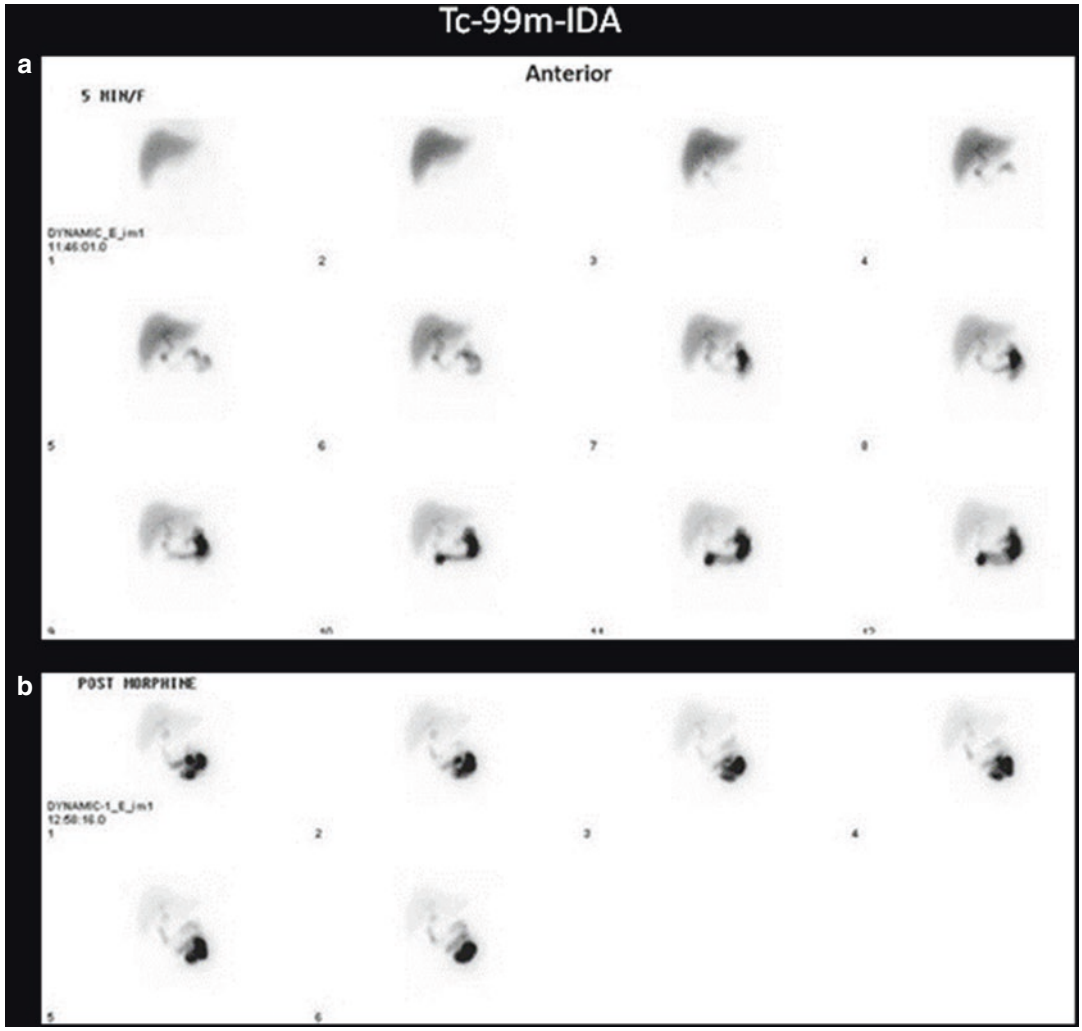

Fig. 10.31 Hepatobiliary study showing nonvisualization of gall bladder during routine study (**a**) and after low-dose morphine injection (**b**) in a patient suspected of having acute cholecystitis. The CBD and small bowel are promptly visualized but the gallbladder is not visualized up to 60 min. Following morphine administration, the gall bladder did not show filling. The finding indicates obstruction of the cystic duct which indicates acute cholecystitis in the clinical setting of this patient

In brief, in addition to its logistic advantage (shortening the imaging time), morphine augmentation provides more specific diagnosis for acute cholecystitis than does delayed imaging. Sincalide pretreatment, when administered at the physiological rate, will be helpful in conditions in which functional resistance to tracer flow into the gallbladder may be present. However, morphine augmentation will further improve the efficacy of the test even after sincalide pretreatment. The technique is therefore recommended for routine clinical use when the gallbladder is not visualized at 1 h.

10.2.6 Hyperbilirubinemia

Cholescintigraphy is often performed to differentiate surgical jaundice (CBD obstruction and biliary atresia) from medical jaundice (intrahepatic cholestasis and/or hepatocellular disease) in both adults and neonates. Alternatively, CBD obstruc-

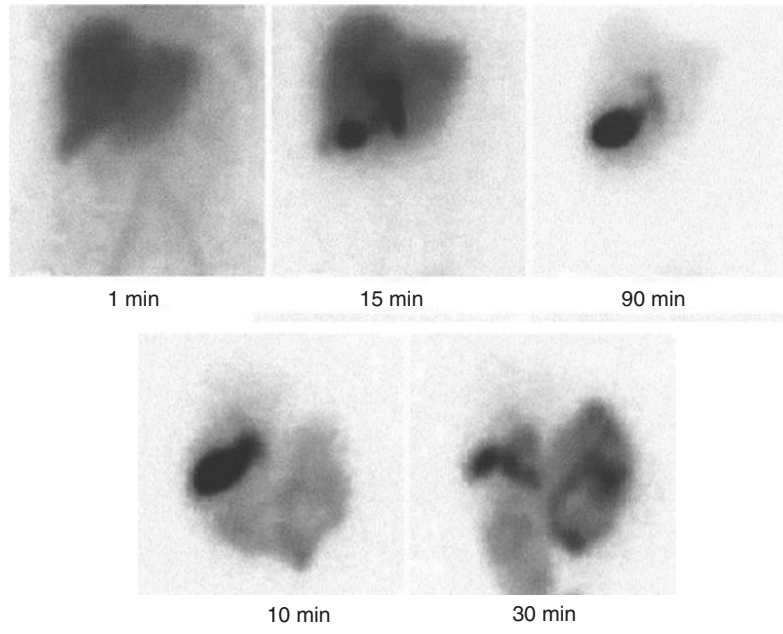

Fig. 10.32 The patient was pretreated with sincalide before receiving an injection of Tc-99m-IDA. The gallbladder filling is prompt but bowel activity is not identified until 90-min postinjection (**a**). Following administration of a second dose of sincalide (**b**), there is prompt tracer excretion into the bowel, which excludes common duct obstruction

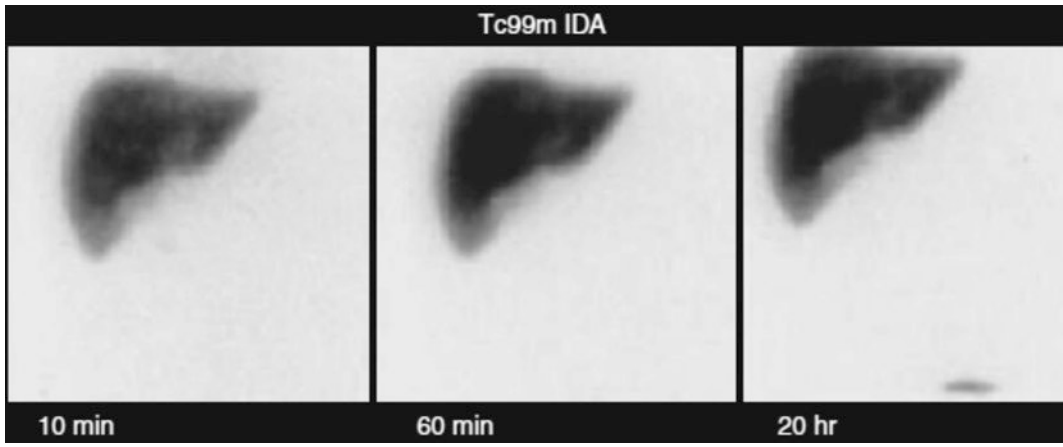

Fig. 10.33 The pattern of acute CBD obstruction imaged with Tc-99m-IDA. The initial hepatic uptake is prompt, with prolonged retention and no evidence of intestinal excretion throughout the study and on delayed image at 20 h pot injection

tion or intrahepatic cholestasis is occasionally detected incidentally on cholescintigraphy performed in patients who present with abdominal pain.

10.2.6.1 Common Bile Duct Obstruction

Cholescintigraphy is useful to diagnose biliary obstruction in patients with normal ultrasonography and who are not clearly jaundiced and only mild liver dysfunction as if serum bilirubin levels are high, bilirubin occupies the available receptors and blocks the IDA uptake since both have the same mechanism for uptake by hepatocytes. Prompt hepatic uptake of IDA that persists 2–4 h (sometimes even up to 24 h) without evidence of biliary excretion is the obstructive pattern that has been commonly described (Fig. 10.33) [167,

168]. The presence of an obvious photopenic defect in the area of the porta hepatis corresponding to dilated bile ducts or slow tracer filling of dilated bile ducts makes CBD obstruction more likely. The presence of intestinal activity without visualization of the CBD makes intrahepatic cholestasis more likely. However, without ancillary findings, the distinction between a high-grade CBD obstruction and a high-grade intrahepatic cholestasis (with relatively preserved hepatocyte function) may be difficult. Ultrasonography may play a complementary role in this situation.

In patients with partial CBD obstruction, cholescintigraphy may demonstrate absence of intestinal activity, delayed biliary-to-bowel transit, and/or a prominent ductal pattern persistent for 2 h [168]. When CBD obstruction is suspected, the patient should not be pretreated with sincalide, which may cause prompt gallbladder filling with delayed biliary-to-bowel transit, as discussed earlier. Poor hepatic uptake with persistent blood pool activity of IDA in jaundiced patients generally indicates hepatocellular disease, regardless of the presence or absence of bowel activity (Fig. 10.32).

Quantification of hepatocyte function by measuring the hepatocyte extraction fraction (HEF) of IDA agents with deconvolutional analysis was reported to be useful for the distinction between CBD obstruction and hepatocellular dysfunction [169–171]. Despite profound hyperbilirubinemia, patients with CBD obstruction typically have only slightly reduced HEF values compared with normal controls, whereas patients with hepatocellular dysfunction have markedly reduced HEF values.

10.2.6.2 Neonatal Hyperbilirubinemia

Persistent jaundice is considered to be pathological beyond 3 weeks of age in full-term babies and 4 weeks in preterm babies. Cholestasis with conjugated hyperbilirubinemia can be due to a wide variety of abnormalities including extrahepatic biliary tree abnormalities (i.e., extrahepatic biliary atresia (EHBA) and choledochal cyst) or intrahepatic diseases (i.e., interlobular bile duct paucity or neonatal hepatitis syndrome).

The cause and pathogenesis of biliary atresia remain largely unknown [172–174]. Both chronic and acute inflammatory changes have been shown histopathologically. Biliary atresia is typically a progressive panductular obliterative process. Without correction of bile flow obstruction within 2–3 months of life, irreversible hepatic damage and complete obliteration of the extrahepatic biliary tree will result. This process could be progressive even after surgical correction of the obstruction [175, 176]. The neonatal hepatitis syndrome includes various kinds of diseases such as idiopathic neonatal hepatitis, infectious hepatitis, and hepatitis from metabolic or genetic causes.

The urgency in correctly diagnosing EHBA is reflected in the surgical results following portoenterostomy (Kasai procedure). Sustained bile flow is significantly greater in infants operated on before 60 days of age (91%), compared with those operated on after 3 months (17%) [177]. The preoperative distinction of EHBA from the other disorders causing severe cholestasis is essential if the correct patients are to be selected for surgery.

Cholescintigraphy has been known to have 100% sensitivity for the diagnosis of extrahepatic biliary atresia, but low specificity [178–181]. In neonates, normal cholescintigraphy should show prompt and uniform uptake of tracer in the liver with a maximum tracer accumulation within 5 min [182, 183]. The gallbladder may be visualized as early as 10 min, but nonvisualization of the gallbladder can be a normal variant in the neonatal period. The hepatic, cystic, and common bile ducts are generally not visualized in the neonatal period even when there is normal excretion and gallbladder visualization. Bowel activity is seen usually by 30–40 min.

In general, cholescintigraphy performed in patients with biliary atresia within the first 2 months of life usually shows reasonably good hepatic uptake, nonvisualization of the gallbladder, and prolonged retention of the tracer in the liver with no biliary excretion (Fig. 10.34). In contrast, patients older than 3 months usually show evidence of decreased hepatic function with reduced hepatic extraction fraction and no biliary excretion [183].

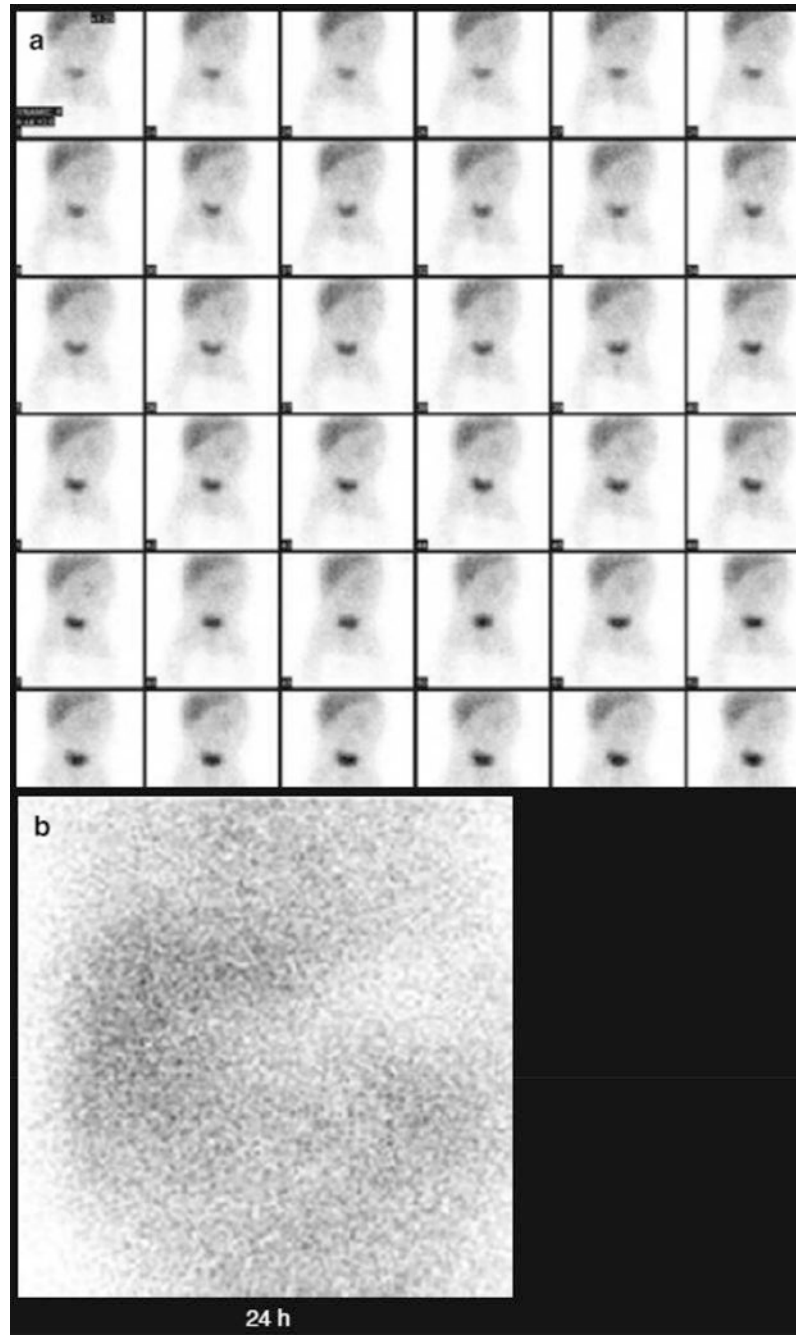

Fig. 10.34 Hepatobiliary study in a neonate carried out for 60 min (**a**) and delayed 24 h image (**b**) illustrating no secretion of activity in the intestine as well as nonvisualization of the gall bladder. Biliary atresia in such case cannot be excluded. However, since the function of the liver is adequate biliary atresia is more likely than neonatal hepatitis

If there is no excretion in an infant less than 2 months of age and the initial uptake suggests liver dysfunction, then the neonatal hepatitis syndrome should be suspected. A repeat study will show the improved function and transit as the condition resolves. In infants under 2 months who do not excrete, those with biliary atresia tend to have better liver-to-heart ratios of radioactivity at 5 min than those with the neonatal hepatitis syndrome. However, no excretion with normal or near normal hepatic uptake may be seen in some cases of severe neonatal hepatitis

syndrome [184]. Cholescintigraphy is most useful in excluding the diagnosis of biliary atresia with a sensitivity and negative predictive value of virtually 100% when intestinal and/or extrahepatic biliary activity is seen. Urine activity in the diaper or contamination of the skin of the abdomen should not be confused with intestinal activity. Acquiring delayed images after cleaning the skin and changing the diaper can prevent this from occurring. The reported specificity ranges from 43 to 90% [179–181, 184–188]. Patients are typically premedicated with phenobarbital, 5 mg/kg daily in two divided doses given for 5 days. Ursodeoxycholic acid, an additional choleretic agent, may also be given at a dose of 20 mg/kg daily in two divided doses in order to optimize bile flow prior to the study.

Phenobarbital stimulates the hepatic transport system for organic anions. This is primarily achieved by induction of hepatic microsomal enzymes, thereby increasing bilirubin conjugation and excretion. Situations.

10.2.6.3 Postoperative Evaluation

Complications After Hepatobiliary Surgery

The increase in the number of laparoscopic cholecystectomy and liver transplantations leads to increased utilization of cholescintigraphy for the evaluation of postoperative complications [189]. Bile duct complications include bile leaks, common bile/hepatic duct injuries or strictures, retained biliary calculi, and obstruction. Most investigators agree that bile leaks are best detected by cholescintigraphy rather than by other anatomical imaging modalities [190–193]. When acquiring scintigraphic images, it is often helpful to enhance image intensity for accurate assessment of the extent of extravasation (Fig. 10.35). The extent of leak is often better identified on

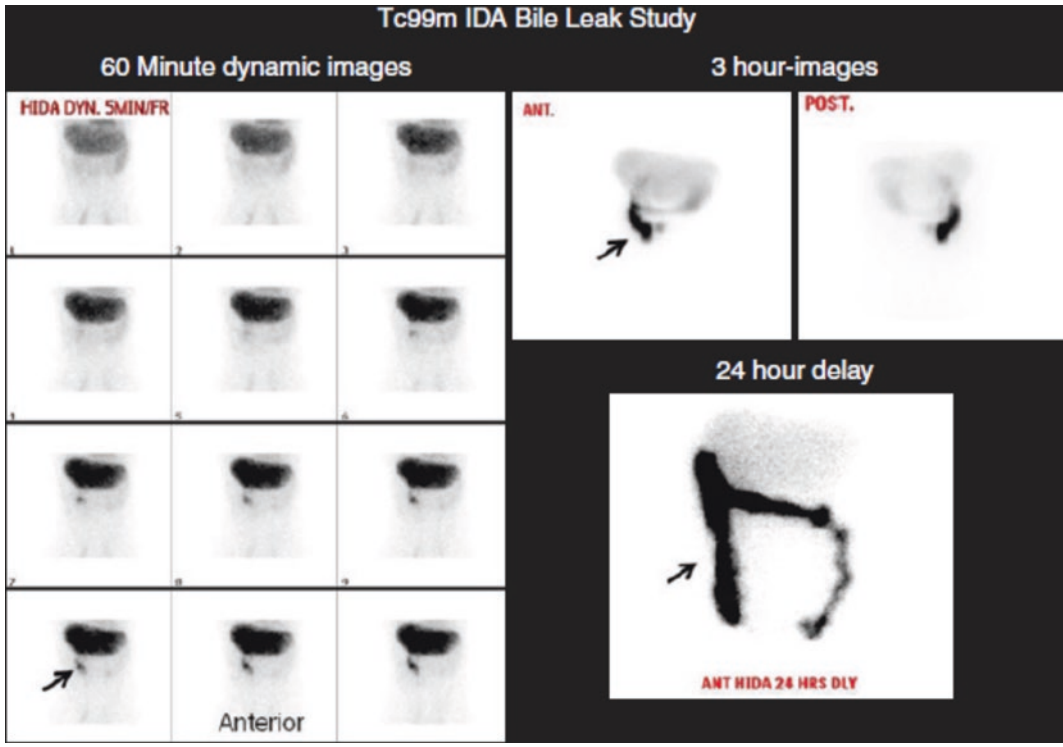

Fig. 10.35 Bile leak study of a patient who underwent liver transplantation 20 days earlier and was referred to rule out possible bile leak. The study shows bile activity early through the study which increased on later images in a linear pattern and appears to be confined within the intestines and colon with no extravasation. Accordingly the study does not show evidence of bile leak

delayed images [194]. Endoscopic retrograde cholangiopancreatography and/or percutaneous transhepatic cholangiography can be a supplement as needed for more definitive diagnosis and treatment [195, 196]. When ultrasonography or CT shows a fluid collection, cholescintigraphy can be helpful not only in confirming but also in excluding biloma [109]. The addition of SPECT/CT imaging can help in localization and improving the accuracy of the study.

The image obtained at 40 min after injection of Tc-99m-IDA reveals intense tracer accumulation, localized only in the gallbladder fossa. However, a subsequently obtained image at an increased intensity (50 min) shows that the leak is more extensive. Delayed images best delineate the extent of the leak (reprinted from Kim [109] with permission).

Clinically insignificant leaks usually heal spontaneously. However, if a major leak is present, reoperation, percutaneous transhepatic biliary drainage, or endoscopic sphincterotomy with placement of a stent or nasobiliary drainage catheter is required. The effectiveness of such interventional procedures may be assessed with cholescintigraphy if clinically indicated (Fig. 10.36).

10.2.6.4 H Miscellaneous

Patients with sclerosing cholangitis were evaluated with planar and SPECT imaging using Tc-99m-IDA [197]. Planar imaging showed beading or band-like constrictions of the biliary tract corresponding to lesions seen on cholangiography. The SPECT images demonstrated multiple focal areas of tracer retention, representing bile stasis in intrahepatic bile ducts.

In patients with cystic fibrosis, ERCP often shows changes consistent with sclerosing cholangitis, with beading and stricturing of the intrahepatic ducts [198]. While various scintigraphic findings in these patients have been described, the most common finding appears to be retention of tracer in the intrahepatic ducts [198–201]. It was suggested that cholescintigraphy is valuable for monitoring the therapeutic responses of cystic fibrosis patients with liver disease to ursodeoxycholic acid therapy [199] and in the early detection of liver involvement [201].

Cholescintigraphy was found to be a useful noninvasive screening test in HIV-positive patients with right upper quadrant pain who are suspected of having AIDS-related sclerosing cholangitis, for the purpose of determining who should be referred for ERCP [202, 203]. The response to specific antimicrobial or surgical intervention can be monitored with cholescintigraphy [203].

Cholescintigraphy is a useful noninvasive test which complements an anatomical finding on ultrasonography in the diagnosis of choledochal cyst [204, 205]. And in assessing the effectiveness of anti-enterogastric reflux procedures (e.g., Roux-en-Y diversion).

Investigators have found cholescintigraphy useful for assessing the patency of a biliary-enteric bypass [206–209]. A case was reported in which biliary stasis seen in the region of the biliary-enteric anastomosis in the supine images disappeared almost completely when the images were repeated after 30 min with the patient in an upright position [210]. We have observed a similar finding in a patient postoperatively. These cases illustrate the importance of imaging in the upright position when biliary or afferent loop stasis is seen in postoperative patients.

10.2.7 Summary

Cholescintigraphy plays a pivotal role in the evaluation of various biliary tract diseases, particularly when coupled with pharmacological intervention. The physician monitoring the study should be familiar with the most optimal technique for the pharmacological intervention and with conditions and medications that affect gallbladder contraction. It is also important to be aware of the various physiological and pharmacological effects on imaging findings, i.e., not only those findings that are normal but also the undesirable variants. Failure to recognize such effects can lead to incorrect interpretations.

Radionuclide imaging of the liver using the various tracers provides unique functional information, i.e., the functional reserve, presence or absence of hepatocytes/Kupffer's cells, and RBC

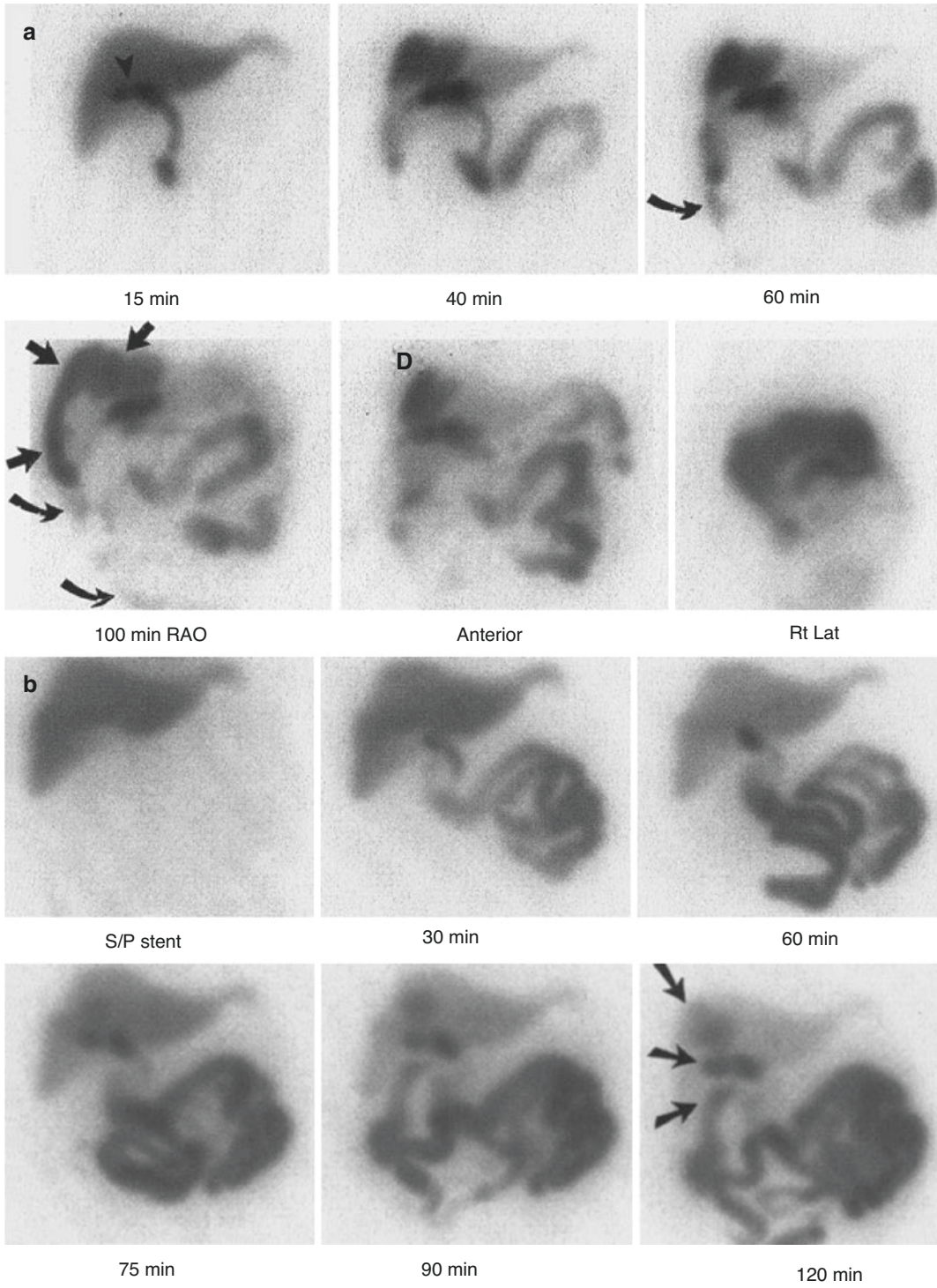

Fig. 10.36 (**a**, **b**) Post-liver transplantation Tc-99m-IDA scan. (**a**) After removal of the t-tube, a bile leak is first noted at 15 min (*arrowhead*). The anterior images show localization of extravasated activity predominantly at the dome (*D*) of the liver. The right anterior oblique (*RAO*) image better delineates extravasated activity over the superior and posterolateral surface of the liver (*straight arrows*), in addition to the right paracolic gutter (*curved arrows*). (**b**) A repeat study after CBD stent placement shows markedly improved drainage of bile into the intestine. However, a milder degree of leak is still evident on the images acquired during the second hour (*arrows*). (Reprinted from Kim [108] with permission)

pooling. This has been augmented further by the improved resolution with multi-head SPECT systems. Advances in instrumentation such as PET and development of new radiopharmaceuticals, including PET tracers specifically for the evaluation of the liver, will likely expand clinical applications further.

References

1. Kuo B, Urma D (2006) Esophagus-anatomy and development. GI Motility online
2. Mittal RK (2011) Upper esophageal sphincter. In: Mittal RK (ed) Motor function of the pharynx, esophagus and its sphincters. Morgan and Claypool Life Sciences, San Rafael. https://www.ncbi.nlm.nih.gov/books/NBK54282
3. Sama SK, Daniel EE, Waterfall WE (1977) Myogenic and neural control systems for esophageal motility. Gastroenereology 73:1345–1352
4. Richards WG, Stamler JS, Kobzik L et al (1995) Role of nitric oxide in human esophageal circular smooth muscle in vitro. J Thorac Cardiovasc Surg 110: 157–164
5. Meyer GW, Gerhardt DC, Castell DO (1981) Human esophageal response to rapid swallowing: muscle refractory period or neural inhibition? Am J Phys 241:G129–G136
6. Sidhu AS, Triadafilopoulos G (2008) Neuroregulation of lower esophageal sphincter function as treatment for gastro-esophageal reflux disease. World J Gastroenterol 14:985–990
7. Wong RKH, Waysonovitch CL (1995) Achalasia. In: Castell DO (ed) The esophagus, 3rd edn. Little Brown, Boston, pp 219–245
8. Oude Nijhuis RAB, Zaninotto G, Roman S, Boeckxstaens GE, Fockens P, Langendam MW et al (2020) European guidelines on achalasia: United European Gastroenterology and European Society of Neurogastroenterology and Motility recommendations. United European Gastroenterol J 8(1):13–33
9. Lacy BE, Weiser K (2008) Esophageal disorders: medical therapy. J Clin Gastroenterol 42:652–658
10. Penaginie R, Schoeman MN, Dent J, Tipnett MD, Holloway RH (1996) Motor events underlying gastroesophageal reflux in ambulant patient with reflux esophagitis. Neurogastroenterol Motil 8:131–141
11. Kahrilas PJ (1999) The role of hiatus hernia in GERD. Yale J Biol Med 72:101–111
12. Kahrilas PJ, Manka M, Shi G, Joehl RJ (2000) Increased frequency of transient lower esophageal sphincter relaxation induced by gastric distention in reflux patients with hiatal hernia. Gastroenterology 118:688–695
13. Galmiche JP, Janssens J (1995) The pathophysiology of gastroesophageal reflux disease: an overview. Scand J Gastroenterol Suppl 211:7–18
14. Goldstein JL, Waykins JL, Greger JA, Layden TL (1994) The esophageal mucosal resistance. J Lab Clin Med 123:653–659
15. Minami H, McCallum RW (1984) The physiology and pathophysiology of gastric emptying in humans. Gastroenterology 86:1592–1600
16. Hinder RA, Kelly KA (1977) Human gastric pacesetter potential: site of origin, spread and response to gastric transection and proximal gastric vagotomy. Am J Surg 133:29–33
17. Meyer JH, Ohashi H, Jehn D et al (1981) Size of liver particles emptied from the human stomach. Gastroenterology 80:1489–1496
18. Brener W, Hendrix TR, McHugh PR (1983) Regulation of the gastric emptying of glucose. Gastroenterology 85:76–82
19. Siegel JA, Urbain JL, Adler LP, Charkes ND, Maurer AH, Krevsky B, Knight LC, Fisher RS, Malmud LS (1988) Biphasic nature of gastric emptying. Gut 29:85–89
20. Loo FD, Palmer DW, Soergel KH, Kalbfleisch JH, Wood CM (1984) Gastric emptying in patients with diabetes mellitus. Gastroenterology 86:485–494
21. Horowitz M, Harding PE, Chatterton BE et al (1985) Acute and chronic effects of domperidone on gastric emptying in diabetic autonomic neuropathy. Dig Dis Sci 30:1–9
22. Muller-Lissner SA, Fimmel CJ, Sonnenberg A et al (1983) Novel approach to quantify duodenogastric reflux in healthy volunteers and in patients with type I gastric ulcer. Gut 24:510–518
23. Tolin RD, Malmud LS, Stelzer F et al (1979) Enterogastric reflux in normal subjects and patients with Billroth II gastroenterostomy. Gastroenterology 77:1027–1033
24. Shaffer EA, McOrmond P, Duggant T (1980) Assessment of gall bladder filling and emptying and duodenogastric reflux. Gastroenterology 79:899–906
25. Markowitz JF (1990) Duodenogastric reflux: state of the art. J Pediatr Gastroenterol 10:287–289
26. Elgazzar AH, Fernandez-Ulloa M, Ryan JR et al (1992) Scintigraphic evaluation of duodenogastric reflux: significance in the diagnosis of acute cholecystitis. Am J Physiol Imaging 3(4):239–241
27. Slavin JD, Sharzynski JJ, Spencer RP (1985) High incidence of gastric reflux during hepatobiliary imaging in pancreatitis. Clin Nucl Med 10:5–6
28. Kutchai HC (2000) Gastrointestinal system. In: Berne RM, Levy MN (eds) Principles of physiology, 3rd edn. Mosby, St. Louis, pp 366–371
29. Chandran P, Satthaporn S, Robins A, Eremin O (2003) Inflammatory bowel disease; dysfunction of GALT and gut bacterial flora (I). Surgeon 2:63–75
30. Halsted CH (2003) Absorption of water-soluble vitamins. Curr Opin Gastroenterol 19:113–117

31. Divgi CR, Lisann NM, Yeh SD, Benua RS (1995) Technetium-99m albumin scintigraphy in the diagnosis of protein-losing enteropathy. J Nucl Med 27:1710–1712
32. Bhatnagar A, Lahoti D, Singh AK et al (1995) Scintigraphic diagnosis of protein losing enteropathy using Tc-99m dextran. Clin Nucl Med 20:1070–1073
33. Bhatnagar A, Singh K (1996) Technetium-99m dextran: a promising new protein-losing enteropathy imaging agent. Eur J Nucl Med 23:572–578
34. Hatoum OA, Binion DG (2005) The vasculature and inflammatory bowel disease: contribution to pathogenesis and clinical pathology. Inflamm Bowel Dis 11:304–313
35. Rogler G, Biedermann L, Scharl M (2018) New insights into the pathophysiology of inflammatory bowel disease: microbiota, epigenetics and common signalling pathways. Swiss Med Wkly 148:w14599
36. Wen Z, Fiocchi C (2004) Inflammatory bowel disease; autoimmune or immune-mediated pathogenesis? Clin Dev Immunol 11:195–204
37. Ahmad T, Tamboli CP, Jewell D, Colombel JF (2004) Clinical relevance of advances in genetics and pharmacogenetics of IBD. Gastroenterology 126:1533–1549
38. Old JL, Dusing RW, Yap W, Dirks J (2005) Imaging for suspected appendicitis. Am Fam Physician 71: 71–78
39. Whiteford MH, Whiteford HM, Yee LF, Ogunbiyi OA, Dehdashti F, Siegel BA, Birnbaum EH, Fleshman JW, Kodner IJ, Read TE (2000) Usefulness of FDG-PET scan in the assessment of suspected metastatic or recurrent adenocarcinoma of the colon and rectum. Dis Colon Rectum 43(6):759–767; discussion 767–70
40. Aabakken L (2005) Non variceal upper gastrointestinal bleeding. Endoscopy 37:195–200
41. Carney BW, Khatri G, Shenoy-Bhangle AS (2019) The role of imaging in gastrointestinal bleed. Cardiovasc Diagn Ther 9(Suppl 1):S88
42. Strate LL, Gralnek IM (2016) Management of patients with acute lower gastrointestinal bleeding. Am J Gastroenterol 111(4):459
43. Zurkiya O, Walker TG (2015) Angiographic evaluation and management of nonvariceal gastrointestinal hemorrhage. Am J Roentgenol 205(4):753–763
44. Gerson LB, Fidler JL, Cave DR, Leighton JA (2015) ACG clinical guideline: diagnosis and management of small bowel bleeding. Am J Gastroenterol 110(9):1265–1287
45. ACR Appropriateness Criteria for LGIB 2014. https://www.acr.org/Clinical-Resources/ACR-Appropriateness-Criteria
46. Stone DN, Mancuso AA, Rice D, Hanafee WN (1981) Parotid CT sialography. Radiology 138:393–397
47. Arroyo V, Bernadi M, Epstein M (1998) Pathophysiology of ascites and functional renal failure in cirrhosis. J Hepatol 6:239
48. Bories P (1986) The treatment of refractory ascites by the Leveen shunts; a multicenter controlled trial of 57 patients. J Hepatol 3:212–218
49. Conn HO (1993) Transjugular intrahepatic portosystemic shunts: the state of the art. Hepatology 17:148–158
50. Singh A (1996) Peritoneovenous shunts: patency studies. In: Henkin RE, Bles MA, Dillehay GL, Halama JR, Karesh SM, Wagner PH, Zimmer AM (eds) Textbook of nuclear medicine. Mosby, New York, pp 1041–1052
51. Desai A, O'Connor M, Neja B, Delaney K, Camilleri M, Zinsmeister AR, Bharucha AE (2018) Reproducibility of gastric emptying assessed with scintigraphy in patients with upper GI symptoms. Neurogastroenterol Motil 30(10):e13365
52. Wang YT, Mohammed SD, Farmer AD, Wang D, Zarate N, Hobson AR et al (2015) Regional gastrointestinal transit and pH studied in 215 healthy volunteers using the wireless motility capsule: influence of age, gender, study country and testing protocol. Aliment Pharmacol Ther 42(6):761–772
53. Kostamo KL (1996) Evaluation of gastrointestinal bleeding by nuclear medicine techniques. In: Henkin RE, Bles MA, Dillehay GL, Halama JR, Karesh SM, Wagner PH, Zimmer AM (eds) Textbook of nuclear medicine. Mosby, New York, pp 1016–1022
54. Nicholson ML, Neoptlemos JP, Sharp JF et al (1989) Localization of lower gastrointestinal bleeding using in vivo technetium 99m-labeled red blood cell scintigraphy. Br J Surg 76:358–361
55. Nogueira HJV (2020) Detection of ectopic gastric mucosa using scintigraphy in pediatric patients
56. Gyorke T, Duffek L, Bratfai K et al (2000) The role of nuclear medicine in inflammatory bowel disease. A review with experiences of a specific bowel activity using immunoscintigraphy with 99mTc anti-granulocyte antibodies. Eur J Radiol 3: 183–192
57. Lantto E (1994) Investigation of suspected intra-abdominal sepsis: the contribution of nuclear medicine. Scand J Gastroenterol Suppl 203:11–14
58. Perlman SB, Hall BS, Reichelderfer M (2013) PET/CT imaging of inflammatory bowel disease. Semin Nucl Med 43:420–426
59. Saha GB (2009) Fundamentals of nuclear pharmacy, 6th edn. Springer, New York
60. Sarkady E, Sapi Z, Toth V, Kiss S (1999) Warthin-like tumor of the thyroid: a case report. Pathol Oncol Res 5:315–317
61. Loutfi I, Nair MK, Ebrahim AK (2003) Salivary gland scintigraphy: the use of semi quantitative analysis for uptake and clearance. J Nucl Med Technol 31(2): 81–85
62. Rypins EB, Evans DG, Hinrichs W et al (1997) Tc-99m-HMPAO white blood cell scan for diagnosis of acute appendicitis in patients with equivocal clinical presentation. Ann Surg 226:58–65
63. Kipper SL (1999) The role of radiolabeled leukocyte imaging in the management of patients with acute appendicitis. Q J Nucl Med 43:83–92
64. Bourgeois S, Van Den Berghe I, De Geeter F (2016) Incidental finding of silent appendicitis on F-FDG

PET/CT in a patient with small cell lung adenocarcinoma. Hell J Nucl Med 19:164–166
65. O'Connor A (2021) The Urea Breath Test for the noninvasive detection of Helicobacter pylori. In: Helicobacter pylori. Humana, New York, pp 15–20
66. Graham DY, Malaty HM, Evans DG et al (1991) Epidemiology of Helicobacter pylori in asymptomatic population in the United States. Gastroenterology 100:1495–1501
67. Peterson WL (1991) Helicobacter pylori and peptic ulcer disease. N Engl J Med 324:1043–1048
68. Parsonnet J, Friedman GD, Vandersteen DP et al (1991) Helicobacter pylori infection and the risk of gastric carcinoma. N Engl J Med 325:1127–1131
69. Logan RP, Dill S, Baner FE et al (1991) The European C13 urea breath test for the detection of Helicobacter pylori. Eur J Gastroenterol Hepatol 3:915–921
70. Philips M (1992) Breath tests in medicine. Sci Am 267:74–79
71. Ormand JE, Talley NJ, Carpenter HA et al (1990) C-14 urea breath test for diagnosis of Helicobacter pylori. Dig Dis Sci 35:879–884
72. Debongnie JC, Pauwels S, Raat A et al (1991) Quantification of Helicobacter pylori infection in gastritis and peptic ulcer disease using a simple and rapid carbon-14-urea breath test. J Nucl Med 32:1192–1198
73. Strubbs JB, Marshall BJ (1993) Radiation dose estimates for the C-14 labeled urea breath test. J Nucl Med 34:821–825
74. Sasaki Y, Lio M, Kameda H et al (1970) Measurement of C-14 lactose absorption in the diagnosis of lactase deficiency. J Lab Clin Med 76:824–835
75. Sasaki Y (1991) Breath test by CO_2 analysis: I. Progress of breath test using isotopes of carbon in Japan. Radioisotopes 40:475–484
76. Sherr HP, Sasaki Y, Newman A et al (1971) Detection of bacterial deconjugation of bile salts by a convenient breath analysis technique. N Engl J Med 285:656–661
77. Sasaki Y (1995) Carbon-14 and carbon 13 breath tests. In: Wagner HN, Buchanan JW, Szabo Z (eds) Principles of nuclear medicine, 2nd edn. Elsevier, Amsterdam, pp 958–965
78. Rassam F, Olthof PB, Richardson H, van Gulik TM, Bennink RJ (2019) Practical guidelines for the use of technetium-99m mebrofenin hepatobiliary scintigraphy in the quantitative assessment of liver function. Nucl Med Commun 40(4):297–307
79. Imura S, Shimada M, Utsunomiya T (2015) Estimation of hepatic functional reserve. Hepatol Res 45:10–19. https://doi.org/10.1111/hepr.12325
80. Katabathina VS, Zafar AM, Suri R (2015) Clinical presentation, imaging, and management of acute cholecystitis. Tech Vasc Interv Radiol 18:256–265
81. Lambie H, Cook AM, Scarsbrook AF, Lodge JPA, Robinson PJ, Chowdhury FU (2011) Tc^{99m}- hepatobiliary iminodiacetic acid (HIDA) scintigraphy in clinical practice. Clin Radiol 66:1094–1105
82. Koizumi K, Uchiyama G, Arai T et al (1992) A new liver functional study using Tc-99m DTPA-galactosyl human serum albumin: evaluation of the validity of several functional parameters. Ann Nucl Med 6: 83–87
83. Yumoto Y, Yagi T, Sato S, Nouso K, Kobayashi Y, Ohmoto M, Yumoto E, Nagaya I, Nakatsukasa H (2010) Preoperative estimation of remnant hepatic function using fusion images obtained by ^{99m}Tc-labelled galactosyl-human serum albumin liver scintigraphy and computed tomography. Br J Surg 97(6):934–944
84. Harvey E, Loberg M, Ryan J, Sikorski S, Faith W, Cooper M (1979) Hepatic clearance mechanism of Tc-99m-HIDA and its effect on quantitation of hepatobiliary function: concise communication. J Nucl Med 20:310–313
85. Tulchinsky M, Ciak BW, Debelke D, Hilsom A, Holes-Lewis KA et al (2010) SNM practice guidelines fir hepatobiliary scintigraphy 4. J Nucl Med Technol 38:210–218
86. Krishnamurthy S, Krishnamurthy GT (1988) Quantitative assessment of hepatobiliary disease with Tc-99m-IDA scintigraphy. In: Freeman LM, Weissman HS (eds) Nuclear medicine annual. Raven, New York, pp 309–330
87. Doo E, Krishnamurthy GT, Eklem MJ, Gilbert S, Brown PH (1991) Quantification of hepatobiliary function as an integral part of imaging with technetium-99m-mebrofenin in health and disease. J Nucl Med 32:48–57
88. Mitsumori A, Nagaya I, Kimoto S, Akaki S, Togami I, Takeda Y, Joja I, Hiraki Y (1998) Preoperative evaluation of hepatic functional reserve following hepatectomy by technetium-99m galactosyl human serum albumin liver scintigraphy and computed tomography. Eur J Nucl Med 25:1377–1382
89. Fujimoto H, Uchiyama G, Araki T et al (1991) Exophytic regenerating nodule of the liver: misleading appearance on iodized-oil CT. J Comput Assist Tomogr 15:495–497
90. Calvet X, Pons F, Bruix J et al (1988) Technetium-99m DISIDA hepatobiliary agent in diagnosis of hepatocellular carcinoma: relationship between detectability and tumor differentiation. J Nucl Med 29:1916–1920
91. Hasegawa Y, Nakano S, Hiyama T et al (1991) Relationship of uptake of technetium-99m(Sn)-N-pyridoxyl-5-methyltryptophan by hepatocellular carcinoma to prognosis. J Nucl Med 32:228–235
92. Boulahdour H, Cherqui D, Charlotte F et al (1993) The hot spot hepatobiliary scan in focal nodular hyperplasia. J Nucl Med 34:2105–2110
93. Kotzerke J, Schwarzrock R, Krischek O et al (1989) Technetium-99m DISIDA hepatobiliary agent in diagnosis of hepatocellular carcinoma, adenoma, and focal nodular hyperplasia (letter). J Nucl Med 30:1278–1280
94. Barwick KW, Rosai J (1996) Liver (non-neoplastic disease). In: Rosai J (ed) Ackerman's surgical pathology. Mosby-Year Book, St Louis, pp 857–942
95. Lin J, Westerhoff M (2021) Vascular neoplasms of the liver. Clin Liver Dis 17:261–266

96. Brant WE, Floyd JL, Jackson DE et al (1987) The radiological evaluation of hepatic cavernous hemangioma. JAMA 257:2471–2474
97. Kudo M, Ikekubo K, Yamamoto K et al (1989) Distinction between hemangioma of the liver and hepatocellular carcinoma: value of labeled RBC-SPECT scanning. AJR Am J Roentgenol 152:977–983
98. Ziessman HA, Silverman PM, Patterson J et al (1991) Improved detection of small cavernous hemangiomas of the liver with high-resolution three-headed SPECT. J Nucl Med 32:2086–2091
99. Langsteger W, Lind P, Eber B et al (1989) Diagnosis of hepatic hemangioma with ^{99m}Tc-labeled red cells: single photon emission computed tomography (SPECT) versus planar imaging. Liver 9:288–293
100. Farlow DC, Chapman PR, Gruenewald SM et al (1990) Investigation of focal hepatic lesions: is tomographic red blood cell imaging useful? World J Surg 14:463–467
101. Krause T, Hauenstein K, Studier-Fischer B et al (1993) Improved evaluation of technetium-99m-red blood cell SPECT in hemangioma of the liver. J Nucl Med 34:375–380
102. Bonanno N, Baldari S, Cerrito A et al (1991) Diagnosis of hepatic hemangiomas with $^{99mTc\text{-}labeled}$ red blood cell scanning: value of SPECT. J Nucl Biol Med 35:135–140
103. Moon DH, Lee MH, Yang SK et al (1992) Diagnosis of hepatic hemangioma (HH) with triple-head (3H) high-resolution SPECT. J Nucl Med 33:918(abstract)
104. Birnbaum BA, Weinreb JC, Megibow AJ et al (1990) Definitive diagnosis of hepatic hemangiomas: MR imaging versus Tc-99m-labeled red blood cell SPECT. Radiology 176:95–101
105. Jhuang J-Y, Lin L-W, Hsieh M-S (2011) Adult capillary hemangioma of the liver: case report and literature review. Kaohsiung J Med Sci 27:344–347
106. Swayne LC, Diehl WL, Brown TD et al (1991) False-positive hepatic blood pool scintigraphy in metastatic colon carcinoma. Clin Nucl Med 16: 630–632
107. Hod N, Pour MC, Juven Y, Horne T (2004) "Positive" Tc-99m red blood cell scintigraphy in a patient with hepatic lymphoma. Clin Nucl Med 29:272–274
108. Kim CK (1998) Scintigraphic evaluation of the liver and biliary tract. In: Gazelle SG, Saini S, Mueller PR (eds) Hepatobiliary and pancreatic radiology: imaging and interventions. Thieme, New York, pp 108–153
109. Zheng JG, Yao ZM, Shu CY, Zhang Y, Zhang X (2005) Role of SPECT/CT in diagnosis of hepatic hemangiomas. World J Gastroenterol 11:5336–5341
110. Schillaci O, Danieli R, Manni C, Capoccetti F, Simonetti G (2004) Technetium-99m-labelled red blood cell imaging in the diagnosis of hepatic haemangiomas: the role of SPECT/CT with a hybrid camera. Eur J Nucl Med Mol Imaging 31:1011–1015
111. Siegel A, Mazurek R (1997) Early dynamic SPECT acquisition for the imaging of hepatic hemangiomas utilizing Tc-99m-labeled red blood cells. Clin Nucl Med 22:745–748
112. Khosa F, Khan AN, Eisenberg RL (2011) Hypervascular liver lesions on MRI. AJR Am J Roentgenol 197:W204–W220
113. Kobayashi S, Maruyama H, Okugawa H, Yoshizumi H, Matsutani S, Ebara M et al (2008) Contrast-enhanced US with Levovist for the diagnosis of hepatic hemangioma: time-related changes of enhancement appearance and the hemodynamic background. Hepato-Gastroenterology 55: 1222–1228
114. Kim CK, Worsley WF, Lentle B (1998) Scintigraphic evaluation of tumors of the liver. In: Murray IPC, Ell PJ (eds) Nuclear medicine in clinical diagnosis and treatment, 2nd edn. Churchill Livingstone, London, pp 775–782
115. Tanasescu D, Brachman M, Rigby J et al (1984) Scintigraphic triad in focal nodular hyperplasia. Am J Gastroenterol 79:61–64
116. Welch TJ, Sheedy PF Jr, Johnson CM et al (1985) Focal nodular hyperplasia and hepatic adenoma: comparison of angiography, CT, US, and scintigraphy. Radiology 156:593–595
117. Salvo AF, Schiller A, Athanasoulis C et al (1977) Hepatoadenoma and focal nodular hyperplasia; pitfalls in radiocolloid imaging. Radiology 125: 451–455
118. Lubbers PR, Ros PR, Goodman ZD et al (1987) Accumulation of technetium-99m sulfur colloid by hepatocellular adenoma: scintigraphic-pathologic correlation. AJR Am J Roentgenol 148:1105–1108
119. Schein CJ (1972) Acute cholecystitis. Harper and Row, New York, p 40
120. Jivegard L, Thornell E, Svanvik J (1987) Pathophysiology of acute obstructive cholecystitis: implications for non-operative management. Br J Surg 74:1084–1086
121. Jivegard L, Thornell E, Bjorck S, Svanvik J (1985) The effects of morphine and enkephaline on gallbladder function in experimental cholecystitis. Inhibition of inflammatory gallbladder secretion. Scand J Gastroenterol 20:1049–1056
122. Greenberger NJ, Isselbacher KJ (1991) Diseases of the gallbladder and bile ducts. In: Wilson JD, Braunwald E, Isselbacher KJ et al (eds) Harrison's principles of internal medicine, 12th edn. McGraw-Hill, New York, pp 1358–1368
123. Freitas JE (1994) Cholescintigraphy. In: Murray IPC, Ell PJ (eds) Nuclear medicine in clinical diagnosis and treatment. Churchill Livingstone, London, pp 77–86
124. Ziessman HA (2014) Hepatobiliary Scintigraphy in 2014. J Nucl Med Technol 42:249–259
125. Ziessman HA (2010) Nuclear medicine hepatobiliary imaging. Clin Gastroenterol Hepatol 8:111–116
126. Kumar V, Abbas A, Aster JC (2014) Robbins and Cotzan, pathologic basis of disease, 9th edn. Saunders, Philadelphia

127. Shea JA, Berlin JA, Escarce JJ et al (1994) Revised estimates of diagnostic test sensitivity and specificity in suspected biliary tract disease. Arch Intern Med 154:2573–2581
128. Ziessman HA (2003) Acute cholecystitis, biliary obstruction and biliary leakage. Semin Nucl Med 38:279–296
129. Kiewiet JJ, Leeuwenburgh MM, Bipat S, Bossuyt PM, Stoker J, Boermeester MA (2012) A systematic review and meta-analysis of diagnostic performance of imaging in acute cholecystitis. Radiology 264:708–720
130. Colletti PM, Cirimelli KM, Radin DR et al (1989) Radionuclide angiography in suspected acute cholecystitis: further observations. Clin Nucl Med 14:867–873
131. Brachman MB, Goodman MD, Waxman AD (1993) The rim sign in acute cholecystitis. Comparison of radionuclide, surgical, and pathologic findings. Clin Nucl Med 18:863–866
132. Nahrwold DL (1991) Chronic cholecystitis and cholelithiasis. In: Sabiston DC (ed) Textbook of surgery, 14th edn. Saunders, Philadelphia, pp 1057–1063
133. Weedon D (1984) Pathology of the gallbladder. Masson, New York
134. Bolen G, Javitt NB (1982) Biliary dyskinesia: mechanisms and management. Hosp Pract 17:115–130
135. Misra DC Jr, Blossom GB, Fink-Bennett D et al (1991) Results of surgical therapy for biliary dyskinesia. Arch Surg 126:957–960
136. Hogan WJ, Geenen JE (1988) Biliarydyskinesia. Endoscopy 20:179–183
137. Coelho JC, Wiederkehr JC (1996) Motility of Oddi's sphincter: recent developments and clinical applications. Am J Surg 172:48–51
138. Sostre S, Kalloo AN, Spiegler EJ et al (1992) A noninvasive test of sphincter of Oddi dysfunction in postcholecystectomy patients: the scintigraphic score. J Nucl Med 33:1216–1222
139. Ziessman HA (1992) Atlas of cholescintigraphy: selective update. In: Ziessman HA, Van Nostrand D (eds) Selected atlas of gastrointestinal scintigraphy. Springer, Berlin, pp 1–34
140. Fink-Bennett D (1991) Augmented cholescintigraphy: its roles in detecting acute and chronic disorders of the hepatobiliary tree. Semin Nucl Med 21:128–139
141. Madacsy L, Velosy B, Lonovics J et al (1994) Differentiation between organic stenosis and functional dyskinesia of the sphincter of Oddi with amyl nitrite-augmented quantitative hepatobiliary scintigraphy. Eur J Nucl Med 21:203–208
142. Freeman LM, Sugarman LA, Weissmann HS (1981) Role of cholecystokinetic agents in ^{99m}Tc-IDA cholescintigraphy. Semin Nucl Med 11:186–193
143. Fink-Bennett D, DeRidder P, Kolozsi WZ et al (1991) Cholecystokinin cholescintigraphy: detection of abnormal gallbladder motor function in patients with chronic acalculous gallbladder disease. J Nucl Med 32:1695–1699
144. Halverson JD, Garner BA, Siegel BA et al (1992) The use of hepatobiliary scintigraphy in patients with acalculous biliary colic. Arch Intern Med 152:1305–1307
145. Reed DN Jr, Fernandez M, Hicks RD (1993) Kinevac-assisted cholescintigraphy as an accurate predictor of chronic acalculous gallbladder disease and the likelihood of symptom relief with cholecystectomy. Am Surg 5:273–277
146. Zech ER, Simmons LB, Kendrick RR et al (1991) Cholecystokinin enhanced hepatobiliary scanning with ejection fraction calculation as an indicator of disease of the gallbladder. Surg Gynecol Obstet 17:21–24
147. Ziessman HA, Fahey FH, Hixson DJ (1992) Calculation of a gallbladder ejection fraction: advantage of continuous sincalide infusion over the three-minute infusion method. J Nucl Med 33:537–541
148. Kim CK, Worsley DF, Machac J (1996) Interventions in gastrointerventional nuclear medicine. In: Freeman LM (ed) Nuclear medicine annual. Raven, New York, pp 213–257
149. Ziessman HA, Muenz LR, Agarwal AK, ZaZa AA (2001) Normal values for sincalidecholescintigraphy: comparison of two methods. Radiology 221:404–410
150. DiBaise JK, Richmond BK, Ziessman HH, Everson GT, Fanelli RD, Maurer A, Ouyang A, Shamamian P, Simons RJ, Wall LA, Weida TJ, Tulchinsky M (2011) Cholecystokinin-cholescintigraphy in adults: consensus recommendations of an interdisciplinary panel. Clin Gastroenterol Hepatol 9:376–384
151. Fisher RS, Rock E, Malmud LS (1987) Effects of meal composition on gallbladder and gastric emptying in man. Dig Dis Sci 32:337–344
152. Maton PN, Selden AC, Fitzpatrick ML, Chadwick VS (1985) Defective gallbladder emptying and cholecystokinin release in celiac disease: reversal by gluten-free diet. Gastroenterology 88:391–396
153. Masclee AAM, Jansen JBMJ, Corstens FHM, Lamers CBHW (1989) Reversible gallbladder dysfunction in severe pancreatic insufficiency. Gut 30:866–872
154. Masclee AA, Jansen JB, Driessen WM, Geuskens LM, Lamers CB (1991) Gallbladder sensitivity to cholecystokinin in coeliac disease. Correlation of gallbladder contraction with plasma cholecystokinin-like immunoreactivity during infusion of cerulein. Scand J Gastroenterol 26:1279–1284
155. Oster-Jorgensen E, Qvist N, Pedersen SA, Rasmussen L, Hovendal CP (1992) Postprandial gallbladder emptying is related to intestinal motility at the time of meal ingestion. Scand J Gastroenterol 27:699–702
156. Brugge WR (1991) Motor function of the gallbladder: measurement and clinical significance. Semin Roentgenol 16:226–231
157. Kloiber R, Molnar CP, Shaffer EA (1992) Chronic biliary-type pain in the absence of gallstones: the value of cholecystokinin cholescintigraphy. AJR Am J Roentgenol 159:509–513

158. Torsoli A, Corazziari E, Habib FI, Cicala M (1990) Pressure relationships within the human bile tract. Normal and abnormal physiology. Scand J Gastroenterol Suppl 175:52–57
159. Murphy P, Solomon J, Roseman DL (1980) Narcotic anesthetic drugs: their effect on biliary dynamics. Arch Surg 115:710–711
160. Dedrick DF, Tanner WW, Bushkin FL (1980) Common bile duct pressure during enflurane anesthesia: effects of morphine and subsequent naloxone. Arch Surg 115:820–821
161. Chen CC, Holder LE, Maunoury C et al (1997) Morphine augmentation increases gallbladder visualization in patients pretreated with cholecystokinin. J Nucl Med 38:644–647
162. Kim CK, Goyal M, San Pedro E et al (1995) The effect of CCK pretreatment on gallbladder visualization on delayed or morphine-augmented imaging (abstract). J Nucl Med 36:74
163. Klingensmith WC (1988) Hepatobiliary imaging: normal appearance and normal variations. In: Gottschalk A, Hoffer PB, Potchen J (eds) Diagnostic nuclear medicine. Williams and Wilkins, Baltimore, pp 575–581
164. Kim CK, Palestro CJ, Solomon RW et al (1990) Delayed biliary-to-bowel transit in cholescintigraphy after cholecystokinin treatment. Radiology 176:553–556
165. Oates E, Achong DM (1992) Incidence and significance of enterogastric reflux during morphine-augmented cholescintigraphy. Clin Nucl Med 17:926–928
166. Shih WJ, Lee JK, Magoun S et al (1995) Morphine-augmented cholescintigraphy enhances duodenogastric reflux. Ann Nucl Med 9:225–228
167. Zeman RK, Lee C, Jaffe MH et al (1984) Hepatobiliary scintigraphy and sonography in early biliary obstruction. Radiology 153:793–798
168. Miller DR, Egbert RM, Braunstein P (1984) Comparison of ultrasound and hepatobiliary imaging in the early detection of acute total common bile duct obstruction. Arch Surg 119:1233–1237
169. Juni JE, Reichle R (1990) Measurement of hepatocellular function with deconvolutional analysis: application in the differential diagnosis of acute jaundice. Radiology 177:171–175
170. Lieberman DA, Brown PH, Krishnamurthy GT (1990) Improved scintigraphic assessment of severe cholestasis with the hepatic extraction fraction. Dig Dis Sci 35:1385–1390
171. Balistreri WF, Grand R, Hoofnagle JH et al (1996) Biliary atresia: current concepts and research directions. Summary of a symposium. Hepatology 23:1682–1692
172. Bezerra JA, Tiao G, Ryckman FC et al (2002) Genetic induction of proinflammatory immunity in children with biliary atresia. Lancet 360(9346):1653–1659
173. Perlmutter DH, Shepherd RW (2002) Extrahepatic biliary atresia: a disease or a phenotype? Hepatology 35(6):1297–1304
174. Miyano T, Fujimoto T, Ohya T, Shimomura H (1993) Current concept of the treatment of biliary atresia. World J Surg 17:332–336
175. McEvoy CF, Suchy FJ (1996) Biliary tract disease in children. Pediatr Clin N Am 43:75–98
176. Kasai M, Suzuki K, Ohashi E et al (1978) Technique and results of operative management of biliary atresia. World J Surg 2:571–580
177. Gerhold JP, Klingensmith WC III, Kuni CC et al (1983) Diagnosis of biliary atresia with radionuclide hepatobiliary imaging. Radiology 146:499–504
178. Spivak W, Sarkar S, Winter D et al (1987) Diagnostic utility of hepatobiliary scintigraphy with 99mTc-DISIDA in neonatal cholestasis. J Pediatr 110:855–861
179. Ben-Haim S, Seabold JE, Kao SC et al (1995) Utility of Tc-99m mebrofenin scintigraphy in the assessment of infantile jaundice. Clin Nucl Med 20:153–163
180. Cox KL, Stadalnik RC, McGahan JP et al (1987) Hepatobiliary scintigraphy with technetium-99m disofenin in the evaluation of neonatal cholestasis. J Pediatr Gastroenterol Nutr 6:885–891
181. Howman-Giles R, Moase A, Gaskin K, Uren R (1993) Hepatobiliary scintigraphy in a pediatric population: determination of hepatic extraction fraction by deconvolution analysis. J Nucl Med 34: 214–221
182. Howman-Giles R, Uren R, Bernard E, Dorney S (1998) Hepatobiliary scintigraphy in infancy. J Nucl Med 39:311–319
183. Majd M, Reba RC, Altman RP (1981) Effect of phenobarbital on ^{99m}Tc-IDA scintigraphy in the evaluation of neonatal jaundice. Semin Nucl Med 11:194–204
184. Balistreri WF (1985) Neonatal cholestasis. J Pediatr 106:171–184
185. Larrosa-Haro A, Caro-Lopez AM, Coello-Ramirez P et al (2001) Duodenal tube test in the diagnosis of biliary atresia. J Pediatr Gastroenterol Nutr 32: 311–315
186. Lin WY, Lin CC, Changlai SP et al (1997) Comparison technetium of Tc-99m disofenin cholescintigraphy with ultrasonography in the differentiation of biliary atresia from other forms of neonatal jaundice. Pediatr Surg Int 12(1):30–33
187. Johnson K, Alton HM, Chapman S (1998) Evaluation of mebrofenin hepatoscintigraphy in neonatal-onset jaundice. Pediatr Radiol 28:937–941
188. Kim CK, Heyman S (1994) Scintigraphic evaluation of liver transplants. In: Murray IPC, Ell PJ (eds) Nuclear medicine in clinical diagnosis and treatment. Churchill Livingstone, London, pp 69–75
189. Rayter Z, Tonge C, Bennett C et al (1991) Ultrasound and HIDA: scanning in evaluating bile leaks after cholecystectomy. Nucl Med Commun 12: 197–202
190. Brugge WR, Rosenberg DJ, Alavi A (1994) Diagnosis of postoperative bile leaks. Am J Gastroenterol 89:2178–2183

191. Walker AT, Shapiro AW, Brooks DC et al (1992) Bile duct disruption and biloma after laparoscopic cholecystectomy: imaging evaluation. AJR Am J Roentgenol 158:785–789
192. Banzo I, Blanco I, Gutierrez-Mendiguchia C, Gomez-Barquin R, Quirce R, Carril JM (1998) Hepatobiliary scintigraphy for the diagnosis of bile leaks produced after T-tube removal in orthotopic liver transplantation. Nucl Med Commun 19:229–236
193. Worsley DF, Kim CK (1994) Hepatic and splenic trauma. In: Murray IPC, Ell PJ (eds) Nuclear medicine in clinical diagnosis and treatment. Churchill Livingstone, London, pp 63–67
194. Trerotola SO, Savader SJ, Lund GB et al (1992) Biliary tract complications following laparoscopic cholecystectomy: imaging and intervention. Radiology 184:195–200
195. Peters JH, Ollila D, Nichols KE et al (1994) Diagnosis and management of bile leaks following laparoscopic cholecystectomy. Surg Laparosc Endosc 4:163–170
196. Rodman CA, Keeffe EB, Lieberman DA et al (1987) Diagnosis of sclerosing cholangitis with technetium 99m-labeled iminodiacetic acid planar and single photon emission computed tomographic scintigraphy. Gastroenterology 92:777–785
197. O'Brien S, Keogan M, Casey M et al (1992) Biliary complications of cystic fibrosis. Gut 33:387–391
198. Colombo C, Castellani MR, Balistreri WF et al (1992) Scintigraphic documentation of an improvement in hepatobiliary excretory function after treatment with ursodeoxycholic acid in patients with cystic fibrosis and associated liver disease. Hepatology 15:677–684
199. Dogan AS, Conway JJ, Lloyd-Till JD (1994) Hepatobiliary scintigraphy in children with cystic fibrosis and liver disease. J Nucl Med 35:432–435
200. O'Connor PJ, Southern KW, Bowler IM et al (1996) The role of hepatobiliary scintigraphy in cystic fibrosis. Hepatology 23:281–287
201. Buscombe JR, Miller RF, Ell PJ (1992) Hepatobiliary scintigraphy in the diagnosis of AIDS-related sclerosing cholangitis. Nucl Med Commun 13: 154–160
202. Quinn D, Pocock N, Freund J et al (1993) Radionuclide hepatobiliary scanning in patients with AIDS-related sclerosing cholangitis. Clin Nucl Med 18:417–422
203. Kim OH, Chung HJ, Choi BG (1995) Imaging of the choledochal cyst. Radiographics 15:69–88
204. Camponovo E, Buck JL, Drane WE (1989) Scintigraphic features of choledochal cyst. J Nucl Med 30:622–628
205. Rosenthall L, Fonseca C, Arzoumanian A et al (1979) ^{99m}Tc-IDA hepatobiliary imaging following upper abdominal surgery. Radiology 130:735–739
206. Zeman RK, Lee C, Stahl RS et al (1982) Ultrasonography and hepatobiliary scintigraphy in the assessment of biliary-enteric anastomoses. Radiology 145:109–115
207. Weissmann HS, Gliedman ML, Wilk PJ et al (1982) Evaluation of the postoperative patient with 99mTc-IDA cholescintigraphy. Semin Nucl Med 12:27–52
208. Belli G, Romano G, Monaco A et al (1988) HIDA scan in the follow-up of biliary-enteric anastomoses. HPB Surg 1:29–32
209. Aigner RM, Fueger GF, Schimpl G, Sauer H, Nicoletti R (1997) Cholescintigraphy in the evaluation of bile flow after Roux-en-Y hepatico-jejunostomy and hepatico-antrostomy in infants with choledochal cysts. Pediatr Radiol 27:850–854
210. Lucas MH, Elgazzar AH, Cummings DD (1995) Positional biliary stasis: scintigraphic findings following biliary-enteric bypass surgery. J Nucl Med 36:104–106